UDC 55 **CODEN – GEOME 2** **ISSN 0352 – 1206**

GEOLOGICA MACEDONICA

Geologica Macedonica	Год.	**24**	Број	1	стр.	1–74	Штип	2010
Geologica Macedonica	Vol.		No		pp.		Štip	

Geologica Macedonica	Год.	**24**	Број	1	стр.	1–74	Штип	2010
Geologica Macedonica	Vol.		No		pp.		Štip	

GEOLOGICA MACEDONICA

Published by: – Издава:

The "Goce Delčev" University, Faculty of Natural and Technical Sciences, Štip, Republic of Macedonia

Универзитет „Гоце Делчев“, Факултет за природни и технички науки, Штип, Република Македонија

Language editor	Лектура
Marijana Kroteva	**Маријана Кротева**
(English)	(англиски)
Georgi Georgievski, Ph. D.	**д-р Георги Георгиевски**
(Macedonian)	(македонски)
Technical editor	Технички уредник
Blagoja Bogatinoski	**Благоја Богатиноски**
Proof-reader	Коректор
Alena Georgievska	**Алена Георгиевска**

Address	Адреса
GEOLOGICA MACEDONICA	**GEOLOGICA MACEDONICA**
EDITORIAL BOARD	**РЕДАКЦИЈА**
Faculty of Natural and Technical Sciences	**Факултет за природни и технички науки**
P. O. Box 96	**пошт. фах 96**
MK-2000 Štip, Republic of Macedonia	**МК-2000 Штип, Република Македонија**
Tel. ++ 389 032 550 575	**Тел. 032 550 575**

E-mail: todor.serafimovski@ugd.edu.mk

400 copies	Тираж: 400
Published yearly	Излегува еднаш годишно
Printed by:	Печати:
2ri Avgust – Štip	2ри Август – Штип
Price: 500 den	Цена: 500 ден.
The edition was published in December 2010	Бројот е отпечатен во декември 2010

Photo on the cover:	На корицата:
Argillitic alteration, Kadiica, Republic of Macedonia	Аргилитска алтерација, Кадиица, Република Мекедонија

Geologica Macedonica	Год.	**24**	Број	1	стр.	1–74	Штип	2010
Geologica Macedonica	Vol.		No		pp.		Štip	

СОДРЖИНА

Geologica Macedonica	Год.	**24**	Број	1	стр.	1–74	Штип	2010
Geologica Macedonica	Vol.		No		pp.		Štip	

TABLE OF CONTENTS

Geologica Macedonica, Vol. **24**, No 1, pp. 1–12 (2010)
GEOME 2 ISSN 0352 – 1206
Manuscript received: March 20, 2010 UDC: 550.380
Accepted: September 27, 2010

Original scientific paper

THE STRUCTURE OF THE BIG MAGNETIC STORMS

Spomenko J. Mihajlović[1], Rudi Čop[2], Paolo Palangio[3]

[1]*Geomagnetic Institute, Geomagnetic Observatory Grocka, Belgrade, Serbia, 11306 Grocka,*
[2]*Higher Education Center Sezana, Laboratory for Geomagnetism and Aeronomy, Slovenia,*
[3]*INGV, Osservatorio Geofisico, Castello Cinquecentesco, 67100 L'Aquila, Italia*
mihas@sezampro.rs //rudi@artal.si // palangio@ingv.it

A b s t r a c t: The records of geomagnetic activity during Solar Cycles 22 and 23 (which occurred from 1986 to 2006) indicate several extremely intensive A-class geomagnetic storms. These were storms classified in the category of the Big Magnetic Storms. In a year of maximum solar activity during Solar Cycle 23, or more precisely, during a phase designated as a post-maximum phase in solar activity (PPM – Phase Post maximum), near the autumn equinox, on 29, October 2003, an extremely strong and intensive magnetic storm was recorded. In the first half of November 2004 (7, November 2004) an intensive magnetic storm was recorded (the Class Big Magnetic Storm). The level of geomagnetic field variations which were recorded for the selected Big Magnetic Storms, was $\Delta D_{st} > 350$ nT. For the Big Magnetic Storms the indicated three-hour interval indices geomagnetic activity was $K_p = 9$. This study presents the spectral composition of the D_i – variations which were recorded during magnetic storms in October 2003 and November 2004.

Key words: magnetic storms; geomagnetic activity; variations in the geomagnetic field; spectrum of variations

INTRODUCTION

During the solar cycles (about 11.5 years) observatories recorded several events of geomagnetic disturbances. These may be the SSC-type geomagnetic storms (SSC – ***s**udden **s**torm **c**ommencement*) or a g-type geomagnetic storms (g – ***g**radual beginning*). The variations described can be used as the basis for a survey of the compound structure of the external geomagnetic field.

In Observatory yearbooks are contented the average solar daily variation for different months of the year, and even separately for quiet, disturbed and all days. Based on the geomagnetic activity index K_p, and solar activity indices R_i, the five quiet and disturbed days are selected very soon after the end of each month by the ISGI – International Service of Geomagnetic Indices in Paris (France). During Solar Cycles 22 and 23, which took place from 1982 to 2005, on the basis of the geomagnetic data recorded at several mid-latitude European observatories diurnal geomagnetic activity variations geomagnetic disturbances and class intensive geomagnetic storms were analyzed.

The amplitudes of the regular daily variation will reach a maximum value during the summer solstices and a minimum value during the winter solstice. This property is proof that the regular daily variations have a seasonal character and that they depend on solar activity changes. At the mid-latitude geomagnetic observatories the measured variation amplitudes during the summer were about 60 nT and during winter 20 nT (nano Teslas, nT).

The sunlight daily variation is directly connected to the upper atmosphere electrical conductivity and to the motions of the atmospheric gas through the geomagnetic field lines of force. These motions and their complex interactions with the field, create an electrical current system in the ionosphere detectable on the Earth's surface as a slow modulation of the three components of the geomagnetic field that can be observed clearly.

At the Geomagnetic Observatory Grocka GMO (GCK) (Serbia), the geomagnetic storms which occurred during the period 1958–1990 were classified (Mihajlović J. S.; 1996a). Classification

as well as statistics and spectral analysis were made for a group (family) of 150 geomagnetic storms. Geomagnetic storms with sudden commencement (SSC-type) and geomagnetic storms with gradual commencement (g-type), were chosen from the 150 classified geomagnetic storms and analysed (Mihajlović J. S.; 1996b). In addition, the intensive magnetic storms which occurred during the period 1986–2005 were also classified; these storms were recorded at Mid-latitude European Geomagnetic Observatories (Cander Lj. R., Mihajlović J. S.; 2005).

Table 1 presents the coordinates of the geomagnetic observatories which made the geomagnetic storm classification, and Table 2 presents the parameters of the Big Magnetic Storms which occurred during the period 1982–2005.

Table 1

Mid-latitude European geomagnetic observatories

Observatory	Code	Geographical latitude
Panagjurishte	PAG	40.6°N
Ebro	EBR	40.8°N
L'Aquila	AQU	42.4°N
Grocka	GCK	44.6°N
Tihany	TIH	46.3°N
Chambon-la-Foret	CLF	50.1°N
Belsk	BEL	50.2°N
Niemegk	NGK	54.1°N
Wingst	WNG	54.5°N
Brorfelde	BFE	55.6°N

At several European GMO's the total of 37 ssc-type magnetic storms were analyzed. The parameters used for magnetic storm classification are: magnetic storm level and magnetic storm duration. The maximum change in the geomagnetic field, which was recorded over the disturbance interval, defines the magnetic storm level. For the magnetic storms analyzed there was registered a maximum intensity change in the geomagnetic field's horizontal component as follows: $\Delta H_{max} = \Delta H_{level} > 200$ nT. The magnetic storms lasted about seventy-two hours or $\Delta t_{st} \geq 72$ hr's (Δt_{st} – the storm time intervals). Table 2 contains a group of eight Big Magnetic Storms which were taken from the total number of the selected magnetic storms.

The Class of Big Magnetic Storms (Table 2) were compared with the magnetic storm categories designated during observation at the Japanese observatories of Kakioka (KAK), Memambetsu (MEM) and Kanoya (KNY) (Tsunomura S.; 1999a) and also with the monthly reports on the rapid variations which were recorded at the worldwide network of magnetic observatories and published by ISGI (International Service of Geomagnetic Indices, Publications, Office Monthly Bulletin – Preliminary Report on Rapid Variations)).

On the basis of the geomagnetic data recorded at several mid-latitude European geomagnetic observatories during Solar Cycles 22 and 23, which took place from 1986 to 2005, the daily geomagnetic-activity variations, geomagnetic disturbances, and the intensive magnetic storm classes were analyzed.

Table 2

The List of Big Magnetic Storms which were recorded during Solar Cycles 22 and 23 which occurred from 1986 to 2006 (Indices g.m.a. K = 9)

Magnetic storm	Duration (start)	Duration (end)	Level amplitude (nT)
1982, July 11th	13 Jul 1982 16:17 UT	15 Jul 1982| 22:00 UT	420
1986, February 6th	06 Feb 1986 13:15 UT	10 Feb 1986 23:45 UT	445
1989, March 13th	13 Mar 1989 01:28 UT	15 Mar 1989 21:50 UT	574
1990, April 9th	09 Apr 1990 08:44 UT	15 Apr 1990 06:00 UT	584
1991, October 17th	17 Oct 1991 13:33 UT	21 Oct 1991 19:20 UT	392
2000, July 14th	14 July 2000 06:46 UT	17 July 2000 13 54 UT	478
2003, October 29th	29 Oct 2003 06:12 UT	01 Nov 2003 21:00 UT	700
2004, November 7th	07 Nov 2004 02:57 UT	11 Nov 2004 14:00 UT	500

GEOMAGNETIC DISTURBANCE

Geomagnetic activity may be analyzed during a month on the basis of mid-time values and in this way regular and periodic variations may be selected as components of the geomagnetic structure. During certain days of the month recorded data for geomagnetic activity may show disordered, irregular and non-periodic variations in the geomagnetic field. They emerge at irregular time intervals and have different periods; the amplitudes/intensity of these variations may have several tens to several hundreds of nT.

The group of authors in period 1960–1972 have been defined another kind of division of the *D* field, based on physical considerations (Akasofu S.-J., Chapman S.; and M. Sugiura). These are associated with theoretical ideas as to the electric current systems by which the *D* field is produced. They are denoted by *DCF*, *DR* and *DP*: *D* for disturbance; *CF* for corpuscular flux; *R* for ring current and *P* for polar.

The *DCF* field is produced by electric currents flowing near the surface of the hollow carved by geomagnetic field in the solar stream or cloud that generates magnetic storms. The current flows as long as the corpuscular flux continues. The main effect of the *DCF* field at the earth's surface is to increase H component in low and middle latitudes, more on the dayside than on the night side of the Earth.

The *DR* field is produced by enhanced west ward electric current round the Earth during the storm. This current is associated with the motions of energetic particles in the outer geomagnetic field. The main effect of the *DR* field at the earth's surface during storms is to reduce H component in low and middle latitudes. The *DCF* and *DR* currents flow at distances of a few earth radii far above the main terrestrial ionosphere.

The *DP* field is produced by currents flowing in the ionosphere. They are driven by elelctromotive forces in the auroral zones. This *DP* field has a different time scale from that of magnetic storm.

They may be a fourth addition to the preexisting fields during the storm. The solar gas may carry with it a magnetic field transported away from the Sun. This field may be denoted by *DSM* (Disturbing Solar Magnetism).

The disturbing field *D* during a magnetic storm may be divided into the following four main parts:

$$D = DCF + DP + DR + DSM.$$

In the disturbed category of geomagnetic activity come disturbed daily variations and non-periodic disturbed variations, as well as short-term periodic changes in the geomagnetic field, which are observed as pulsations. All the aforementioned geomagnetic field variations which have all the aforementioned characteristics, or some of them, constitute a geomagnetic disturbance.

Sugiura and Akasofu, Chapman, (1961, 1972) and other researchers selected some morphological characteristics common to all geomagnetic disturbances by analyzing and investigating a great number of magnetic storms and other magnetic disturbances. Each geomagnetic disturbance is composed of: the regular part of the geomagnetic field's disturbance (*DS*); non-periodic variations (D_{st}), and the irregular part of the geomagnetic field's disturbance (D_i).

Selecting the days when geomagnetic disturbances were recorded as the days for analysis and applying the method of geomagnetic field variation processing, it is possible to regard the morphology of the variations, which are integral parts of the geomagnetic disturbances, in a different light. The geomagnetic field variations which may be expressed as the mid-time variation values for the days during the disturbance are defined as the regular part of geomagnetic disturbance or the DS-variation of the geomagnetic field. The subtraction of the geomagnetic field variations, which were recorded during the geomagnetic storm, from the defined *DS*-variation will present the non-periodic and irregular part of the geomagnetic disturbance.

One of the most important attributes of magnetic storms is that these geomagnetic disturbances have three phases: the initial phase, the main phase and the recovery phase (Figure 1, Figure 2). The appearance of an SSC impulse in the recorded data signifies the beginning of a magnetic storm (SSC impulse – ***S**udden **S**torm **C**ommencement*). It is followed by a sudden change ("jump") in the intensity of the geomagnetic field's horizontal component (ΔH) which is recorded over a short interval, which can last 3–5 minutes (Figure 1, Figure 2). These are very important parameters which describe the morphology of the SSC impulse and announce the sudden commencement of SSC-type magnetic storm.

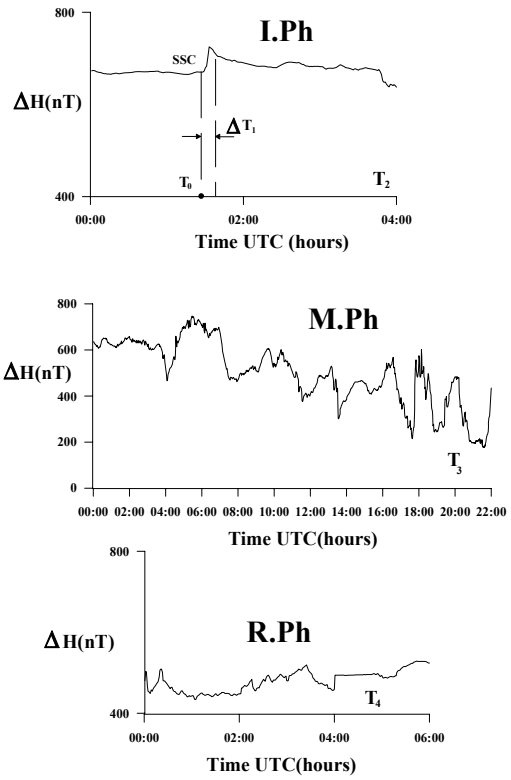

Fig. 1. The morphology of a geomagnetic storm shown in three phases
a) the initial phase (I.Ph); b) the main phase (M.Ph);
c) the recovery phase (R.Ph)

Changes in the Earth's Magnetic Field, without a predetermined period and different amplitudes, are determined as geomagnetic disturbances. The most typical geomagnetic disturbances are magnetic storms. They are represented by intensive variations in the geomagnetic field. These variations have a complex morphology.

The line of increase in the geomagnetic field's horizontal component values determines the initial phase of a magnetic storm. The initial phase can last for 30 minutes to a few hours (Figure 1, Figure 2). The main phase of a magnetic storm starts with the moment of decrease in the intensity of the geomagnetic field's horizontal component. The decrease in the field's intensity can last for a few hours to a few days. During the main phase of a magnetic storm, geomagnetic field variations with different amplitudes and periods can be recorded. It can be assumed that the recovery phase of a magnetic storm starts when the horizontal component values start their return to the level before registration of the storm (Figures 1, Figure 2).

The described geomagnetic field changes which occur during magnetic storm are a macrostructural model of the magnetic storm. This model highlights the cumulative, principal characteristics associated with the magnetic storm phenomenon.

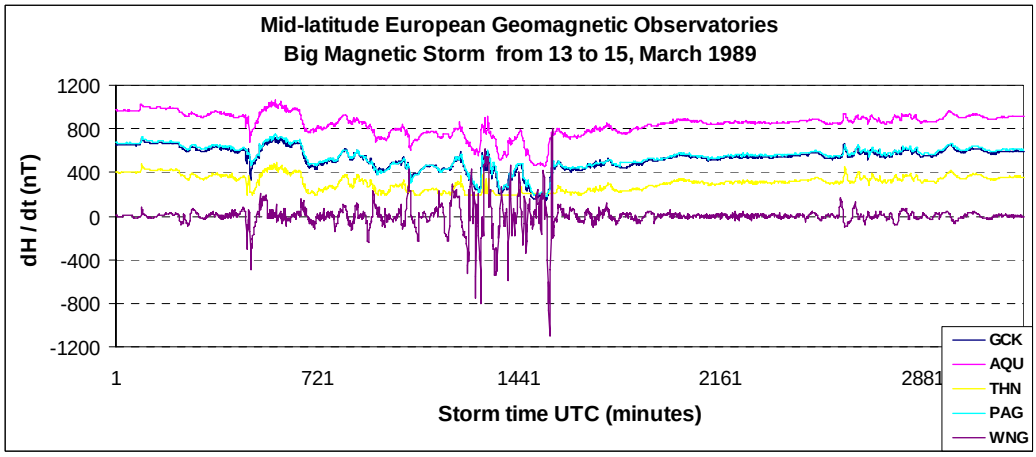

Fig. 2. The variations recorded in the horizontal component of the geomagnetic field during the Big Magnetic Storm on 13, March 1989, at Mid-latitude European Geomagnetic Observatories

The described methodology for geomagnetic field variation analysis during a geomagnetic disturbance was used for the intensive geomagnetic storms recorded on February 6, 1986 and on March 13, 1989 (Villante U. et al. 1990; Chander R. Lj., Mihajlović J. S., 1998). The data from these two geomagnetic storms which were recorded at mid-latitude geomagnetic observatories were used for the analysis (Table 1, Table 2, Figure 1, Figure 2).

The recorded variations mean hours values for the geomagnetic field's horizontal components (H or X component) may be determined for the geomagnetic storms' time intervals, on the basis of the study of a great number of geomagnetic storms during various seasons. When the described analytic procedure is applied to geomagnetic disturbances, the result is a regular variation of the geomagnetic field according to certain rules, which is

essential for all recorded changes in the geomagnetic storm and this is called the non-periodic variation (D_{st}). The geomagnetic field's non-periodic variation (D_{st}) is linked to the time (t_{st}) when the geomagnetic storm starts. Referring to its basic interpretation this variation is defined as the storm time variation (D_{st}), or variation over the interval which starts with the magnetic storm's commencement and finishes when the geomagnetic storm ends (Akasofu S-J. and Chapman S. 1961, 1972; Bartels J.; 1963).

The deviation in the geomagnetic field's variation – presented in minutes and measured during the geomagnetic storm interval – from the determined D_{st}-variation, illustrates the irregular part of the geomagnetic field's disturbance. This deviation is the result of subtraction: the disturbed daily variation (S_D) & non-periodic variation (D_{st}) minus the geomagnetic field's variation which was recorded during the geomagnetic storm. Such a geomagnetic field variation is called an irregular variation (D_i). This type of geomagnetic field variation is composed of a complex signal which characterizes a "chaotic, irregular" feature of the geomagnetic disturbance. The structure of the geomagnetic field's irregular variation (D_i) contains the individual characteristic of each geomagnetic storm (Mihajlović J. S., 2000; Cander Lj. R., Mihajlović, 2005).

If we can say for the D_{st} variation that it is a picture of the magnetic storm (the morphology of the magnetic storm), then the D_i variation is the rhythm of each magnetic storm (the power of the magnetic storm).

This study presents the methodology for analysing the geomagnetic field variation, using the recorded data at several mid-latitude geomagnetic observatories, during the two Big Magnetic Storms on 29, October 2003 and on 07, November 2004 (Table 1, Table 2).

Big Magnetic Storm on 29. October 2003

In 2003 during the last ten days of October, intensive and very turbulent changes in the solar radiation spectrum were recorded in both solar activity and the sun's magnetic field. The recorded phenomena: solar storms, explosive and hyperactive solar flares with strong coronal mass ejection (CME) caused large magnetic storms in the geomagnetic field, which were classified in the clas or category of the Big Magnetic Storms.

The beginning of the intensive magnetic storm in October (29, October 2003) was signified by an SSC (A) impulse. The amplitude of the SSC (A) impulse which was recorded at the Geomagnetic Observatory Grocka (GCK; φ = 43.4°), was ΔX = –54 nT, ΔY = –40 nT, ΔZ = –10 nT. Figure 3 shows the October Big Magnetic Storm which was recorded at the mid-latitude European GMO's.

In the interval from the start (the time when the sudden storm commencement impulse was recorded) through the approximately 120 or 150 minutes of minute values changes in the geomagnetic field's H-component intensity at the listed geomagnetic observatories reached $\Delta H > -700$ nT (Figure 3). Therefore, it is necessary to mention, as this storm's particular feature or individual characteristic, that extremely high values in the geomagnetic field's intensity were recorded constantly during the initial phase. The extremely high sunspot group activity continued over the next few days, and disturbed geomagnetic activity and the geomagnetic storm lasted till November 2nd 2003.

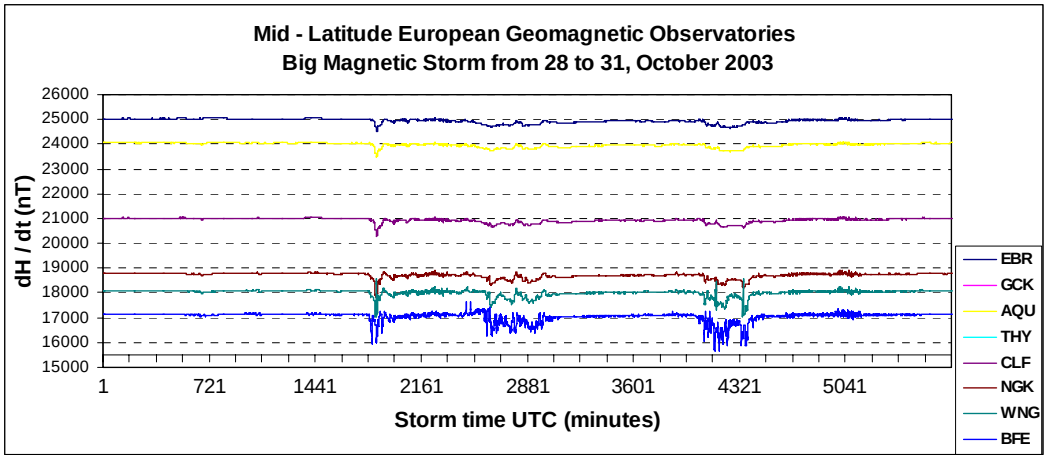

Fig. 3. The October's Big Magnetic Storm which was recorded at the mid-latitude European Geomagnetic Observatories

The specific characteristic of the October Big Magnetic Storm was its non-periodic variation (D_{st}). Figure 4 shows the D_{st}-variation of the October Big Magnetic Storm which was recorded at the mid-latitude European geomagnetic Observatories (last diagram) and the D_{st}-variation data recorded at the Geomagnetic Observatories: GCK, AQU and WNG which are shown separately (first diagram). The maximum changes in the geomagnetic field's horizontal components (H or X component) are represented by the mean hours values witch during the October's Big Magnetic Storm were greater than four hundred nano Teslas $\Delta H > -400$ nT (Fig. 4.).

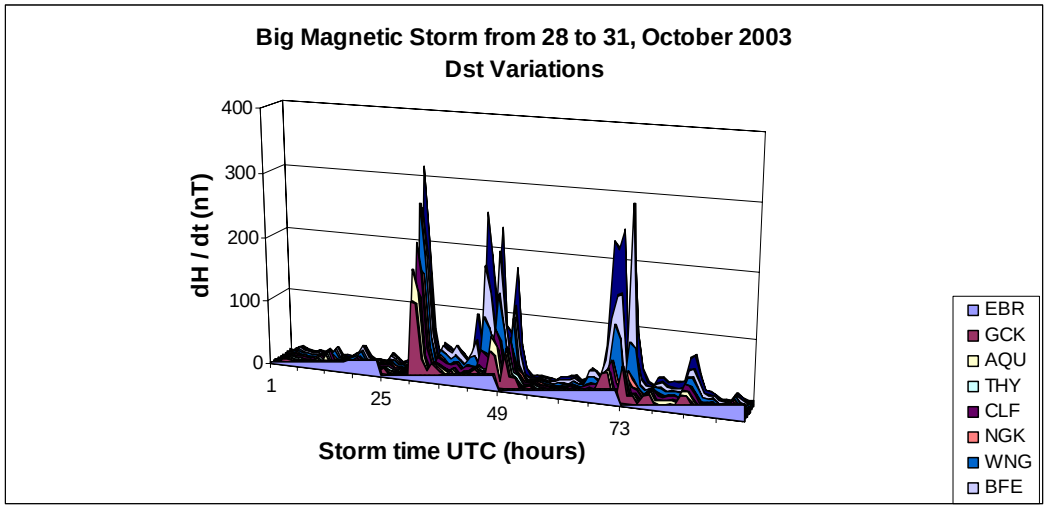

Fig. 4. The D_{st} variation structure which was recorded during the October's Big Magnetic Storm

The results of the analysis and surveys of the March Big Magnetic Storm (13, March 1989) showed that the recorded data of the D_{st}-variation have a tendency to reduce the geomagnetic field's horizontal component intensity (a depression in the horizontal component intensity). This may be taken as a standard or regular morphology and structure of the non-periodic variation (D_{st}) (Cander R. LJ., and Mihajlović J. S.; 1998).

In the D_{st}-variation structure, during the main phase of the October's Big Magnetic Storm, three cycles of intensity reduction in the geomagnetic field's horizontal component were recorded. The cycles of intensity reduction in the geomagnetic field's H-component lasted about ten hours. On diagrams on Figure 5 is shown the amplitude spectrum of the non-periodic variation (D_{st}) signal recorded at the GMO (GCK).

The Fourier transformation of the non-periodic variation (D_{st}) signal, which was recorded during October Magnetic Storm, showed that the changes in the geomagnetic field's H-component intensity came about in cycles with a frequency from $\Delta\omega = 0.05$ to $\Delta\omega = 0.38$ cycles per hour, that is their periods were $\Delta T = 150 - 180$, $\Delta T = 200 - 240$, $\Delta T = 500$, $\Delta T = 600$ and $\Delta T = 1000 - 1200$ minutes (Figure 5.). In the amplitude spectrum of the non-periodic variation (D_{st}) signal the dominant changes were the changes in the geomagnetic field's H-component intensity, which were from $\Delta H = 2$ nT/minute to $\Delta H = 6$ nT/minute, and they were recorded at the Geomagnetic Observatory Grocka (GCK), (Figure 5.).

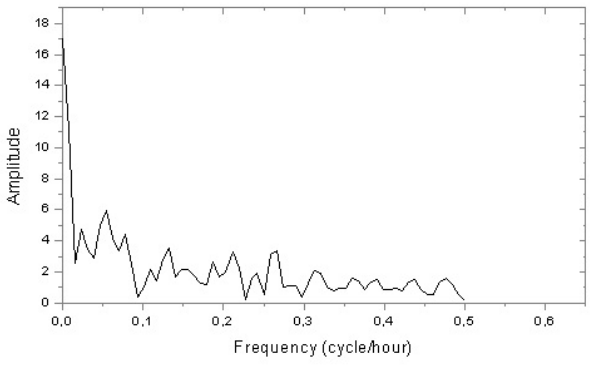

Fig. 5. The amplitude spectrum of the non-periodic variation (D_{st}) signal which was recorded during the October Big Magnetic Storm at the Geomagnetic Observatory Grocka (GCK)

In anlysis October's Big Magnetic Storm, the geomagnetic field's irregular variation (D_i) was extracted (Cander R. LJ., and Mihajlović J. S.; 2005). By taking a Fourier transformation of the irregular-variation signal (D_i), which was recorded

during the October Magnetic Storm, the characteristics of the amplitude spectrum and the frequency spectrum of the geomagnetic storm's recorded variations were obtained. Diagrams on Figure 6 show the morphology and amplitude spectrum of an irregular variation (D_i) during the October's Big Magnetic Storm which was recorded at several European GMO's.

In this amplitude spectrum of the D_i variations which have frequencies from $\Delta\omega$ = 0.025 to $\Delta\omega$ = 0.5 cycles/minute were recorded (Fig. 6). It is a complex spectrum of electromagnetic pulsations with periods from two to fifteen minutes, and with an maximum amplitude of several hundred nT.

The specific characteristics of the irregular variation (D_i), which were recorded during the October's Big Magnetic Storm, are a very complex amplitude spectrum and frequency spectrum. During intervals which lasted from 100 to 150 minutes, a complex geomagnetic field variation spectrum was recorded; the complex spectrum of the P_c1 – P_c5 classes of geomagnetic pulsations (or changes in the Earth's magnetic and electromagnetic fields with periods from ΔT = 1 sec to ΔT = 20 minutes was also recorded. The solar flare group activity, the proton fluxes and the coronal mass ejections (CMEs) caused induction of the geomagnetic activity's irregular variation (D_i) with a complex spectrum.

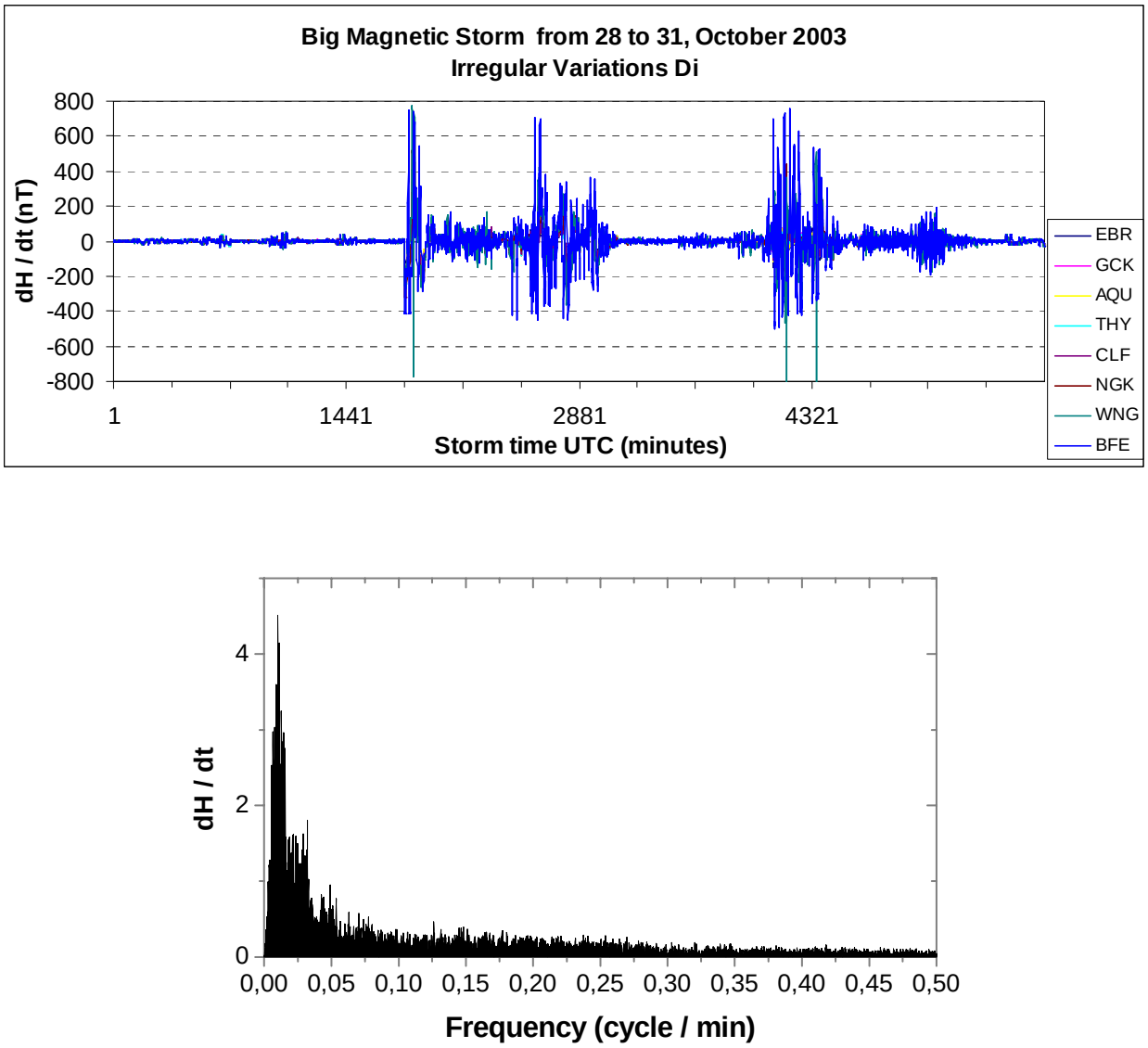

Fig. 6. The D_i irregular variation of geomagnetic field which was registered during the October Big Magnetic Storm a) the D_i irregular variation signal (upper diagram); (b) the D_i irregular variation amplitude spectrum which was recorded at the Geomagnetic Observatory Grocka (GCK) (bottom diagram)

Big Magnetic Storm on 07, November 2004

At 2:57 UT on 07, November 2004, an SSC (A) impulse was registered. It marked the start of the geomagnetic disturbance. The amplitude of the SSC (A) impulse which was recorded at the Geomagnetic Observatory Grocka (GCK) was ΔX = +4.1 nT; ΔY= –2.3 nT; ΔZ = –0.5 nT. After the first SSC impulse, geomagnetic activity conditions were moderately disturbed. This situation lasted about eight hours. A second SSC (A) impulse was recorded at 10:52 UT with an amplitude of ΔX = +14.0 nT, ΔY = +4.0 nT, ΔZ = –2.3 nT. The second SSC (A) impulse signified the development of the magnetic storm.

During the initial interval, which lasted 80 minutes, an increase in the geomagnetic field's *X*-component intensity was recorded; this increase signified the start of the November's Big Magnetic Storm's initial phase. The increase in the geomagnetic field's X-component was about ΔX = 30 nT. On Figure 7 are shown the registrations of the November's Big Magnetic Storm which were recorded at mid-latitude European Geomagnetic Observatories.

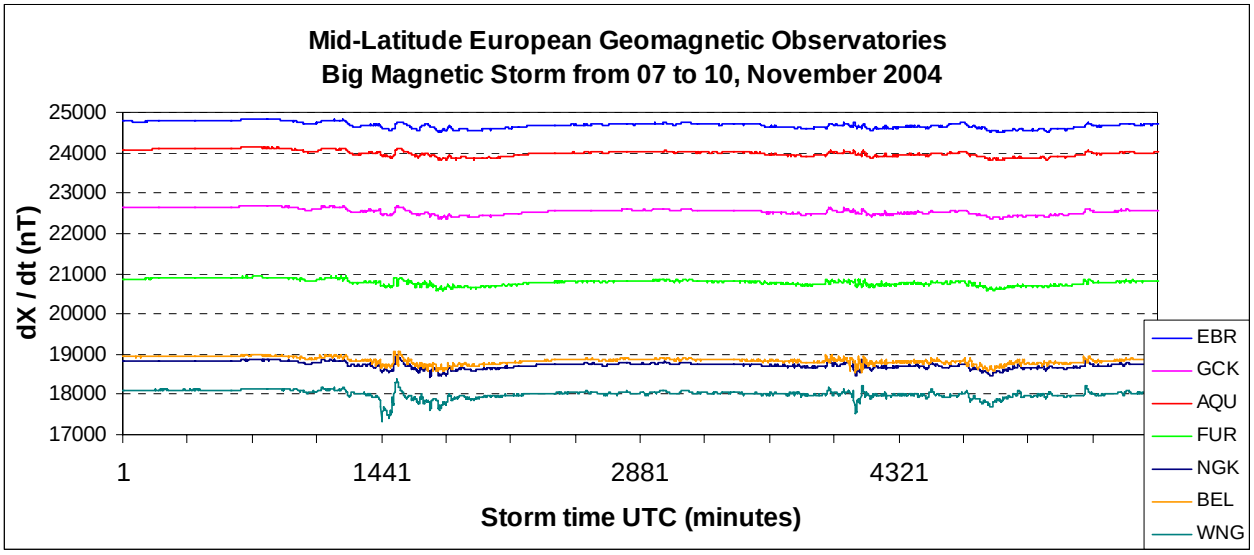

Fig. 7. The November's Big Magnetic Storm which was recorded at the mid-latitude European Geomagnetic Observatories

The recorded geomagnetic data during the November's Big Magnetic Storm show that the main phase development started after the geomagnetic field's X-component increased. The specific characteristic of the November Storm's main phase is the X-component reduction, which occurred in time interval which lasted approximately ten hours (Fig. 7.).

In the D_{st}-variations structure, during the main phase of the November's Big Magnetic Storm, a reduction in the geomagnetic field's X-component intensity was recorded over two cycles (depression). Figure 8 shows the non-periodic variation (D_{st}) signal recorded at the Geomagnetic Observatories of Grocka (GCK), L'Aquila (AQU) and Niemegk (NGK).

By taking the Fourier transformation of the non-periodic variation (D_{st}), which was recorded during the November Magnetic Storm, the periods of the changes in the geomagnetic field's X-component intensity were obtained (Fig. 8.)

The irregular variation (D_i) of the geomagnetic field which was registered during the November magnetic storm is illustrated in Figure 9. In the morphology of the irregular variation (D_i), two signals with extremely high values of the geomagnetic field's horizontal component $\Delta X > \pm 300$ nT can be observed.

Figure 9 illustrates the amplitude spectrum of the irregular variation (D_i) in the geomagnetic field. In this amplitude spectrum, the D_i variations with frequencies from $\Delta\omega$ = 0.025 to $\Delta\omega$ = 0.35 cycles/minute and periods from ΔT = 40 minutes to ΔT = 3 minutes were recorded. This is basically a complex pulsation spectrum; during the interval when the November Big Magnetic Storm was recorded these pulses had amplitudes greater than ±200 nT.

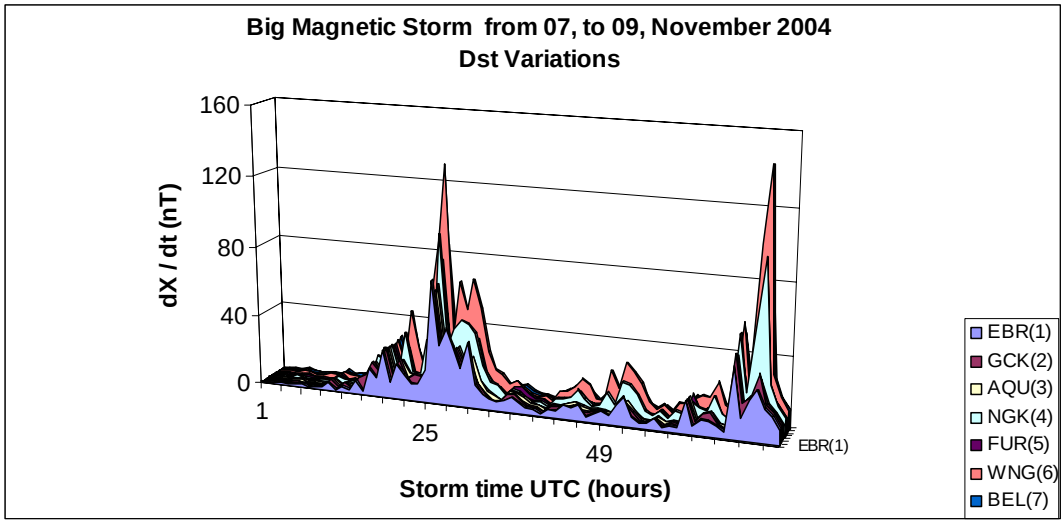

Fig. 8. The D_{st}-variation structure which was recorded during the November Big Magnetic Storm

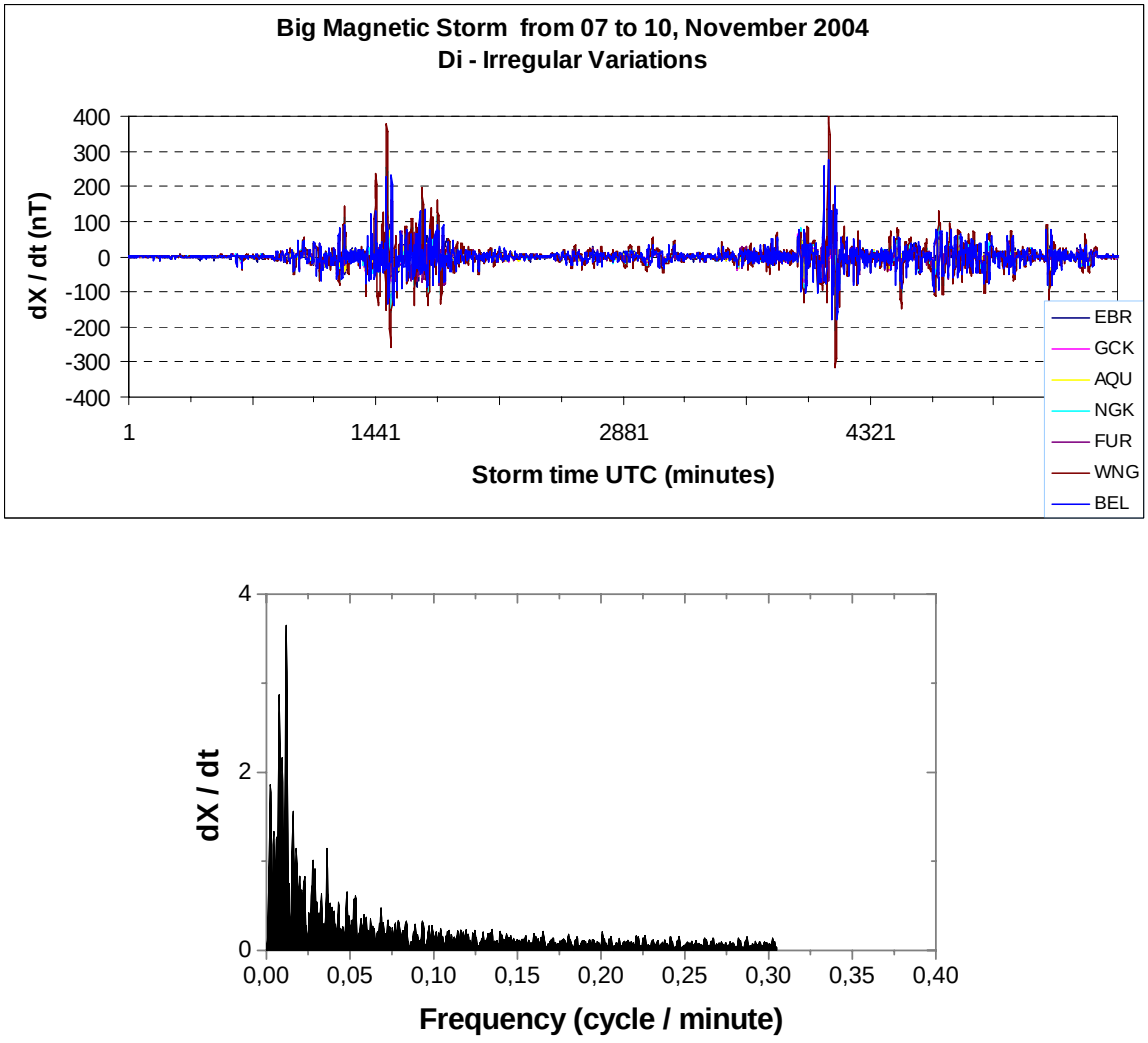

Fig. 9. The Di irregular variation of geomagnetic field which was registered during the November Big Magnetic Storm (a) the D_i irregular variation signal (upper diagram); b) the D_i irregular variation amplitude spectrum which was recorded at the Geomagnetic Observatory Grocka (GCK) (bottom diagram)

CONCLUSIONS

The structure of the geomagnetic activity disturbance is illustrated with graphs of three Big Magnetic Storms (in March 1989, in October 2003 and in November 2004) which were recorded at Mid-latitude European Geomagnetic Observatories. During the months in which these three storms were recorded the types of daily variations in the geomagnetic field were analyzed. These variations were designated as the daily variations for magnetically quiet days (S_q) and the daily variations for magnetically disturbed days (S_d).

By defining the type of daily variation in the geomagnetic field, which was recorded during the duration of the extreme geomagnetic storms (Δt_{st} – the storm time interval), the individual characteristics of these Big Magnetic Storms were determined. The types of variations in the geomagnetic field which were analyzed are: non-periodic variation (D_{st}) and irregular variation (D_i).

Referring to the literature, many groups of authors have carried out research in which they defined the D_{st}-variation as the long-term periodic changes in the geomagnetic field during the storm time interval. These changes represent the trend ("depression") in the intensity of the geomagnetic field's horizontal component during the main phase of a geomagnetic storm (Sugiura M., Chapman S., Bartels J., Akasofu S. -J., 1960–1972; Tsurutani B. T., Gonzales W. D., 1994–2004; Yago K. and Kamide Y., 2003; Cander Lj. R. and Mihajlović J. S., 1996–2005).

The non-periodic variation of the geomagnetic field (D_{st}), which was recorded during the Extreme Geomagnetic Storm in March 1989, had a distinctive line of reduction in the intensity of the geomagnetic field in one cycle. The structure of the D_{st}-variation which was recorded during the main phase of the March Big Magnetic Storm is, on the whole, equivalent to the definition of the standard (regular) macro-structural model of the non-periodic variation type.

The structure of the D_{st}-variation which was recorded during the main phase of the October Big Magnetic Storm has three cycles of reduction in intensity in the geomagnetic field's horizontal component, and the structure of the D_{st}-variation which was recorded during the main phase of the November Big Magnetic Storm has two cycles of reduction (depression) in the intensity of the geomagnetic field's horizontal component. The cycles of the intensity changes in the geomagnetic field's *H*-component lasted about ten hours.

The spectral analysis of the irregular variation signal (D_i) which was recorded during the October Big Magnetic Storm, showed that the geomagnetic field's variations were predominantly within the frequency band from $\Delta\omega = 0.025$ to $\Delta\omega = 0.5$ cycles per minute, or with periods approximately from $\Delta T = 2$ to 15 minutes with the distribution of the changes in the geomagnetic field's *H*-component intensity approximately $\Delta H > \pm 500$ nT. The spectral components of the irregular variation signal (D_i), which was recorded during the November Big Magnetic Storm, showed that the geomagnetic field's variations were predominantly within the frequency band from $\Delta\omega = 0.025$ to 0.35 cycles per minute, or with periods approximately from $\Delta T = 3$ to 40 minutes with the distribution of the changes in the geomagnetic field's *H*-component intensity approximately $\Delta H > \pm 300$ nT.

In these two extreme magnetic storms during the initial time interval of approximately 100 to 150 minutes the following data were recorded: the complex spectrum of the geomagnetic field's variations, and the complex spectrum of the P_c1–P_c5 class of geomagnetic pulsation – these were changes in geomagnetic activity and changes in the Earth's electromagnetic field with periods lasting from 10 seconds to 20 minutes.

The complex spectrum of the irregular variations (D_i) of the geomagnetic field which were recorded during the October and November Big Magnetic Storms indicates extremely strong processes in energy exchange in the solar magnetic field, and extremely high incidences of solar flares, proton fluxes and CMEs which induced very major changes in interplanetary conditions – and consequently in solar-geophysical conditions and geomagnetic activity conditions.

Acknowledgments: Results of researching of geomagnetic field variations and geomagnetic disturbances (geomagnetic storms), which are registered on European observatories of middle geomagnetic latitude, are shown on workmanship assemblies and workshops, in international MEM Project, which last from 2004 to 2008. In this work is shown the part of results of those researching...

I want to express acknowledgement lider partners of MEM Project: Regione Abruzzo, Osservatorio Geofisico L'Aquila, Instituto Nazionale Geofisica e Vulcanologia (INGV), Roma, Italia, which enabled to me to realize role in the MEM Project :"Geomagnetic field spatial modeling on regional scale".

REFERENCES

Akasofu S.-I. and Chapman S., 1972: *Solar – Terrestrial Physics, Chapter V–VIII*; Oxford University.

Akasofu S. -I. and Chapman S., 1961: A Study of magnetic Storms and Auroras; *Scientific Report No. 7.; Geophysical Institute of the University of Alaska*; March 1961.

Bartels J., 1963: Discussion of Time-Variations of Geomagnetic Activity, Indices Kp and Ap, 1932–1961, *Extrait des Annales de Geophisyque;* Tome 19, No. 1. Janvier-Mars.

Cander R. Lj. and Mihajlovic J. S., 1998: Forecasting ionospheric structure during the great geomagnetic storms; *J. Geophys. Res*., **103**, A1, 391–398, January 1.

Cander Ljiljana R. and Spomenko J. Mihajlovic, 2005: Ionospheric spatial and temporal variations during the 29–31 October 2003 storm; *Journal of Atmospheric and Solar-Terrestrial Physics,* **67**, 1118–1128; Elsevier Ltd.

Mihajlović Spomenko J., 1996a: "Morfologija varijacija geomagnetskog polja registrovanih na geomagnetskoj opservatoriji Grocka u periodu 1958-1990. godine" – Monografija, Izdanja Geomagnetskog instituta Grocka, pp. 1-63; Beograd, 1996.

Mihajlović Spomenko J., 1996b: "Morfologija geomagnetskih bura registrovanih na opservatorijama Jugoistočne Evrope", *Doktorska disertacija*, pp. 1-107, Beograd, 1996.

Mihajlović J. S; Rašić M., 2000: Solarno-geofizički procesi i geomagnetski poremećaji, *10. Kongres fizičara Jugoslavije; Zbornik radova*, Knjiga II; pp. 913–920.; Jugoslovensko Društvo Fizičara; Beograd.

Sugiura M. and Chapman S. 1960: The average morfology of geomagnetic storms with sudden commencement, *Abb. Akadem. Wissensch. Gottingen*; Math-Physik; KI.; Sond 4. Gottingen.

Sugiura M., 1961: A Study of the Morfology of Magnetic Storms, *Final Report, Geophysical Institute of the University of Alaska*; October 1961.

Tang F., Tsurutani B.T. et al. 1994: Solar Sources of Interplanetary Southward B_Z Events Responsible for Major Magnetic Storms (1978–1979), *JGR;* **94**, A4, 3535–3541, April 1.

Tsunomura S. et al. 1999a: A study of geomagnetic storm on the basis of magnetic observations in the Japanese chain observatories, *Memories of the Kakioka magnetic observatory*, vol. **27**, pp. 1–105, Japan.

Tsurutani B. T. et al. 1998: Magnetic Storms, *Geophysical Monograph*, Series 98, American Geophysical Union (AGU); Washington, DC, USA.

Tsurutani B. T. and Suess S. T. (editors), 1998: *From the Sun: Auroras, Magnetic Storms, Solar Flares, Cosmic Rays*; Copyright 1998 by the American Geophysical Union; Washington, DC, USA.

Tsurutani B. T., Gonzales W. D., et al. 2004a: Properties of slow magnetic clouds; *JASTP,* **66**, 2, January, pp 147–151, Published in Association with U.R.S.I., Elsevier Ltd.

Tsurutani B. T., Gonzales W. D., et al. 2004b: Prediction of peak – D_{st} from halo CME/magnetic cloud-speed observations, *JASTP,* **66**, 2, January, pp 161–165, Published in Association with U.R.S.I.; Elsevier Ltd.

Villante V.; Villante U.; et al. 1990: The strong geomagnetic storms of March 13, 1989, Analysis at a low latitude station, *Annales Geophysical*, 8, 337–342.

Yago K.; Kamide Y., 2003: Use of lognormal distributions in D_{st} variations for space weather forecast, *Space Weather*, **1**, 1, 1004, Winter, AGU.

The Data Sources

Solar Influences Data Analysis*, Sunspot bulletin*, 2004, No. 11, Monthly Summary of Solar and Geomagnetic Activity.

Solar Influences Data Analysis, *Sunspot Bulletin,* 2003, No. 10, Monthly Summary of Solar and Geomagnetic Activity.

ISGI Publications, *Office Monthly Bulletin*, No. 3–10, October, 2003; No. 4–11, November, 2004.

www.sidc.be, April 2007.

Р е з и м е

СТРУКТУРА НА ГОЛЕМИТЕ МАГНЕТНИ БУРИ

Споменко Ј. Михајловиќ[1], Руди Чоп[2], Паоло Паланџио[3]

[1]Геомагнетен Институт 11306 Гроцка, Геомагнетна Опсерваторија Гроцка, Белград, Србија,
[2]Центар за високо образование Сежана, Лабораторија за геомагнетизам и аерономија, Словенија,
[3]INGV, Osservatorio Geofisico, Castello Cinquecentesco, 67100 L'Aquila, Italia,
mihas@sezampro.rs //rudi@artal.si // (palangio@ingv.it)

Клучни зборови: geomagnetina aktivnost; geomagnetina bura, varijacii na geomagnetnoto pole; spektar na varijacii

Евиденцијата на геомагнетна активност за време на соларните циклуси 22 и 23 (кој се случија 1986–2006) укажуваат на неколку исклучително интензивни А-класа геомагнетни бури. Овие бури се класифицираат во категоријата на големи магнетни бури. Во година на максимална сончева активност во текот на Сончевиот циклус 23, или поточно, за време на фазата назначена како пост-максимална фаза во сончевата активност (PPM – Phase Post maximum – фаза на пост-максимум), во близина на есенската рамнодневица, на 29, октомври 2003 година, евидентирана е исклучително силна и интензивна магнетна бура. Во првата половина на ноември 2004 година (07. ноември, 2004), евидентирана е интензивна магнетна бура (Класа Голема Магнетна бура). Нивото на варијации на геомагнетното поле кои се снимени за избраните Големи Магнетни бури, беше $\Delta D_{st} > 350$ nT. За големите магнетни бури наведениот тричасовен интервал покажува геомагнетна активност беше $K_p = 9$.

Оваа студија претставува спектрален состав на D_t-варијации што беа снимени за време на магнетни бури во октомври 2003 и ноември 2004 година.

Geologica Macedonica, Vol**. 24**, No 1, pp. 13–21 (2010)
GEOME 2 ISSN 0352 – 1206
Manuscript received: March 13, 2010 UDC: 551.24(497.7))
Accepted: October 3, 2010

Original scientific paper

OF REPEAT STATIONS AND TECTONIC REGIONALIZATION OF THE REPUBLIC OF MACEDONIA

Marjan Delipetrev[1], Jean L. Rasson[2], Blagica Doneva[1], Todor Delipetrov[1]

[1]Faculty of Natural and Technical Sciences, Department of Geology and Geophysics
The "Goce Delčev" University,
Goce Delčev 89, MK-2000, Štip, Republic of Macedonia
[2]Royal Meteorological Institute- Geomagnetic Observatory Dourbes, Belgium
marjan.delipetrev@ugd.edu.mk // blagica.doneva@ugd.edu.mk

A b s t r a c t: Geomagnetic field is vector sum of causes deep in the Earth's interior and their influence can be felt in the whole Earth. There are sources of magnetic fields which are characterized for larger regions and local anomalous geomagnetic fields. When selecting the location of base station, regions where local geomagnetic anomalies are present, should be avoided, with aim to receive measured results which gives the geomagnetic field characteristic for that region. The territory of the Republic of Macedonia has complex relief, and also has complex geological structure and these features have high influence on the regional geomagnetic field. Bearing in mind the complex relief and geological structure, strict procedure of geomagnetic field observations were conducted for every selected location for repeat station. Maps from the measurements in 2004 are also presented in this paper.

Key words: repeat station; geomagnetic field; declination; inclination; total field

INTRODUCTION

This paper presents neotectonic regionalization of the Republic of Macedonia. In the central part of Macedonia, Vardar zone is located. On the eastern side of it is Eastern Macedonian zone (Serbian–Macedonian massif), and on the west is Western Macedonian zone. These mega structures have their influence on the geomagnetic field and in that way create the characteristic field for this region (GETECH, 1997)

When forming the net of the repeat stations (first order net), the arrangement of the measured points should be such as to cover the territory of the Macedonia as much as homogenous.

Conducted procedure when selecting the measured points, i.e. homogenity of the geomagnetic field, horizontal and vertical, must satisfy the standards of INTERMAGNET (Delipetrov T., 2004).

The maps of the elements of the geomagnetic fields are presented in this paper. They are compiled from the measurements on the net of the repeat stations done by Dr. Jean Rasson and MSc. Marjan Delipetrev.

The method of declination, inclination and total field measurements was used (Delipetrov T., 1991, 1996, 2003;. Delipetrov T., et al. 2006; Slimak Š, 1996).

NEOTECTONIC CHARACTERISTICS AND REGIONALIZATION OF THE TERRITORY OF THE REPUBLIC OF MACEDONIA

The geological evolution during the Neocene and Quaternary in all of Macedonia is characterized by continental development, uplift, overthrust and subsidence. .During this period, volcanic activity, the outflow of large andesite-dacite volcanic masses and tuffs occurred only in the area of Zletovo. Along reactivated deep faults there was outflow of volcanic material of some 1000 km^3. A

similar volcanic mass also developed in the area of Kožuf–Vitačevo. According to data, the volcanic activity took place periodically, although it started earlier in the Zletovo area. In the area of Kožuf it continued to the beginning of the Quaternary.

Modern relief was formed in limnic basins due to active neotectonic processes. Terrigenous layers of molasse with interbeds of coal were deposited in the depressions. During the Pliocene the terrigenous material became coarse as a result of atomization caused by tectonic movements. These processes have continued to the present time and manifest themselves as earthquakes (Skopje in 1963, Valandovo in 1931 etc.). At the end of the Pliocene and at the beginning of the Quaternary the volcanic activity consisted of outflows of basalts near Nagoričani and some other localities. Today, only traces of this activity can be seen in the area of Ohrid (the village of Kosel) in the form of sulphatara – fumarola.

All geotectonic units mentioned, starting in the Neocene, developed as continental phase. During the first phase, peneplenisation of structures developed through orogenic processes (end of Paleocene–Oligocene). In the second phase, commencing in the Miocene, a neotectonic phase took place and basic structures seen today as modern relief were formed. Mountainous massifs formed as elements of uplift and depressions formed in areas of relative subsidence.

The neotectonic processes spurred the development of new structures and at the same time reactivated structures formed earlier. Many of the underthrust faults reactivated such as the Drim fault zone, some in the Vardar zone and other places.

Neotectonic regionalization of the Republic of Macedonia took place (Fig. 1). In the western part, morpho-structures of uplift up to 2000 m in size formed. These structures of uplift are blocks elongated with meridian strike. Graben structures were formed with meridian strike as well.

This indicates that during the neotectonic stage the pattern of general uplift was an east–west expansion. The morphostructures in the Vardar zone are characterized by mountainous massif morph structures of uplift of 1000 to 1500 m (500 m lower than those structures in western Macedonia).

In the Vardar zone, depressions were the dominant structures. Skopska I, Ovčepolska II, Tikveška III, are situated above the older structures and consist of complex shapes of 100 to 400 m height. From the intensity of vertical movements, whose impact can be seen in the modern relief, and based on higher order morph structures, it is concluded that the horizontal component of extension is of a different orientation in the zones.

Unlike the Vardar zone, the morphostructures of uplift in eastern Macedonia are present as mountainous massifs 1600 – 1800 m high and the depressions are present as grabens oriented east–west. The main strain is of vertical extension, whereas the axis of extension is of meridian strike.

The neotectonic zones of Western Macedonian, Vardar, and Eastern Macedonia are rather different.

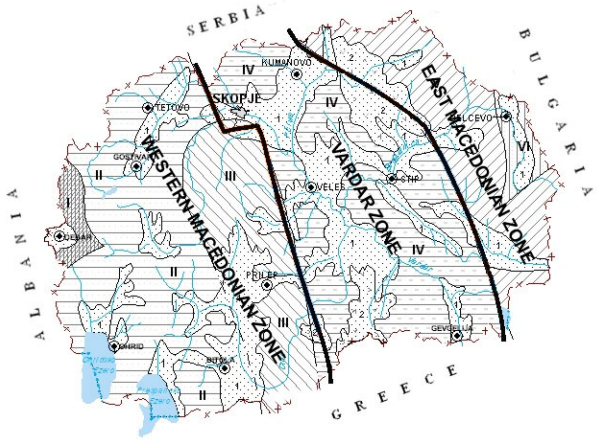

Fig. 1. Neotectonic map of the Republic of Macedonia

NET OF GEOMAGNETIC STATIONS

For complete monitoring of the geomagnetic field of a given space, it is necessary to have a basic network of stations for periodic observations of the field and geomagnetic observatory which permanent measures the weather changes of the geomagnetic field.

For definition of the coefficients of dependence of the geomagnetic field from geographic latitude and longitude of a point to a particular area (usually the state), despite the existence of geomagnetic observatory which is a benchmark point, required is relatively homogeneous network of geomagnetic stations. Performed extensive field studies, allowed defining of the 15 points on the territory of the Republic of Macedonia, which made up the network of geomagnetic repeat stations (Table 1, Figure 2).

The basic network of the repeat stations is used for periodical measurements of that point in the interval of 3 to 5 years. According the relation that follows, for a given epoch (a period of five years) we can calculate the value of any component of the geomagnetic field for a given point that belongs to region (state) that covers geomagnetic observatory with coordinates φ_0 and λ_0.

$$E(\Delta\phi,\Delta\lambda) = a_1 + a_2\Delta\phi + a_3\Delta\lambda + a_4\Delta\phi^2 + \\ + a_5\Delta\lambda^2 + a_6\Delta\phi\Delta\lambda$$

where is:

– $E(\Delta\phi,\Delta\lambda)$ is the value of the normal field at the point with geographic coordinates φ_1 and λ_1;

– φ_1 and λ_1 is geographic latitude and longitude of the point;

– φ_0 and λ_0 is geographic latitude and longitude of the reference point;

– $\Delta\varphi = \varphi_1 - \varphi_0$ is difference of geographic latitude in minutes;

– $\Delta\lambda = \lambda_1 - \lambda_0$ is difference of geographic longitude in minutes;

– a_i is coefficients of the differences in *nT*/minutes, minutes/minutes, or *nT* and minutes.

Table 1

GPS coordinates of the geomagnetic stations

Measured point	Geographic		Altitude
	latitude	Longitude	(m)
1. "Bajlovce"	42° 13' 16"	21° 55' 17"	592
2. "Crna Skala"	41° 59' 41"	22° 47' 28"	833
3. "Gradot Island"	41° 23' 15"	21° 57' 06"	317
4. "Egri"	40° 57' 56"	21° 26' 54"	626
5. "Galičica"	40° 57' 23"	20° 48' 51"	1684
6. "Luke"	42° 20' 39"	22° 16' 29"	1180
7. "Mavrovo"	41° 42' 58"	20° 43' 38"	1418
8. "Nikolić"	41° 15' 54"	22° 44' 36"	300
9. "Plačkovica" – location for geomagneticobservatory	41° 47' 41"	22° 18' 13"	677
10. "Ponikva"	42° 01' 35"	22° 21' 29"	1618
11. "Prilep Lake"	41° 24' 11"	21° 36' 32"	870
12. "St. Marija Precesna"	41° 37' 38"	21° 11' 36"	837
13. "Slivnica"	41° 36' 54"	22° 51' 46"	1252
14. "Tetovo-Želino"	41° 59' 09"	21° 04' 46"	522
15. "Vodno"	41° 58' 40"	21° 24' 57"	569

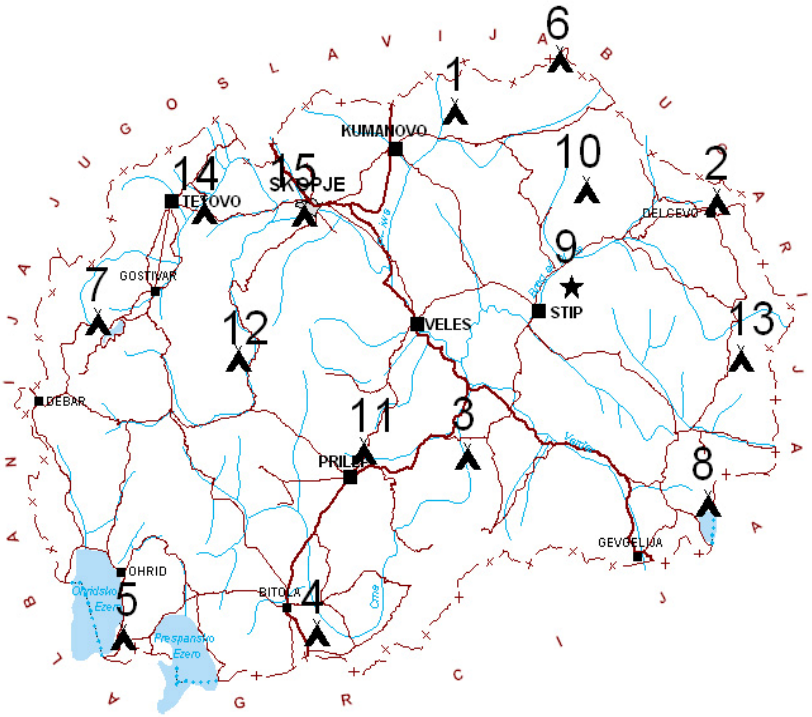

Fig. 2. Map of the geomagnetic stations in Macedonia

Galicica Magnetic Repeat Station Description

Coordinates of the Repeat Station

WGS84 / GPS

Longitude :	20°48’51"	20.8141°
Latitude :	40°57’23"	40.9563°
Altitude :	1684 m	

Hermannskogel / Bessel 1841

Longitude :	20°49’09”	20.8192°
Latitude :	40°57’21”	40.9558°
Altitude :	1635 m	

Location Maps

Yugoslavian topographic map 1:25000 1971
Ljubanista 2-1
190-2-1
Ohrid

Driving and Regional Details

From Ohrid, take the road Southwards to Sveti Naum.

Reaching the village of Trpejca you take left uphill following signs for the national park of Galicica.

After heavy ascending on a sinuous road the climb almost ends with a big turn. You have reached the mountain pass (Fig. 3). There is a parking place on the right side with a small religious monument overlooking over spectacular cliffs the Ohrid Lake and Sveti Naum.

Fig. 3. Access road to geomagnetic station Galicica (J. Rasson, 2004)

Access

Leave the car on the abovementioned parking and start climbing on foot towards uphill on the left side of road (towards NE). You should climb up to a little plateau seen on **Error! Reference source not found.** 3. When you cross an eroded ditch remaining from a previous Balkan trench warfare you have arrived on site.

We plan to drive a pin marker into this rock to locate the station more accurately.

Station Marker

Location: The marker is located on a little plateau. It is on a local maximum in height.

Description: The marker is a big rock firmly seated into ground (**Error! Reference source not found.** 4) and painted yellow. The very station place is the highest part of the rock.

Fig. 4. Photo of measurement point Galicica (J. Rasson, 2004)f

Targets for Declination Measurement

Target description and Azimuth

Meteo Station in Albania: red/white antenna at 275° magnetic

Date of measurement:		8 august 2003
Azimuth:	282.4969°	282°29'49"

Target B description and Azimuth

Meteo Station in Albania: left corner of house at 275° magnetic

Date of measurement:		20 october 2002
Azimuth:	282.4437°	282°26'38"

Target C description and Azimuth

Sveti Naum Church Tower left at 229° magnetic

Date of measurement:		20 october 2002
Azimuth:	232.7148°	232°42'54"

Target D description and Azimuth

Antenna on Albanian Border in color red/white at 300° magnetic.

This target was used in oct 2002 for declination measurement.

Date of measurement: 20 october 2002
Azimuth: 306.6588° 306°39'32"

Target E description and Azimuth

Kalishta Struga Church right of hotel at 320° magnetic

Date of measurement: 20 october 2002
Azimuth: 326.4650° 326°27'54"

Target F description and Azimuth

Minaret Livada North from Struga at 340° magnetic

Date of measurement: 20 october 2002
Azimuth: 347.1383° 347°08'18"

Target G description and Azimuth

Top of Mountain like camel in direction of Prespansko lake

Date of measurement: 20 october 2002
Azimuth: 94.3919° 94°23'31"

Remarks

Magnetic Cleanliness

Survey made in october 2002. To be repeated in 2004

Proton survey with 1 pace separation; 46000nT + … nT

Other

Both Ohrid and Prespa lakes are visible from the station (Figs. 5, 6 and 7,).

Temperature is rather cold in morning, wear warm clothes even in summer.

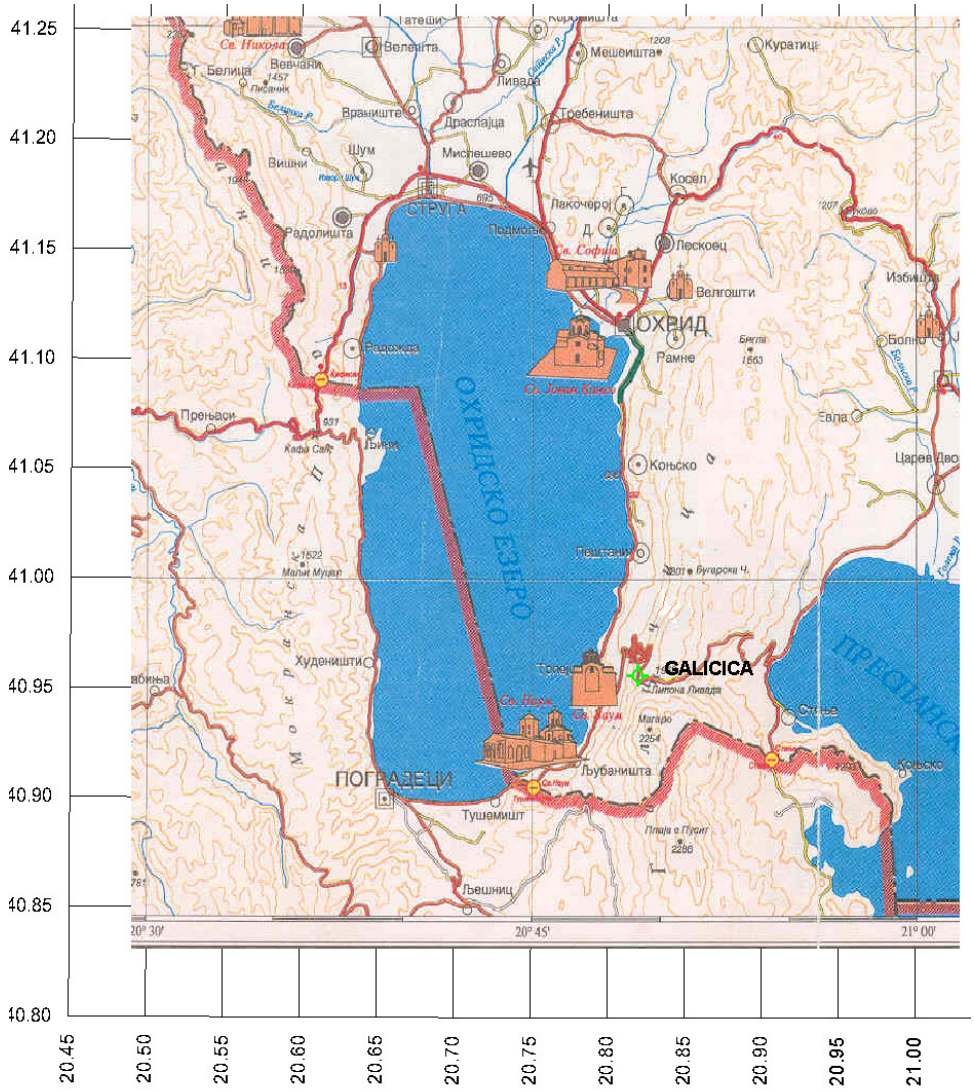

Fig. 5 Part of travel map of Macedonia - point Galicica

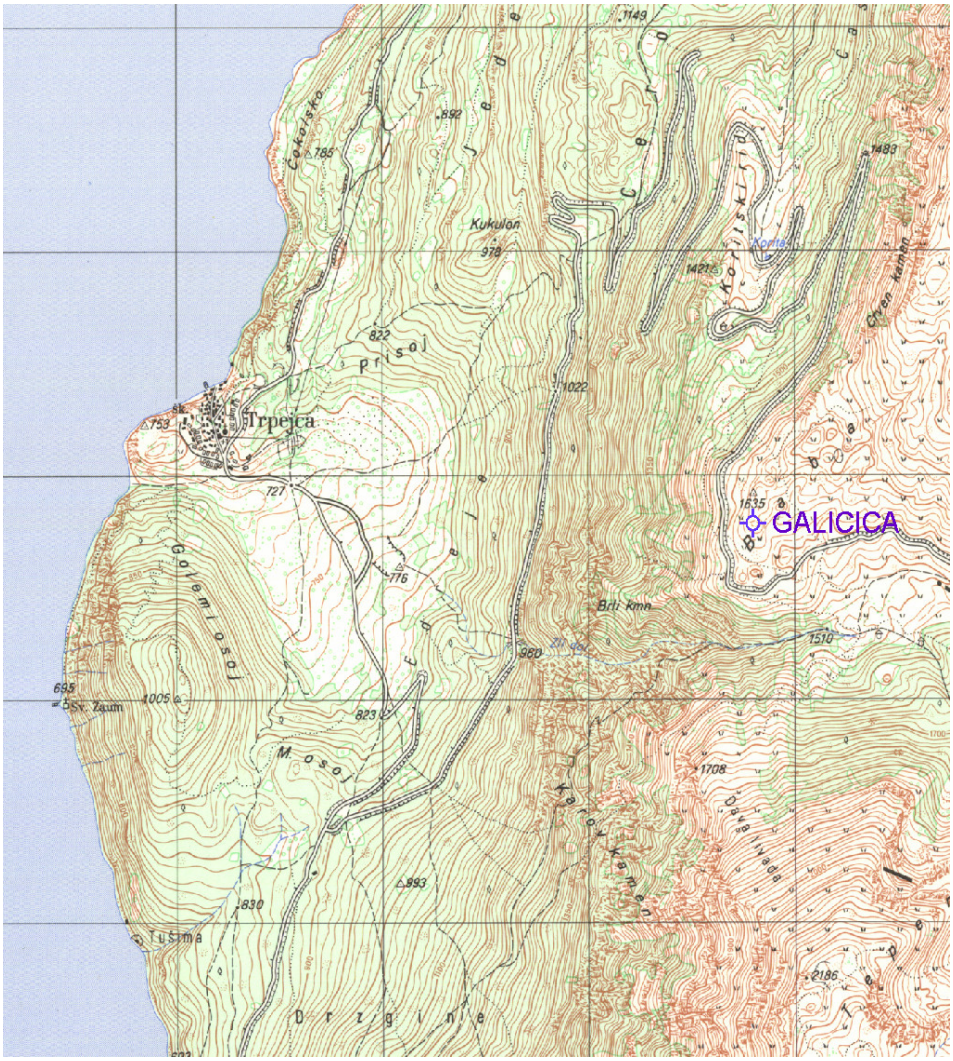

Fig. 6. Topographic map of measurement point Galicica

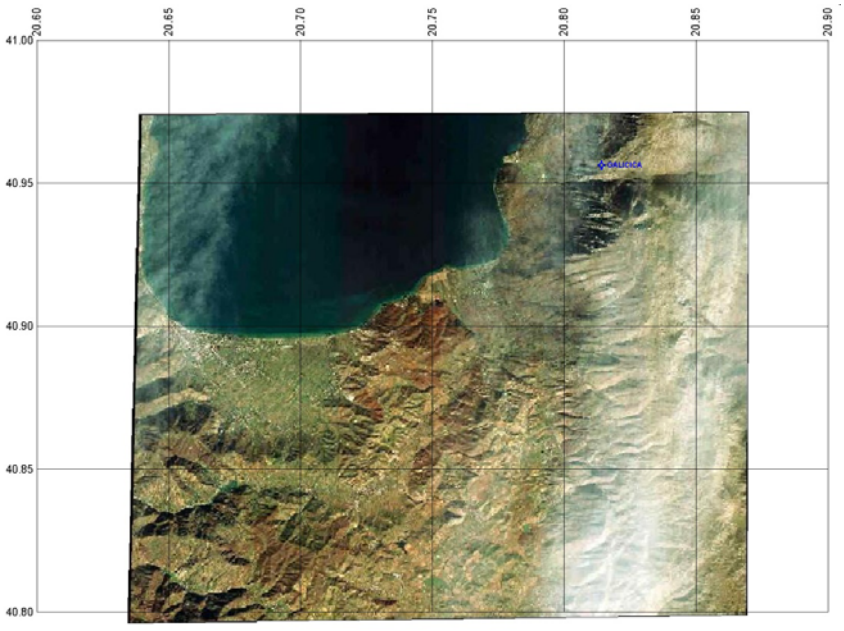

Fig. 7. Satelite photo of the terrain

GEOMAGNETIC MAPS

According the measurements on the established net of the repeat stations in 2004, maps of the magnetic field elements were compiled (Table 2, Fig. 8 – 10).

Table 2

Results from the measurements 2004

Geomagnetic stations 2004.5		Total field T	Inclination I	Declination D
Code	Locality	Mean value		
BAI	Bailovce	46758.4	59.269	2.997
CRN	Crna skala	46920.4	58.883	3.260
EGR	Egri	46430.1	57.765	3.097
GAL	Galicica	46291.2	57.694	2.955
GRA	Ostrovot Gradot	46438.4	58.083	3.576
LKA	Luke	47036.7	59.390	3.337
MVR	Mavrovo	46561.4	58.577	3.058
NIK	Nikolic	46594.8	58.203	3.146
PLC	Plackovica	46679.2	58.619	3.229
PON	Ponikva	46825.7	58.994	2.868
PRP	Prilepsko Ezero	46665.8	58.277	3.101
SLI	Slivnica	46696.9	58.509	3.442
SMP	St. Marija Precesna	46562.2	58.443	3.137
TET	Tetovo	46747.1	58.762	3.186
VOD	Vodno	46740.1	58.787	3.274

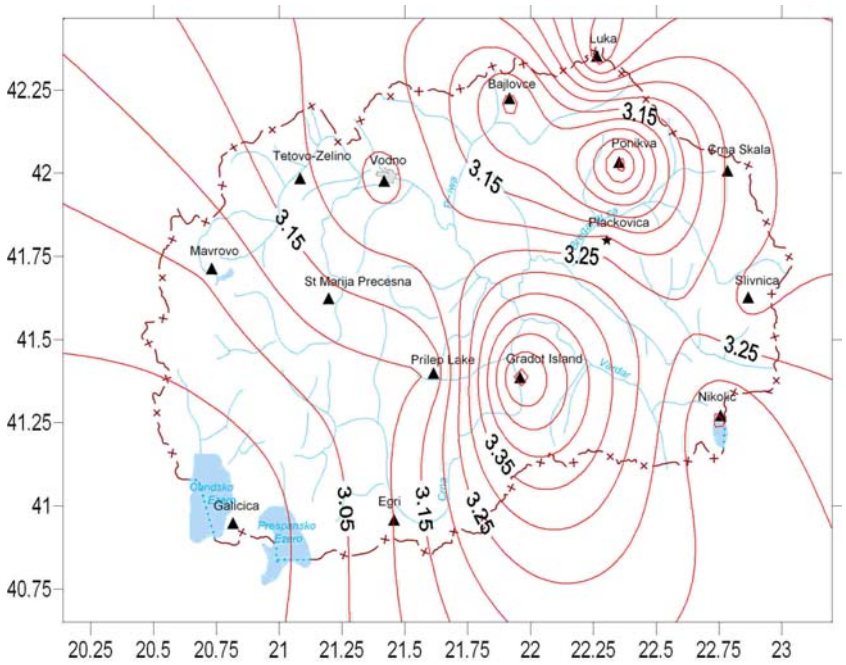

Fig. 8. Map of declination, D for 2004 (M. Delipetrev, 2004)

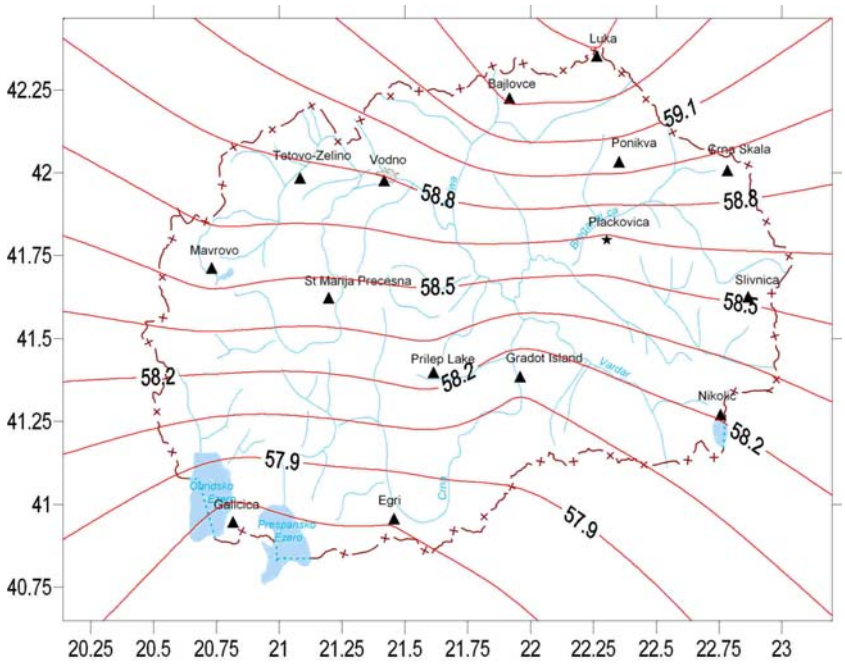

Fig. 9. Map of inclination, I for 2004 (M. Delipetrev, 2004)

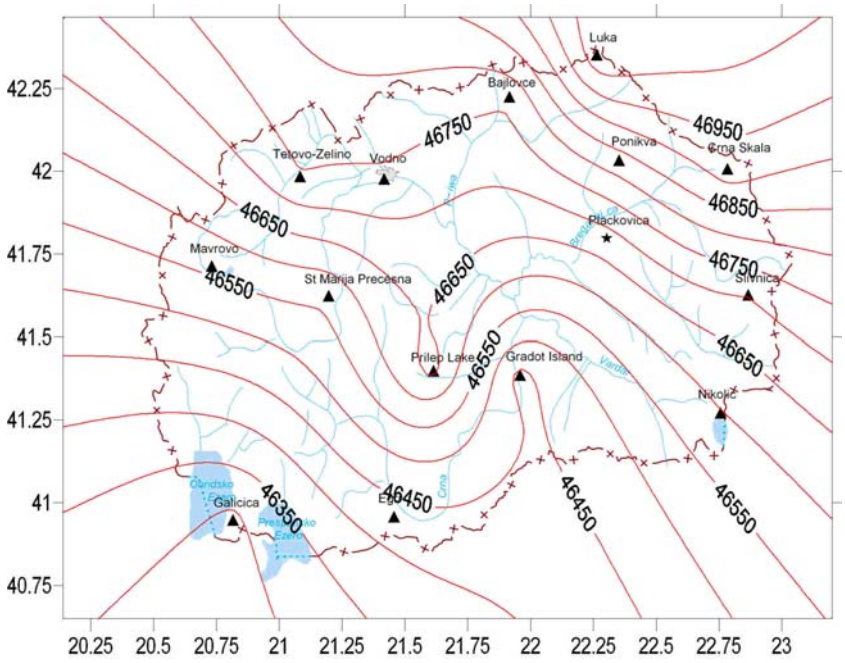

Fig. 10. Map of total field, T for 2004 (M. Delipetrev, 2004)

CONCLUSION

Net of 15 repeat stations satisfy criteria for geomagnetic net of first order;

– Number of measurement points is adequate, bearing in mind the complex relief and the geological structure;

– Elements of the geomagnetic fields of the investigated area vary for:

Total vector	≤ T ≤
Inclination	≤ I ≤
Declination	≤ D ≤

– Geomagnetic field is in good correlation with neotectonic regionalization of the Republic of Macedonia.

REFERENCES

Delipetrov, T., 2003: *Basics of Geophysics*, Faculty of Mining and Geology, Štip, R. Macedonia.

Delipetrov, T., 1996: *Geophysical explorations*, Faculty of Mining and Geology, Štip, R. Macedonia.

Delipetrov, T., 1991: *Correlation between crusts and subcrusts structures on the territory of Macedonia and seismicity*, Doctor thesis, Štip, R. Macedonia.

Delipetrov, T., 2004: Report: *Establishing geomagnetic observatory in the Republic of Macedonia according to INTERMAGNET standards*, Štip, R. Macedonia.

Delipetrov, T., Rasson, J., Duma, G., 2006: *Geomagnetic and electromagnetic measurements and quality standards*, RGF.

GETECH (Geophysical Exploration Technology), December, 1997: *Eastern Europe magnetic project (EEMP) Report 8,* Leeds, United Kingdom.

Rasson, J., 2004, *Macedonian 2003 Magnetic Repeat Station Description*, Internar report.

Slimak S., 1996: *Engineering geophysics*, RGF Belgrade.

Р е з и м е

МРЕЖА НА МЕРНИ СТАНИЦИ И ТЕКТОНСКА РЕОНИЗАЦИЈА НА РЕПУБЛИКА МАКЕДОНИЈА

Марјан Делипетрев[1], Жан Л. Расон[2], Благица Донева[1], Тодор Делипетров[1]

[1]Универзитет „ГоцеДелчев“, Факултет за природни и технички науки, Катедра за геологија и геофизика
ул. ГоцеДелчев 89, МК-2000 Штип, Република Македонија
[2]Кралски метеоролошки институт, Геомагнетна Опсерваторија Дурбс, Белгија
marjan.delipetrev@ugd.edu.mk // blagica.doneva@ugd.edu.mk

Клучни зборови: мерна станица; геомагнетно поле; деклинација; инклинација; тотално поле

Геомагнетното поле е векторски збир на причинители кои се наоѓаат длабоко во земјината внатрешност и нивното влијание може да се почувствува на целата Земја. Постојат изнори на магнетни полиња кои се карактеристични за големи региони и локални аномални геомагнетни полиња.

При избирање на локација за мерна станица, треба да се избегнуваат региони каде има локални геомагнетни аномалии, со цел мерните резултати што ќе се добијат, да бидат карактеристични за тој регион.

Територијата на Република Македонија има комплексен релјеф, а исто така и комплексна геолошка градба и овие особини имаат големо влијание на регионалното геомагнетно поле.

Имајќи ги во предвид сложениот релјеф и комплексната геолошка градба, за секоја избрана мерна станица беше спроведена строга процедура за мерење на геомагнетното поле.

Картите креирани од мерењата во 2004 година се презентирани во овој труд.

Geologica Macedonica, Vol. **24,** No. 1, pp. 23–30 (2010)
GEOME 2 ISSN 0352 – 1206
Manuscript received: March 30, 2010 UDC: 552.54(497)
Accepted: September 28, 2010

Original scientific paper

RANGE OF ENGINEERING-GEOLOGICAL PROPERTIES FOR SOME CARBONATE ROCK COMPLEXES FROM BALKAN PENINSULA

Milorad Jovanovski[1], Azra Špago[2], Igor Peševski[1]

[1]*Faculty of Civil Engineering, "Ss. Cyril and Methodius" University in Skopje, Partizanski odredi 24, MK-1000, Skopje, Republic of Macedonia,*
[2]*Faculty of Civil Engineering, "University Djemal Bijedic", Mostar, Bosnia and Herzegovina,*
jovanovski@gf.ukim.edu.mk // Azra.Krvavac@unmo.ba

A b s t r a c t: The Carbonate Rock masses are a geological media with extremely complex states and properties, which has a certain influences on the mechanical and hydraulic behavior during construction and exploitation of engineering structures. Practical aspects of the problem analysis arise from the fact that the areas of Bosnia and Herzegovina, Macedonia and the entire Balkans is characterized by presence of wide areas covered with carbonate complexes, where large number of complex engineering structures have been, or shall be constructed in the future. In this context, their engineering-geological modeling is still a practical and scientific challenge**.** The analysis of engineering-geological properties is one of the main steps in forming of analytical and geotechnical models for complex rock structures. This article gives a data about the range for these properties, according to the results from an extensive investigation program. Some original correlations and testing results are given and they are compared with some published relations from the world.

Key words: carbonate rock complexes; GSI classification; deformation modulus; strength properties

INTRODUCTION

It is known, that the large areas of the Balkan Peninsula are covered with Carbonate Rock Complexes with different geological ages, genesis, degree of karstification, weathering and fracture properties. Such conditions, beside phenomenology of their event, are also important from the practical point if view. This comes from the fact that such complexes are often foundational media for construction of large infrastructural projects. So, knowing of engineering-geological properties is one of the main prerequisites for successful design of important structures. The authors were involved in several large projects and had an opportunity to be involved directly in different phases of investigation, design or analyses for dams "Sveta Petka", "Kozjak" and others in R. Macedonia, as well as "Salakovac", "Grabovica" and others in Bosnia and Herzegovina. Also, data from several tunnels designed in carbonate complexes are collected and analyzed. So, numerous data about physical, mechanical, structural and other important geological and tectonically data exist and allow preparing adequate scientific analyses.

Between other usual investigation methods, an adequate geotechnical laboratory and field investigations have been applied in order to define the strength, deformability and shear strength of the rock masses. All the results are used to establish a numerous correlations between rock mass quality and mechanical properties, to modify some known classification methods and to improve methodology of geotechnical modeling for carbonate rock mass complexes (Јовановски, 2001; Špargo, 2010).

RANGE OF VALUES FOR INTACT ROCK STRENGTH PROPERTIES

Although intact rock parts characteristics are obtained from the examination of examples on compressive strength and tension, their practical use in solving engineer's problems is limited,

mainly the values of these strengths can be useful parameters that indicate on the quality of rock mass. So it is very often they are used as enter information for classification of rock, or as value for defining some failure criteria.

In order to know interval in which the values of strengths for intact parts of rock mass vary, in this paper we show some results of examination of uniaxial compressive strength σ_{ci} for carbonate rocks from the area in Bosnia and Herzegovina and Republic of Macedonia.

In Table 1 and Table 2, results from testing of uniaxial compressive strength from location of ″Salakovac″ dam on Neretva River, Bosnia and Herzegovina, and ″Sveta Petka″, on Treska River, R. Macedonia are given.

Table 1

Average values of uniaxial compressive strenght σ_{ci} vertical on bedding planes in MPa, samples of limestone for "Salakovac" dam

Condition	Sample					
	1.	2.	3.	4.	5.	6.
Dry	171.5	162.3	152.3	150.6	158.2	153.2
Water logged	164.4	145.4	139.6	135.1	138.3	144.8
Frozen samples	156.4	137.7	127.1	129.2	136.8	143.3

In Table 4. it can be seen that the most frequent values of uniaxial compressive strength for rocks on the location of "Sveta Petka" dam are in diapason from σ_{ci} = 40 – 50 MPa.

These results are under usuall values for carbonate rocks, that can be explained by influence of microscopic deffects made with earlier tectonic influences, although if we look it macroscopicaly, the samples are in fresh state. By parameter of strenght of monoliths, these rocks are medium strong (by Hoek, Brown, 1997).

Beside these results, on Figures 1 and 2, histograms with statistic processed data are presented.

From figures, it can be seen that uniaxial compressive strength of carbonate rock massifs vary in large interval, that can be explained by the influence of crystallization level, decomposition of monolithic parts, strength anisotropy of monolith, different factors of subjective nature etc. Further, results are compared with world's experiences. In this context, with a wider approach, it can be concluded that variations in results are very large, that certainly imply that it is very hard to generalize results from different locations and also indicates of necessity of specific examination for every separate location

Table 2

Values of strenght stress σ_{ci} of intact samples from the location of "Sveta Petka" dam

Nr	Drill hole	Depth (m)	Uniaxial compressive strenght σ_{ci} (MPa)
1	DB-8	21.10–21.30	25.78
2	DB-9	25.2–25.40	35.56
3	DB-9	26.5–27.1	45.05
4	DB-9	27.80–28.00	50.84
5	DB-9	28.5–28.7	64.89
6	DB-9	29.40–29.60	62.76
7	DB-9	30.10–30.30	54.45
8	DB-9	73.10–73.3	32.07
9	DB-10	25.10–25.30	27.26
10	DB-10	23.50–23.80	42.35
11	DB-11	33.70–33.90	33.06
12	DIL-2	25.20–25.40	35.12
13	DIL- 2	26.10–26.30	24.91
14	DIL- 2	32.60–32.80	55.88
15	DIL- 2	37.60–37.80	24.91
16	DIL- 2	38.5–38.7	75.96
17	PS-1	32.20–32.40	54.45
18	PS-2	31.60–31.80	41.33
21	PS-2	69.70–69.90	49.47
22	S-3	28.10–28.30	61.28
23	PS-4	25.40–25.60	41.20
24	PS-5	25.40–25.60	33.09
25	S-6	30.40–30.60	42.71
26	DVZ-1	17.30–17.50	26.59
27	DZ-1	28.20–28.40	44.96
29	DR-3	16.10–16.30	38.07

Table 3

Overview of diapason of variation of values for uniaxial compressive strenght for different types of carbonate rock massifs (Hawkins, 1998)

	Direction of testing	Sample 1 (MPa)	Sample 2 (MPa)	Sample 3 (MPa)	Average (MPa)
Limestone type "Shelly"	Parallel	94	107	115	105
	Vertical	119	139	131	131
	Oblique	109	109	121	113
Crinoids limestone	Parallel	154	157	153	154
	Vertical	169	163	152	161
	Oblique	144	159	179	161
Oolitic limestone	Parallel	118	156	206	179
	Vertical	207	142	156	176
	Oblique	165	141	151	166
Micritic limestone	Parallel	217	225	211	218
	Vertical	222	233	244	233
	Oblique	225	216	235	225
Dolomite	Parallel	227	258	269	251
	Vertical	242	229	248	240
	Oblique	270	259	254	261

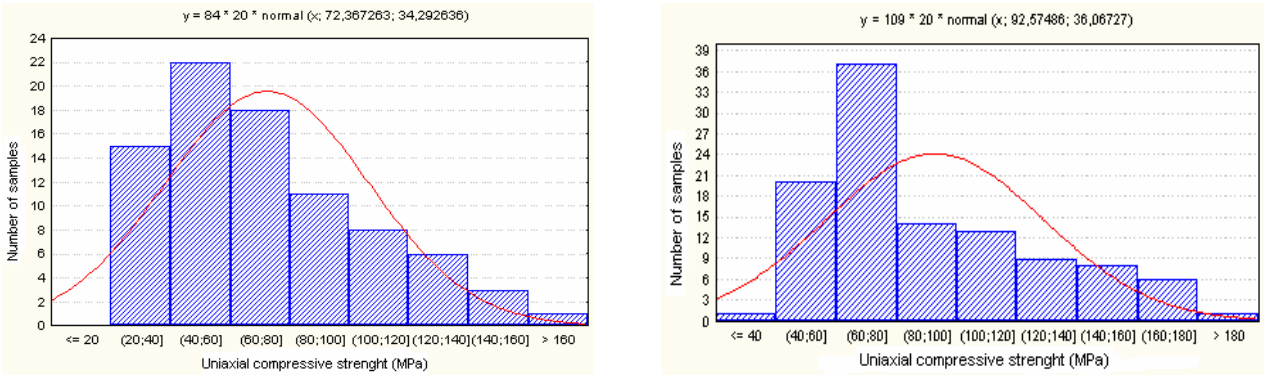

a) b)

Fig 1. a) Histogram of distribution of uniaxial compressive strength of intact parts of carbonate rock massifs;
b) Histogram of distribution of uniaxial compressive strength of monolithic samples from the location of dam "Sveta Petka" (Jovanovski, Krvavac-Špago, Ilijovski, Peševski, 2008)

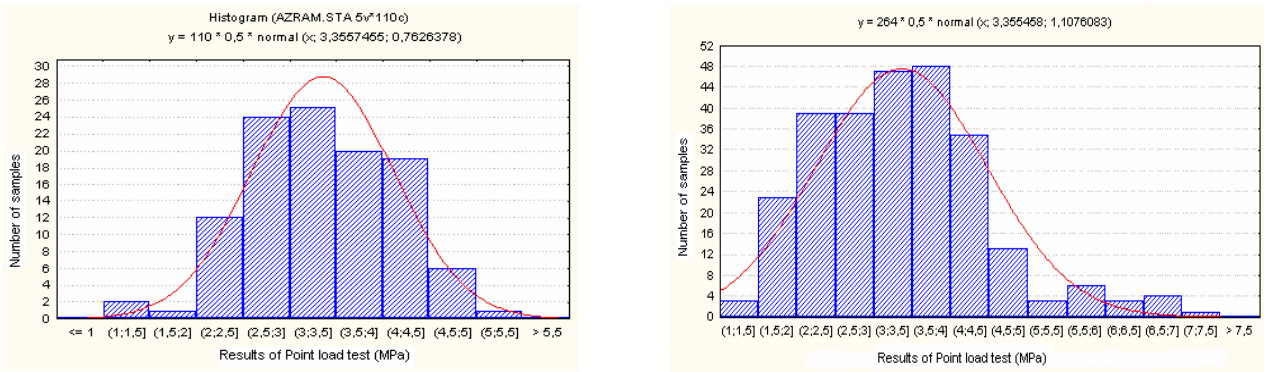

a) b)

Fig. 2. a) Histogram of distribution of results of Point load test of intact parts of carbonate rock massifs;
b) Histogram of distribution of results of Point load test for samples from the location of dam "Sveta Petka" (Jovanovski, Krvavac-Špago, Ilijovski, Peševski, 2008)

In Table 4, some results from tension strength testing on intact samples of rock from the location on "Sveta Petka" dam, by Brazilian method. Values of tension strength vary, where at lower values are considered for weathered rock variations, and higher values on fresh intact parts. On Figure 3 is given histogram with categories of carbonate rock mass by RMR system from R.Macedonia and Bosnia and Herzegovina.

Table 4

Tests results of tension strenght on monolith by Brasillian method for "Sveta Petka" dam

Num.	Drill hole	Depth m	σ_{t1} MPa	σ_{t2} MPa	σ_{t3} MPa
1.	PS–4	28.60 – 28.80	6.76	9.11	–
2.	S–6	25.60 – 25.90	7.06	11.25	9.52
3.	DB–8	22.60 – 22.90	14.39	15.15	7.56
4.	DM–1	18.30 – 18.50	3.43	0.33	6.79
5.	DM–1	25.10 – 25.30	3.95	7.28	6.30
6.	DZ–1	30.40 – 30.60	3.66	–	3.45

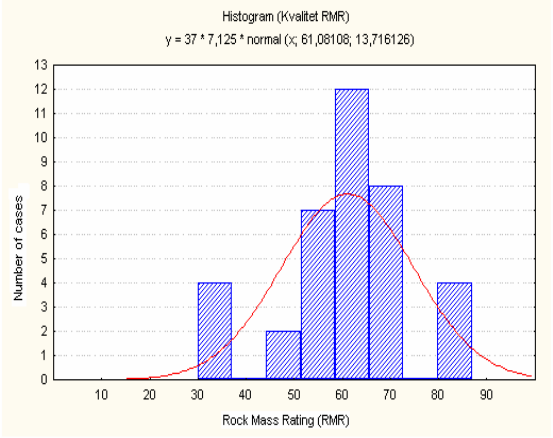

Fig. 3. Histogram with overview of categories of rock mass by RMR system (Jovanovski, Krvavac-Špago, Ilijovski, Peševski, 2008)

CORRELATIONS AND MODELS FOR PREDICTION OF MODULUS OF DEFORMABILITY OF CARBONATE ROCK MASSES

After collecting, testing and statistical analysis of examined samples, numerous correlations between obtained parameters, as well as creation of analytical models for prediction of other important rock mass parameters, are established.

The most simple correlation that can be established is the one that connects the results from the point load test ($Is_{(50)}$ – Index of point load strength for sample diameter d = 50 mm) and the value of uniaxial compressive strength. For the case of marbles from dam "Sveta Petka" the factor of correlation is 16.832, and for limestone of a round area of Ohrid this factor is 39.508.

When compared with known correlation from for various limestone's with values 5–27 for the correlation factor it is obvious that the correlation factors for carbonate rock mass of different geological age, mineral structure, weathered and macro and micro structural characteristics vary in large interval. Variation of results again indicates the need of determining of these correlations for every specific location itself. Also important is the scale effect, with the new knowledge that by increasing the size of examined samples, average value of uniaxial strength actually stays unchanged, and only dispersion of results is decreasing i.e. the variation of uniaxial strength.

Further we show the procedure for making analytical models that are used for prediction of possible intervals of modulus of deformation D, cohesion c and friction angleφ, depending on uniaxial compressive strength of intact elements of rock mass. Models are made using software RocLab. On the Figure 4 are shown several examples of analytical models for prediction of possible interval of modulus of deformation D of carbonate rock mass depending on uniaxial compressive strength of intact part of rock mass σ_{ci} for different values of GSI. The GSI classification strongly depends on the uniaxial compressive strength of intact rock as well as the structure of the rock.

For analysis of modulus of Deformation D software RocLab is used (Hoek, Carranza-Torres and Corkum, 2002):

for $\sigma_{ci} \le 100$ MPa $\rightarrow$

$$E_{rm} = \left(1 - \frac{D}{2}\right)\sqrt{\frac{\sigma_{ci}}{100}}\,10^{\left(\frac{GSI-10}{40}\right)} \text{ MPa}$$

for $\sigma_{ci} > 100$ MPa$\rightarrow$

$$E_{rm} = \left(1 - \frac{D}{2}\right)10^{\left(\frac{GSI-10}{40}\right)} \text{ MPa}$$

The term modulus of deformation is marked as E_{rm} based on English term and not D as it is the usual case in the literature and in our speaking area, and on the other hand to distinguish it from the term for D (disturbance factor). For deformation modulus D double logarithmic (Power) model of regression is formed which in general form is $D = a \times \sigma_{ci}^{\ b}$.

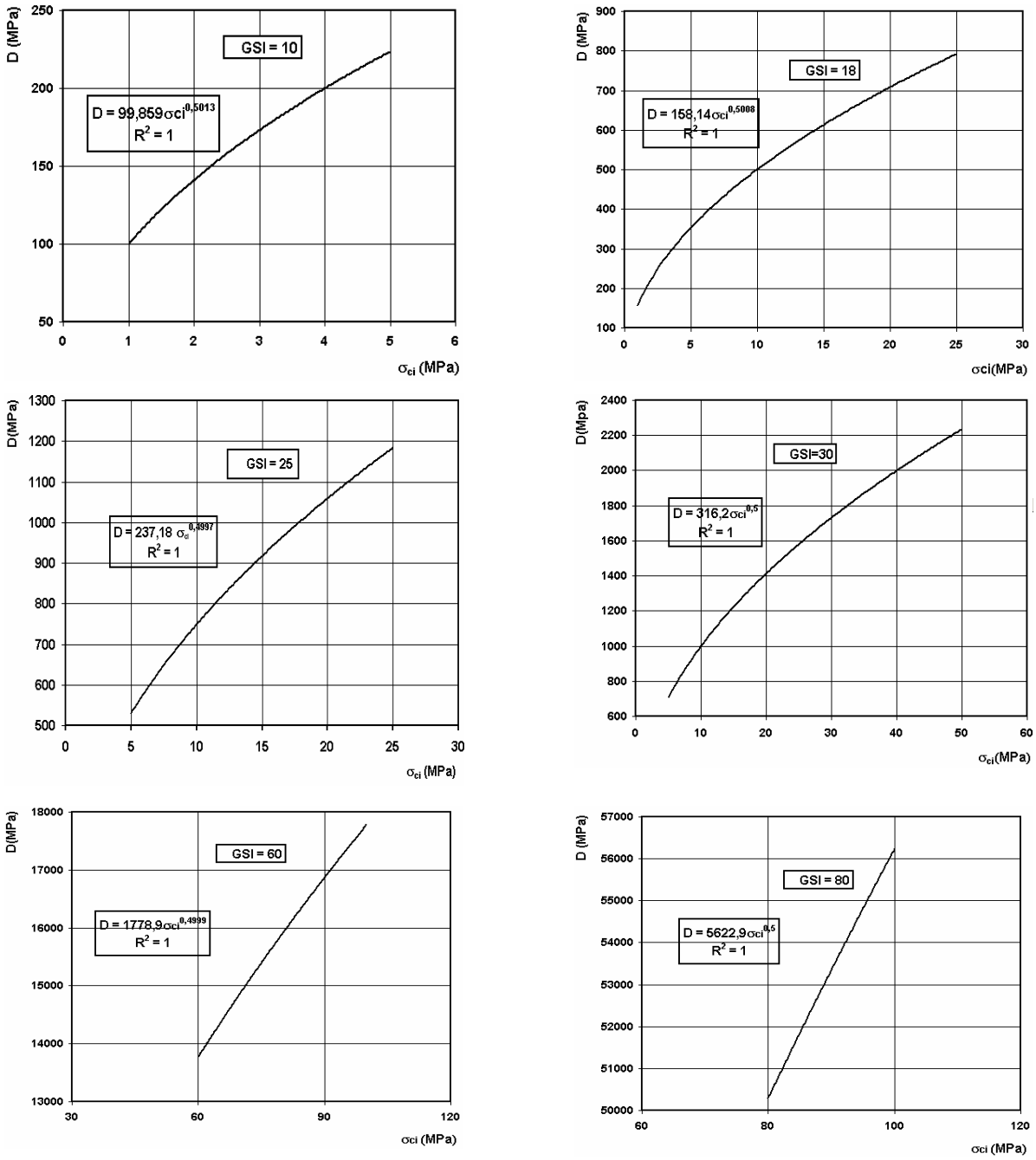

Fig. 4. Analytical models for prediction of possible deformation modulus interval D of carbonate rock mass depending on uniaxial compressive strength of intact part of rock mass σ_{ci} for different values of GSI.

Never version of RocLab software uses term:

$$E_{rm} = E_i \left(0{,}02 + \frac{1 - D/2}{1 + e^{((60+15D-GSI)/11}} \right) \text{MPa}$$

The relation is given by Hoek and Diederichs, 2006, and which require knowing of Deformation modulus of intact parts of rock E_i. On Figure 5 is shown model for prediction of deformation modulus D for solid marbles from location of dam "Sveta Petka".

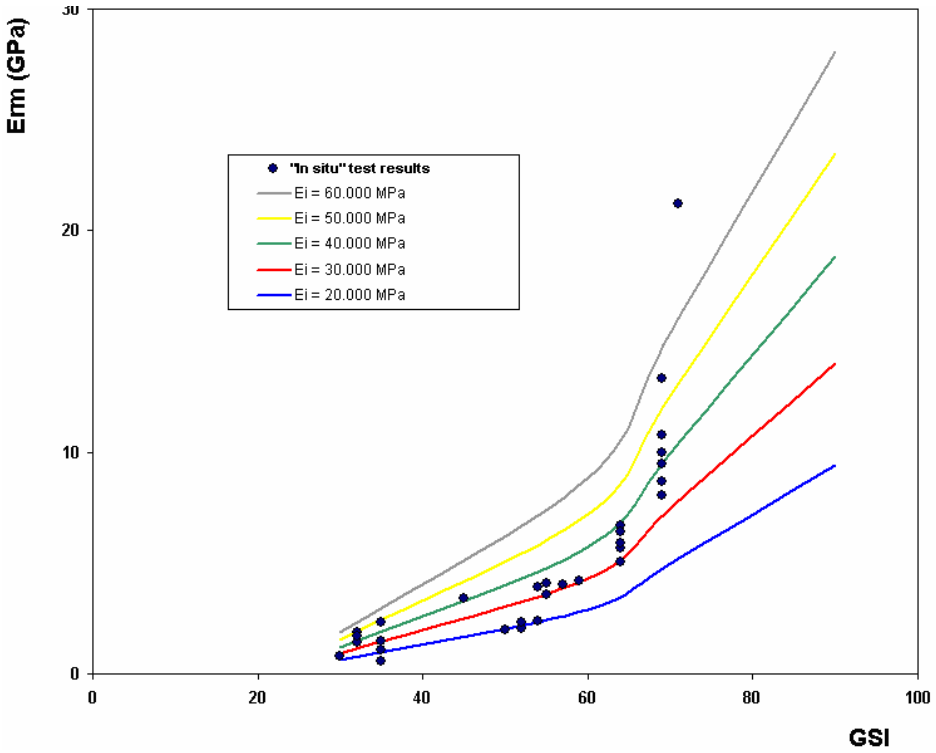

Fig. 5. Comparison of values for rock mass modulus of deformation E_{rm} estimated by Hoek and Diederichs (2006) for deformation modulus of intact parts of rock mass E_i = 20.000 MPa, E_i = 30.000 MPa, E_i = 40.000 MPa, E_i = 50.000 MPa and E_i = 60.000 MPa and disturbance factor D_f = 0, 8 with values of deformation modulus by field investigation through hydraulic flat jack

On monolithic samples taken from different depth of bore hole on the dam location we have got modulus of deformation by lab deformability test. This value of deformation modulus varies in wide interval from 20,000 to 85,000 MPa. So in that way deformation modulus were valued by Hoek and Diederichs, 2006, for values of deformation modulus of intact parts of rock mass E_i = 20,000 MPa, E_i = 30,000 MPa, E_i = 40,000 MPa, E_i = 50,000 MPa and E_i = 60,000 MPa. From the Figure 6, it can be seen that results obtained with *in situ* investigation of deformation modulus with hydraulic flat jack mainly match with those valued by term from Hoek and Diederichs (2006).

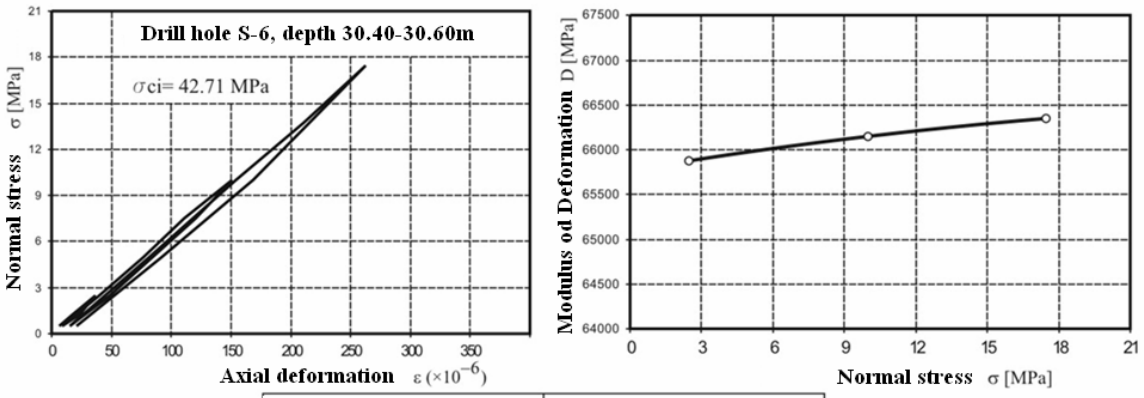

Modulus of deformation D [MPa]		Modulus of elasticity E [MPa]	
I cycle	65869.38	I cycle	70518.98
II cycle	66137.14	II cycle	70041.91
III cycle	66341.10	III cycle	70179.01

Fig. 6. Results of Deformability tests on the samples form dam "Sveta Petka" in three cycled for sample S-6 (a)

In case when we are not able to use values for deformation modulus of intact parts of rock mass E_i or to be able to prepare undisturbed samples for measuring values of E_i, and we do have lab defined values of uniaxial compressive strength of intact parts of rock mass σ_{ci} then we use term:

$$E_i = MR \cdot \sigma_{ci}$$

where MR is relation between deformation modulus of rock mass and modulus of intact rock mass E_{rm}/E_i, which is different depending of the type of the rock.

Model formed by last two terms for carbonate complex of dam "Sveta Petka" is given on Figure 7 (Average value of uniaxial compressive strength σ_{ci} = 44 MPa, disturbance factor D_f = 0.8, which are values for dam "Sveta Petka", value of MR as relation between deformation modulus of rock mass and modulus of intact part of rock mass E_{rm}/E_i = 850 – value for marble) and is showing good overlapping with curve which is gotten by extrapolation of the investigation results on the location of dam "Sveta Petka". The same procedure is done for the cases of dams Grabovica and Salakovac.

From Figure 7 it can be seen, that there exist well correspondence between formed correlative dependences for deformation modulus D and quality of rock mass RMR form location of "Salakovac" dam, "Sveta Petka" dam and correlations given by Jovanovski, Gapkovski, and Ilijoski, 2002. Also curve form the location of "Grabovica" dam is approaching these curves by increasing values of RMR. On the other hand, term gotten by Serrafim and Perreira, 1998, some higher values of deformation modulus D for equal value of RMR. Analytical models formed by term of Hoek, Carranza-Torres, Corkum, 2002, and Hoek and Diederichs, 2006, show well correspondence with curve formed by extrapolation of „in situ“ gotten results on the location for "Sveta Petka" dam.

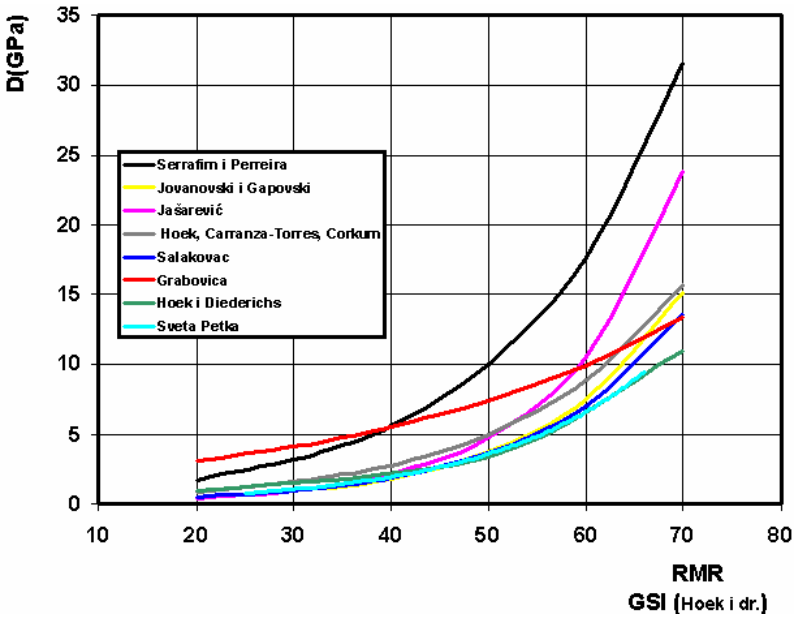

Fig. 7. Comparison of correlative dependences between quality of rock mass RMR (GSI) and deformation modulus D from the location on "Salakovac" dam $D = 0.1369 \times e^{0.0657RMR}$ (GPa), "Grabovica" dam $D = 1.6963xe^{0.0295RMR}$ (GPa) and "Sveta Petka" $D = 0.1104 \times e^{0.0703RMR}$ dam with correlative dependences formed by Jovanovski and Gapovski $D = 1.69^{-6}\ RMR^{3,9}$ (GPa), then Hoek, Carranza-Torres and Corkum (2002) and Hoek and Diederichs (2006) (average value of uniaxial compressive strenght σ_{ci} = 44 MPa, distrubance factor value D_f = 0.8, which are values of the "Sveta Petka" dam, value of MR relation between deformation modulus of rock mass and modulus of intact part of rock mass E_{rm} / E_i = 850 – values for marbles).

CONCLUSIONS

Range of values for strength and deformability parameter of Carbonate rocks are analyzed in this paper. Based on these analyses, some correlations analytical models are formed for obtaining the Modulus of Deformation of carbonate masses through the cases of dam sites "Sveta Petka",

"Salakovac" and "Grabovica". After executed analysis it can be concluded that beside large variations in values, the trend of the correlation curves remains the same for all analyzed cases. However, because of the specific nature of the carbonate rock masses, and the different degree of karstification, folding and fracturing of each location, these analytical models stand only for the subject terrain.

The forming of a universal analytical model is not possible because of these reasons, so given analyses can be used for other structures for lower stages of design, while for larger projects, the adequate testing shall be prepared.

REFERENCES

Hawkins, A. B., 1998: Aspect of rock strength. *Bull Eng Geol Env*, **57 (**17–30), 35–48.

Hoek, E., Brown E. T., 1997: Practical estimates of rock mass strenght. *Intnl. J. Rock Mech & Mining Sci. & Geomechanics,* Abstracts. **34** (8), 1165–1186.

Hoek, E., Carranza-Torres, C., Corkum, B, 2002: Hoek-Brow failure criterion-2002 edition, http://www.rocksciennce.com.

Hoek, E and Diederichs, M.S., 2006: Empirical estimation of rock mass modulus. *International Joural of Rock Mechanics and Mining Sciences*, **43**, 203–215

Јовановски М., 2001: *Прилог кон методологијата на истражување на карпестите маси како работна средина*. Докторска дисертација, Градежен факултет, Скопје.

Jovanovski M., Gapkovski N., Ilijovski Z., 2002: Correlation between Rock Mass Rating and deformability on a profile for arch dam Sveta Petka, *10-th International Conference of the DGKM*, Ohrid.

Јовановски, М., Крвавац-Шпаго, А., Илијовски, З., Пешевски, И., 2008: *Некои зависности за инженерско-геолошките карактеристики на карбонатни карпести маси од Балканскиот полуостров*. Прв конгрес на геолозите на Република Македонија, Охрид.

Serafim, J. L. and Pereira, J. P. 1983: Consideration of the Geomechanics, Classification of Bieniawski. *Proc. Intnl. Symp. Engng. Geol. And Underground Construction.* Lisbon, Portugal, Vol. 1, Part 11, 33-44.

Špago A., 2010: *Methodology of Geotechnical Modeling of the carbonate rock complexes*, Doctoral thesis, Faculty of Civil Engineering, Skopje, 2009.

Р е з и м е

ДИЈАПАЗОН НА ВРЕДНОСТИ НА ИНЖЕНЕРСКО-ГЕОЛОШКИ КАРАКТЕРИСТИКИ НА НЕКОИ КАРБОНАТНИ КАРПЕСТИ КОМПЛЕКСИ ОД БАЛКАНСКИОТ ПОЛУСТРОВ

Милорад Јовановски[1], Азра Шпаго[2], Игор Пешевски[1]

[1]Градежен факултет, Универзитет „Св. Кирил и Методиј“ во Скопје, Партизански одреди 24, МК-1000, Скопје, Република Македонија
[2]Градежен факултет, Универзитет „Џемаил Биједиќ“, Мостар, Република Босна и Херцеговина
jovanovski@gf.ukim.edu.mk // Azra.Krvavac@unmo.ba

Клучни зборови: карбонатни карпи; класификација GSI; модул на деформација; јакостни својства

Карбонатните карпести маси се геолошка средина со екстремно сложени својства и состојби кои имаат и директно влијание врз механичкото и хидрауличкото однесување при изведба и експлоатација на инженерски објекти градени врз нив. Практичните аспекти за анализа на овој проблем произлегуваат од фактот, што големи пространства во Босна и Херцеговина, Македонија и целиот Балкански полуостров се карактеризираат со присуство на вакви комплески, каде се изведени или се планираат за изведба голем број инфраструктурни капитални објекти. Во овој контекст, инженерскогеолошкото моделирање на овие средини е сеуште голем предизвик од научен и практичен аспект. Анализата на инженерско-геолошките својства е еден од најзначајните чекори во припремата на аналитички и геотехнички модели за вака комплексни карпести маси. Така, во овој труд се прикажани одредени дијапазони на варирање на некои инженерско-геолошки својства, а врз основа на резултати од испитување според опширна програма за истражување. Основните аспекти се потенцирани во овој труд, а резултатите можат да послужат како основа за идни анализи. Покрај другото, прикажани се некои оригинални корелации кои се споредени со воспоставени корелации во светот.

GEOME 2
Manuscript received: March 22, 2010
Accepted: September 30, 2010

Geologica Macedonica, Vol. **24** (1), pp. 31–37 (2010)
ISSN 0352 – 1206
UDC: 551.24 : 551.781(497.7)

Original scientific paper

TECTONICS EVOLUTION OF THE PALEOGENE BASINS IN THE REPUBLIC OF MACEDONIA

Goše Petrov[1], Violeta Stojanova[1], Vojo Mirčovski[1], Andrej Šmuc[2], Đorđi Dimov[3]

[1]Faculty of Natural and Technical Sciences, "Goce Delčev" University,
Goce Delčev 89, MK–2000, Štip, Republic of Macedonia
[2]Faculty of Natural and Technical Sciences, Geology Department, University in Ljubljana
Privoz 11, 1000 Ljubljana, Slovenia
[3]Faculty of Computer Sciences, "Goce Delčev" University, ,
Tošo Arsov 14, MK–2000 Štip, Republic of Macedonia
gose.petrov@ugd.edu.mk // violeta.stojanova@ugd.edu.mk

A b s t r a c t: Paleogene sediments on the territory of the Republic of Macedonia are widespread, especially in its central and eastern parts, i.e. in the Vardar zone and Serbo–Macedonian massif (Kraisthide zone). After Laramide orogeny compression, in expansion conditions, along the gravitational faults, continental trenches were created on these spaces, with general direction NW–SE, in which paleogene molassa sediments were accumulated. In the Vardar zone, continental trenches are extended to the north to Skopska Crna Gora mountain (north of Skopje), which includes the Skopje–Kumanovo basin, Ovče Pole basin, Tikveš basin, Gevgelija–Strumica basin and Valandovo basin. In Kraisthide zone continental trenches stretches along the border with Bulgaria and it includes Deve Bair basin and Delčevo basin. Bearing in mind the different thickness of the allocated Paleogene lithozones in the separate basins, and the fact that in some basins lithozones absent, it can be assumed that their spreading along trenches were segmented by cross faults with NE–SW direction. Cross faults are mainly contemporaneous faults.

Key words: Paleogene; molassa sediments; continental trench; contemporaneous fault

INTRODUCTION

After the final closure of the Vardar Ocean and finishing processes of collision with Laramide orogeny phase (Latest Cretaceous–Paleocene), the southern parts of the Balkan Peninsula (the territory of Macedonia, southern Bulgaria, northern Greece and eastern Albania), in the Eocene–Oligocene period, became in the conditions of expansion in the south Balkan extension region (SBER) (Dumurdžanov et al. 2005). This extension system belongs to a much wider area, separated as Aegean extension region (Sengor et al. 2004) (Fig. 1).

Besides the intensive tectonics of Paleogene sediments with Pyrenian orogeny and Savian orogeny compression (folding, faulting and shelling), lithostratigraphy of these sediments is relatively simple. Along the edge parts of the basin, sediments are represented by coarse conglomerates and sandstones, while internal parts are represented by finegranular sediments, marlstone, clay and others. They are transgressive through the older formations, from Precambrian to Mesozoic.

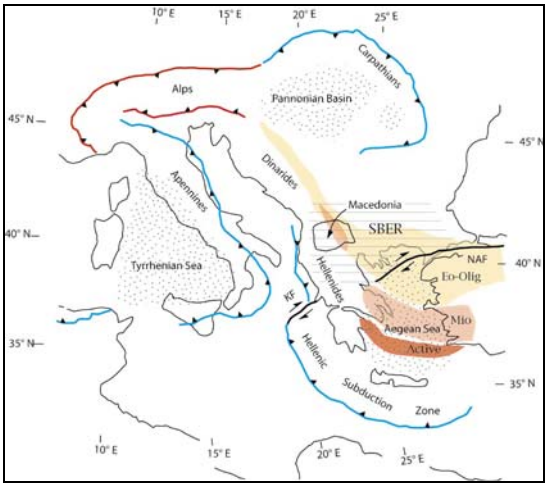

Fig. 1. Simplified tectonic map of the Eastern Mediterranean region showning Southern Balkan Extensional Region (SBER – horizontal lines) in relation to selected tectonic features. In Balkan region, position of the volcanic arcs of Eocene–Oligocene age (Eo-Olig); Miocene (Mio), and Pliocene to Recent (Active); are shown. The location of Macedonia is outlined. KF – Kefalonia fault zone; NAF – North Anadolska fault zone (taken from Dumurdžanov et al. 2005)

In all these basins, Paleogene sediments have been identified as Upper Eocene–Priabonian and Lower Oligocene (Pavlović 1926; Темкова 1958, 1967; Mitrović et al. 1990; Džuranov et al. 1999: Тунева 2000). The total thickness of Paleogene sediments (Upper Eocene–Lower Oligocene) is evaluate at about 3 000–3 500 m.

STRATIGRAPHY OF PALEOGEN IN THE R. MACEDONIA

According to the spatial expansion, Paleogene in R. Macedonia can be divided into 4 main (larger) basins and a few isolated blocks, usually located along the shells with NW-SE orientation. These are: Tikveš, Ovče Pole, Skopje–Kumanovo and Delčevo basin as the main basins and Deve Bair, Dedeli–Rabrovo (near Valandovo) and Ilovica–Štuka in Strumica valley, as isolated blocks (Fig. 2).

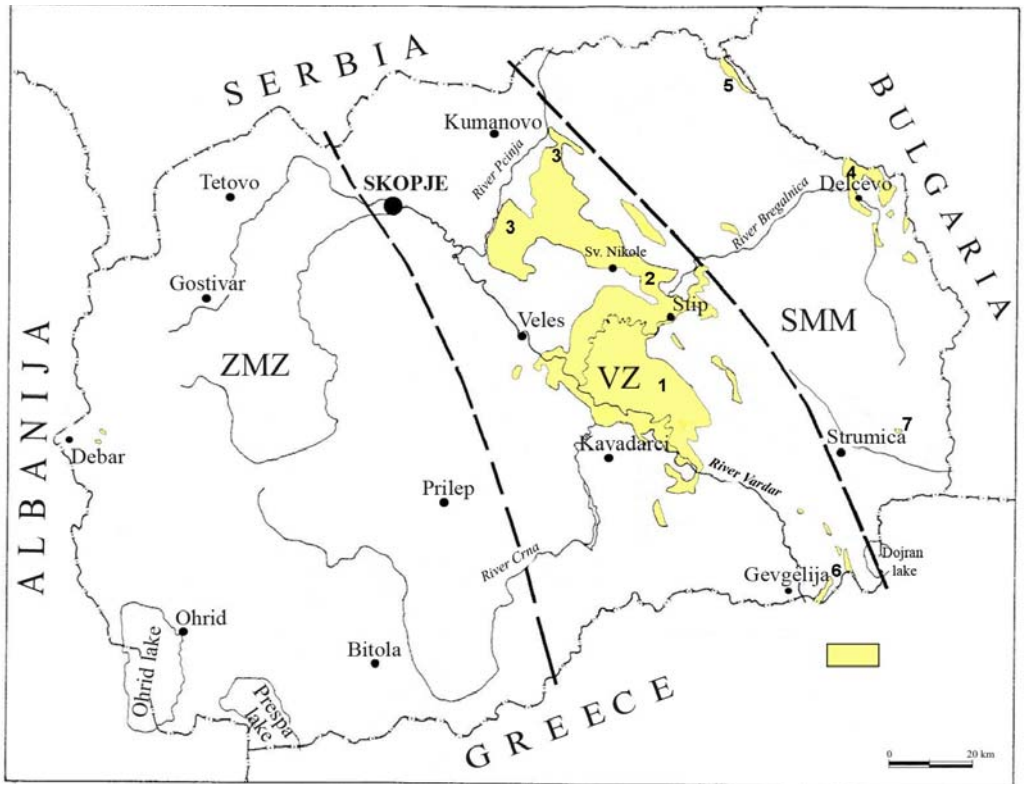

Fig. 2. Distribution of Paleogene sediments in Macedonia
1– Tikveš basin, 2 – Ovče Pole basin, 3 – Skopje–Kumanovo basin, 4 – Delčevo basin, 5 – Valandovo–Gevgelia basin, 6 – Strumica basin, 7– Deve Bair basin

With lithostratigraphical studies to Paleogene sediments in the basins of R. Macedonia, five superpositional lithostratigraphical units (litozones) were separated: basal lithozone, low flysch lithozone, lithozone of yellow sandstones, upper flysch lithozone and Oligocene lithozone (Fig. 3).

Basal lithozone ($^1E_3$) starts with basal conglomerates and sandstones, clay stone and kalkarenits (all in red and purple color) lay above. This zone is presented in all Paleogene basins on the territory of the R. Macedonia. Thickness of this lithozone varies from 350–700 m. Paleontological is documented in the Tikveš basin, with large macrofauna, represented by Molusca and Anthozoa (Maksimović et al. 1954).

Lower flysch lithozone ($^2E_3$) is a thick about 1100 m. It is developed in Tikveš, Ovče Pole and Deve – Bair basin with rhythmically replacement of red and gray conglomerates, sandstones, claystones and marlstone and alevrolites. In Deve Bair basin, in the rhythms of the zone volcanogenetic sediments appear. In the upper stratigraphic levels Priabonian snails, shells, coral and macroforaminifer fauna are determined (Темкова 1958).

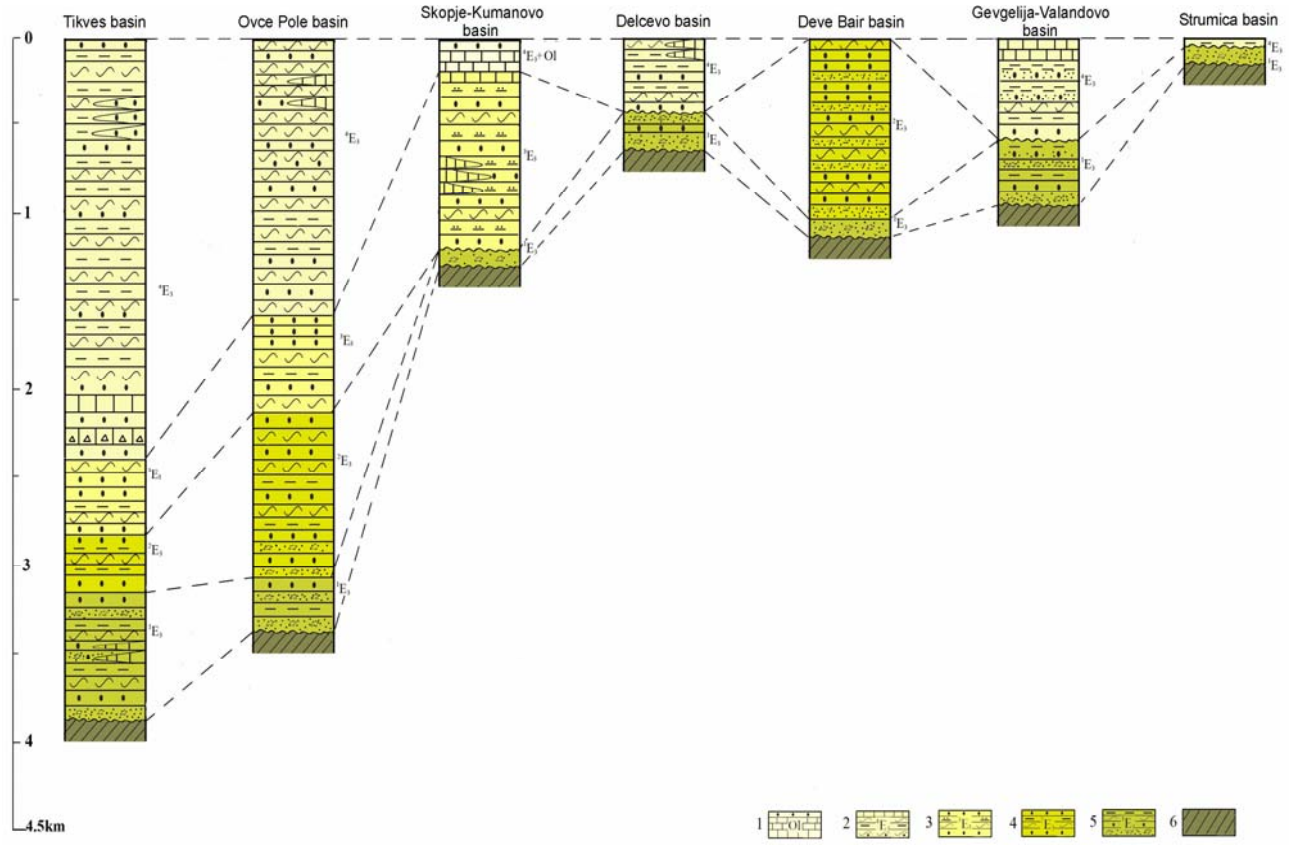

Fig. 3. Correlation of Paleogene basins in the Republic of Macedonia
1 – lower oligocene sediments, 2 – upper flysch lithozone, 3 – lithozone of yellow sandstones, 4 – lower flysch lithozone, 5 – basal lithozone, 6 – paleorelief

Lithozone of yellow sandstones ($^3E_3$) is thick from 600 to 1000 m. It is present in Tikveš and Ovče Pole basin, where vertical and lateral passes in the top flysch lithozone, while in Skopje–Kumanovo basin sediments that belong to this lithozone were moved out into the sediments with Oligocene age. Lithozone of yellow sandstones is determined as Priabonian with large foraminifer fauna, snails, corals, shells and more (Темкова 1967).

Upper flysch lithozone ($^4E_3$) is thick from 1000 – 2000 m. The greatest thickness (about 2000 m) is presented in Tikveš basin (based on data from drilling). Characteristic for this lithozone is its gray color. In the upper flysch lithozone gray sandstone, marls and claystones are present and on the top are limestones, with obvious gradation, convolution and lamination.

All levels of the lithozone are rich in snails, shels and foraminifer fauna, while in the upper limestone layers are determined: *Nummulites fabiani, Nummulites incrassatus, Nummulites budensis, Operculina alpina, Discocyclina angastae* (Maksimović et al. 1954, Ракичевиќ et al. 1976) and microforaminifer fauna of Priabonian age (Džuranov et al. 1999).

Oligocene sediments are preserved with thickness from 200–300 m in some parts of Ovče Pole basin (in the vicinity of Kočani) and in Skopje –Kumanovo basin. This lithozone begins with ridge gray limestones, with typical marine fauna the sandstones are above them and on the top ends with clay stones.

Limestones have typical shallow character. In the lower part they are in breccious, and in the upper part move into corale limestone. The age of limestone is problematic, because despite Oligocene types of Nummulti (*Nummulites intermedius* – typical oligocene kind), Anthozoa, Gasteropoda, Bivalvia and Echinodermata (Karajovanović et al. 1975), in fossil association occur species from Eocene to Oligocene. But according to stratigraphy position, lithologic composition and discovered fauna, the age of these sediments is determined as the lower Oligocene.

TECTONICS EVOLUTION OF PALEOGEN AND DEVELOPMENT OF ACUMULATION BASIN IN THE R. MACEDONIA

In terms of expansion and a general trend of segmentation in the wider region of the Balkan Peninsula, wide areas of the territory of the Republic Macedonia, primarily the area of the Vardar zone and Serbo-Macedonian massif (Kraisthide zone) and border areas with Albania (near Debar), during Upper Eocene were covered with differential vertical movements. Such processes of extension and vertical tectonics conditioned the formation of trenches, along which gradually entering marine waters from the south and southeast to the north and northwest. Today preserved Eocene–Oligocene masses with its geological position, extension and orientation suggest that the formation of trenches was controlled by the gravitational faults with a dominant direction NW–SE. Faults in this direction, often represent reactivated older faults, located in the border, very mobile, parts of the Vardar zone with Pelagonian massif (from west), Serbo-Macedonian massif (eastern side) and the newly formed fault lines in the Vardar zone and Serbo-Macedonian massif of the same orientation (NW–SE).

With the intensive transgression, because of the spreading of the sedimentation basin, sedimentation from the trenches expanded and spread to most of the Vardar zone. Towards north reach the terrains northeast of Skopje, and to the east covered the entire central and eastern Vardar subzone, and most of the Serbo – Macedonian massif (and Kraisthide zone). In that way, very wide sedimentary basin that existed in the Upper Eocene was formed.

The accumulation of Upper Eocene sediments began with continental terrigenous sediments, with red and red–violet color, presented by coarse conglomerates, sandstones and clay stones and thin layers of gray kalkarenites. With the gradual deepening of the area, sedimentation become sea type. Vertical sinking of the terrains was the most expressive in Tikveš basin, where sediments are formed by mass with thickness 3 000–3 500 m and in Ovče Pole basin to 3 000 m (Fig. 3).

Paleogene sedimentary masses from Tikveš, Ovče Pole and Skopje–Kumanovo basin presented, more or less, a whole, in places covered by Neogene or Quarter deposit or divided by a narrow neotectonics horst. The general orientation of this mass is NW–SE, conditioned by postlaramie faults segmentation of the area, with which trenches were formed and after which entering Eocene transgression with accumulation of sediments. Most of these fault structures were renewed in posteocene period, and because of that mass maintaining the same orientation. Small deviations in the extension of mass in the WNW–ESE direction are caused by faults of neotectonic stage.

After the forming of Late Eocene–Oligocene sediment mass, in the Lower Oligocene, it was covered with Pyrenian compression, and at the end of Oligocene and Lower Miocene with Savian compression. During these orogeny phases, intensive folding, faulting and sheathing was made towards the west. As a result, widespread Paleogene mass was segmented in a large number of partially or completely isolated blocks. Compression oriented east–west, conditioned folding of Paleogene sediments in discrete anticline and syncline form, often with an orientation NW–SE to N–S. With this compression, parallel with folding, creation of numerous faults and shells with NW–SE to N–S orientation starts.

RESULTS AND DISCUSSION

More conclusions can be done if analyzing the horizontal distribution of Upper Eocene–Lower Oligocene sediments (separated in 5 superpositional lithozone) in individual sedimentary basins, and analysis of the thickness of individual lithozone. Namely, it was mentioned that basal lithozone ($^1E_3$) is present in all Paleogene basins, suggesting that in this period sedimentation took place in relatively calm tectonic conditions. The thickness of the basal lithozone is the largest in Tikveš and Gevgelija–Valandovo basin, which means that in such a relatively calm tectonic conditions southern part of Paleogene sedimentary basin in the territory of the R. Macedonia sinking faster.

During the deposition of the lower flysch lithozone ($^2E_3$), differentiated vertical movements

in sedimentary basin took place. This lithozone is absent in Skopje–Kumanovo, Delčevo, Gevgelija–Valandovo and Strumica basin, which means that these regions were land in that time. This suggests that in addition to faults with spreading NW–SE (after formation of Paleogene trenches) existed transverse fault lines in NE–SW direction (Fig. 4), after which becomes differentiated vertical rising (or sinking).

In the Vardar zone, lower flysch lithozone has larger thickness in the Ovče Pole basin than in Tikveš basin, and it can be concluded that along the transverse contemporaneous fault, Ovče Pole basin is sinking faster. In border areas of Bulgaria (in Kraisthide zone) in the northern trench (Deve Bair basin) sinking was more intense compared to the southern part (Delčevo basin).

Lithozone of yellow sandstones ($^3E_3$), as the lower flysch lithozone is not continuous in all Paleogene basins. It is absent in Delčevo basin, Gevgelija–Valandovo basin and in Strumica basin. The trench in the Vardar zone has the greatest thickness in the Skopje–Kumanovo basin, and along the transverse fault sinked relatively faster compared to Ovče Pole and Tikveš basins. In the Serbo–Macedonian basin lithozone of yellow sendstones is not present, meaning that these areas were land.

In the final phase of Paleogene sedimentation, at the time of deposition of upper flysch lithozone ($^4E_3$), the Vardar zone and Serbo–Macedonian massif (Kraisthide zone) were under water. The southern parts of Vardar zone (Tikveš and Ovče Pole basin) sinking more intense compared to the northern parts (Skopje–Kumanovo basin). In Kraisthide zone southern of the trench (Delčevo basin) sinking more intense compared to the north, where the upper flysch lithozone is eroded.

In the Lower Oligocene (Ol) sedimentation took place mainly in the northern parts of continental trench along the Vardar zone. In Skopje–Kumanovo basin sinking was most intense, and in the SE terrains relative rising was present.

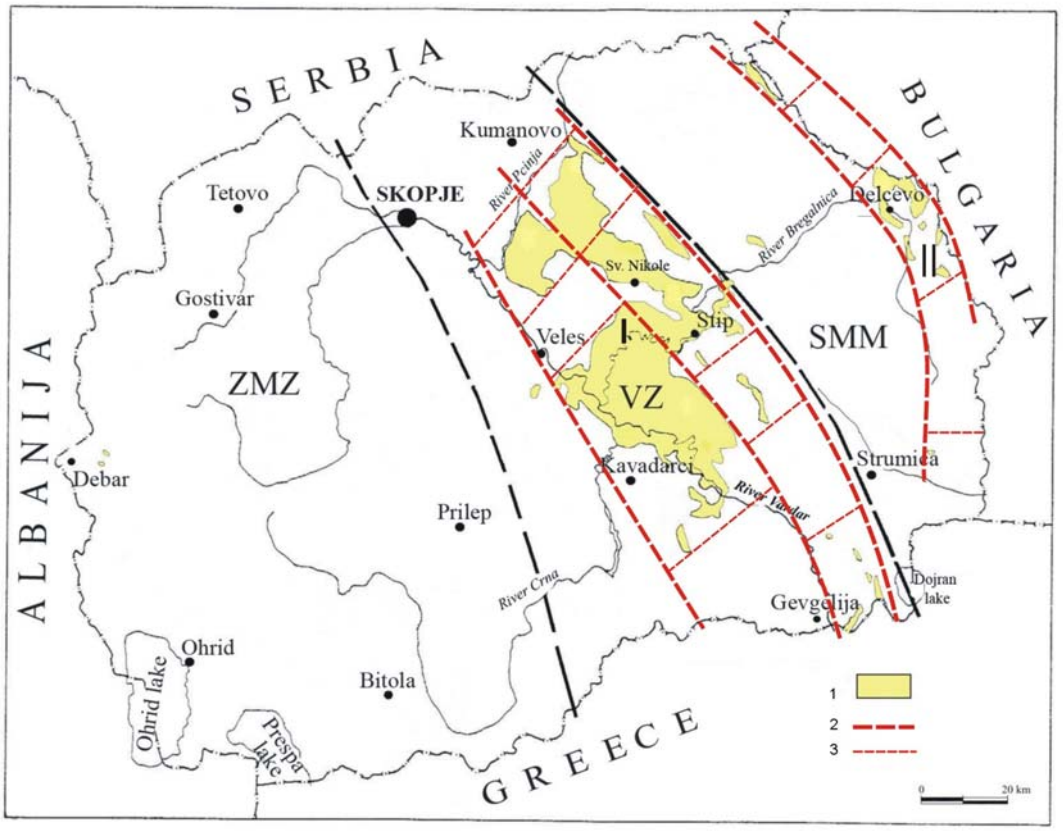

Fig. 4. Simplified tectonic map of the Paleogene in the Republic of Macedonia
Paleogene continental trenches: I – in Vardar zone, II – in Serbo–Macedonian massif (Kraisthide zone); 1 – paleogene sediments, 2 – longitudinal faults, 3 – cross (transverse) faults

CONCLUSION

On the territory of the Republic of Macedonia Paleogene sedimentary basins are present in two continental trenches formed in extension conditions along the gravitational fault lines with direction NW–SE. Continental trench that was formed in Vardar zone, starts north of Skopje–Kumanovo basin. Towards SE structure expands and includes the Ovče Pole basin, Tikveš basin, Gelgelija–Valandovo basin and Strumica basin. In the border belt with Bulgaria, in the Kraisthide zone, relatively narrower continental trench that covered Deve Bair basin and Delčevo basin was formed.

Besides gravitational edge faults, along which the continental trenches were formed, great significance for the course and character of the individual Paleogene sedimentation basins have cross–faults with NE–SW direction. Along these, mainly contemporaneous fault, during the Upper Eocene – Lower Oligocene differentiated vertical movements took place. As a result of such sinking or rising, big differences in thickness of individual lithozone (Fig. 3) appeared. In Tikveš basin and Ovče Pole basin the Paleogene lithostratigraphic columns are complete, while in other Paleogene basins one or two lithozones are missing (lower flysch lithozone and the lithozone of yellow sandstone)

REFERENCES

Arsovski M., Dumurdžanov N., 1995: Alpine tectonic evolution of the Vardar zone and its place in the Balcan region. *Geologica Macedonica*, **9**, 1, 15–22,

Арсовски М., 1997: *Тектоника на Македонија*. Рударско-геолошки факултет, Штип.

Arsovski M., Dumurdžanov N., Petrov G., 1997: *Manifestations of the Alpine orogen phases in the Vardar zone*. Proceeding, Symposium, Dojran.

Dumurdžanov N. et al., 2005: *Cenozoik tectonics of Macedonia and its relation to the South Balkan extensional regime. Soesphere*, Geological Society of America, p. 1–22.

Džuranov S., Tuneva V., Dumurdžanov N., 1999: Microforaminifera findings near the village of Čardaklija in the Ovče pole paleogene basin, Republic of Macedonia. *Geologica Macedonica*, **13**, 57–68.

Јанчевски Ј., 1987: *Класификација на раседните структури по генеза, старост и морфологија со осврт на сеизмичноста на територијата на Македонија*. Докторска дисертација, РГФ, Штип.

Maksimović B., Sikošek B., Marković O., & Veselinović M., 1954: Geološki sastav i tektonska struktura jednog dela Ovčeg Polja i Tikveša sa paleontološkom dokumentacijom. *Trudovi na Geološki Zavod na NRM*, Sv. 4, Skopje, p. 1– 177.

Карајовановиќ М. & Хаџи-Митрова С., 1975: *Толкувач за Основна Геолошка Карта на СФРЈ,* 1:100 000, лист Титов Велес. Геолошки завод. Скопје.

Pavlović P., 1926: Priabonski mekusci sa Ovčeg Polja i Jezevog Brda. *Geol. Anali Balk. Pol*., Kn. VIII, 2, Beograd, p. 231–254.

Петров Г., 2002: *Геодинамика на геотектонските процеси на Вардарската зона со посебен осврт на Алписката орогенеза*. Докторска дисертација, РГФ, Штип.

Петров Г., Стојанова В., Думурџанов Н., Димов Г., 2009: *Корелација на еоценските флишни седименти на Македонија и Словенија и влијанието на регионалното палеогеографско проучување на флишните басени*. Факултет за природни и технички науки, Штип.

Petrović-Mitrović J. et al., 1990: *Paleogene echinoides of Eastern Macedonia*. 13th Congress of the Geologists of Jugoslavia, Kn. 1, p. 369–380.

Ракичевиќ Т., Думурџанов Н., Петковски П., 1976: *Толкувач за Основна геолошка карта на СФРЈ*, 1:100 000, лист Штип. Геолошки завод, Скопје.

Sengor et al. 2004: The North Anatolian Fault. A new look. *Ann. Rev. Earth Planet. Sci*. **33**, 1–75.

Стојанова В., 2008: *Еволуција и стратиграфија на палеогенот на територијата на Република Македонија*. Докторска дисертација, ФРГП, Штип, с. 13–78.

Темкова В., 1958: Палеонтолошка обработка на фауната во Тиквешкиот басен и околината. *Трудови на Геолошки завод на НРМ*, **6**, с. 93–123, Скопје.

Темкова В., 1967: *Палеонтолошка одредба на макрофауната од палеогените седименти на тереноt, лист Штип*. Стручен фонд на Геолошки завод на СРМ, Скопје.

Тунева В., 2000: *Стратиграфија на палеогенот од Овчеполскиот басен според микрофораминиферите*. Магистерка работа. Рударско-геолошки факултет, Штип.

Р е з и м е

ТЕКТОНСКА ЕВОЛУЦИЈА НА ПАЛЕОГЕНИТЕ БАСЕНИ ВО РЕПУБЛИКА МАКЕДОНИЈА

Гоше Петров[1], Виолета Стојанова[1], Војо Мирчовски[1], Андреј Шмуц[2], Ѓорѓи Димов[3]

[1]Универзитет "Гоце Делчев", Факултет за природни и технички науки,
Гоце Делчев 89, МК – 2000 Штип, Република Македонија
[2]Факултет за природни и технички науки, Оддел за геологија, Универзитет во Љубљана
Привоз 11, 1000 Љубљана, Словенија
[3]Универзитет "Гоце Делчев", Факултет за информатика,
Тошо Арсов 14, МК – 2000 Штип, Република Македонија
gose.petrov@ugd.edu.mk // violeta.stojanova@ugd.edu.mk

Клучни зборови: палеоген; моласни седименти; континентален трог; контемпорарен расед.

Палеогените седименти на територијата на Република Македонија се широко распространети, особено во нејзиниот централен и источнен дел, односно во Вардарската зона и Српско-Македонскиот масив (Краиштидната зона). По Ларамиската орогена компресија, во услови на екстензија, на овие простори биле создадени континентални трогови, долж гравитациони раседи со генерален правец на протегање СЗ–ЈИ, во кои се таложеле палеогени моласни седименти.

Во Вардарската зона континенталниот трог на север се простирал до Скопска Црна Гора (северно од Скопје), во кој влегуваат Скопско-Кумановскиот басен, Овчеполскиот басен, Тиквешкиот басен, Гевгелиско-Валандовскиот басен и Струмичкиот басен. Во Краиштидната зона континенталниот трог се протега долж границата со Бугарија и во него влегуваат Девебаирскиот басен и Делчевскиот басен.

Имајќи ја предвид различната дебелина на издвоените палеогени литозони во поедините басени, и фактот што во некои басени некои литозони отсуствуваат, може да се претпостави дека троговите долж нивното протегање биле сегментирани со напречни раседи со протегање СИ–ЈЗ. Напречните раседи главно претставуваат контемпорарни раседи.

Geologica Macedonica, Vol. **24** (1), pp. 39–48 (2010)
ISSN 0352 – 1206
UDC: 553.43(497.7 : 497.11)

GEOME 2
Manuscript received: April 5, 2010
Accepted: September 15, 2010

Original scientific paper

MAJOR ALPINE STRUCTURES AND Cu-PORPHYRY MINERALIZATION IN THE SERBO-MACEDONIAN MASSIF

Todor Serafimovski[1], Goran Tasev[1], Krsto Blažev[1], Aleksandr Volkov[2]

[1]*Institute of geology, Faculty of Natural and Technical Sciences, "Goce Delčev" University, Goce Delčev 89, MK–2000, Štip, Republic of Macedonia,*
[2]*IGEM–Russian Academy of Science, Moscow, Russia*
todor.serafimovski@ugd.edu.mk

A b s t r a c t: The geodynamic evolution of the Serbo-Macedonian massif can be reviewed in few geological and geotectonic epochs, but very specific is the Cenozoic evolution from geodynamic, geotectonic, structural, magmatism and metallogenetic point of view. The Cenozoic longitudinal structures are deep in their origin and represent a boundary to the Vardar Zone on the one side and Struma Zone on the other side. Morphostructural forms of different rank and intensity are of high importance for the spatial distribution of the ore mineralization (Kratovo-Zletovo Pb-Zn-Cu ore district, Bucim-Damjan Cu-Au-Fe ore district, Bukovik-Kadiica Cu-Au-Ag-Fe ore system etc.). Predominant structures within the Serbo-Macedonian massif are those with NW-SE direction, which served as orebearing systems too (ore zone Besna Kobila-Osogovo-Tasos and metallogenetic zone Lece-Chalkidiki).

Key words: Serbo-Macedonian massif; morphostructures; Cenozoic activization; polymetallic mineralizations; ore systems

INTRODUCTION

Serbo-Macedonian massif (SMM) represents remarkable geotectonic unitwithin central parts of the Balkan Peninsula (Dimitrijević, 1958) where have been confirmed numerous structures, morphostructures and significant ore mineralizations (Janković and Petković, 1974; Janković et al. 1980; Serafimovski, 1990). From the geological point of view the SMM has been built mainly of gneisses, mica-schists and Paleozoic schists, while the structural construction has been dominated by plicative structures and disjunctive ruptures. Tertiary magmatism, intruded along Cenozoic structures (Arsovski and Ivanov, 1977; Serafimovski, 1990, 1993), has been related to the polymetallic mineralization of Pb, Zn, Cu, Au, Ag, AS, Sb etc. (Serafimovski et al. 1995; Janković and Serafimovski, 1997 etc.). Significant morphostructural forms in the central parts of the SMM have been related to the productive mineralizations of Cu-Pb-Zn (Plavica type), Cu-Au (Borov Dol type) and Cu ± Au ± Ag ± Mo (Bukovik-Kadiica type). Neotoectonic structures are of SW-NE to E-W direction and within this area they are not related to the mineralization, but they are just seismically active.

REGIONAL GEODYNAMIC EVOLUTION OF THE AREA OF CONSIDERATION

From Paleogene to Recent time, Macedonia was part of the South Balkan exten-sional region, the northern part of the Aegean extensional regime. Extension began in the middle to late Eocene in eastern Macedonia with the formation of a NNW-trending east-tilted half graben lying east of a forearc basin in central Macedonia.

The tectonics of Macedonia from the late Eocene to the present is dominated by two periods of regional extension separated by a short interval of shortening deformation in late Oligocene–early Miocene time. Extensional deformation in Macedonia is part of the broader South Balkan extensional regime that in addition to Macedonia affects northern Greece, Bulgaria, Albania, Serbia, Montenegro, and probably parts of southwestern Romania (Fig. 1; Dumurdžanov et al. 2005).

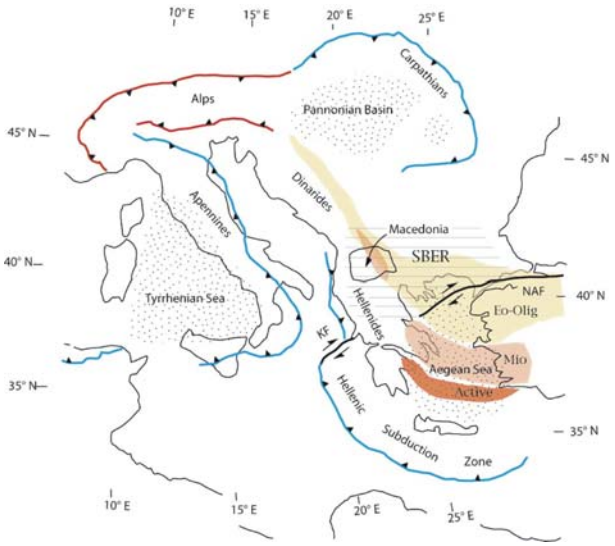

Fig. 1. Simplified tectonic map of Eastern Mediterranean region showing Southern Balkan Extensional Region (SBER; horizontal lines) in relation to selected tectonic features (Dumurdžanov et al. 2005).
Retreating subduction zones (blue) and related areas of backarc extension (dotted pattern) and advancing subduction zones (red) are highlighted. In Balkan region, position of the volcanic arcs of Eocene-Oligocene age (Eo-Olig: yellow), Miocene (Mio: pink), and Pliocene to Recent (Active: red-brown) are shown. The location of Macedonia is outlined. KF – Kefalonia fault zone; NAF – North Anatolian fault zone

Development of the extensional system was diachronous throughout the South Balkans and was related not only to changes at the boundaries of the extensional system, but also to changes in lithospheric rheology. This paper develops the late Eocene to Recent tectonic evolution of Macedonia and relates it to our evolving understanding of the regional South Balkan extensional regime.

Most of the understanding of the tectonic evolution of Macedonia comes from the study of the numerous Cenozoic sedimentary basins that contain the record of its extensional history. Unfortunately, the deeper parts of many of the sedimentary basins of Macedonia are poorly exposed and covered by Quaternary deposits. Thus, much of the data from these basins come from drill holes and limited surface exposures, and the three-dimensional framework of these basins is poorly known.

The crust that underlies the Cenozoic basins of Macedonia has had a long and complicated evolution, and structures within the pre-Cenozoic basement rocks have affected the development of some of the basins. Macedonian pre-Cenozoic basement consists of five major tectonic units from west to east: the Chukali-Krasta zone, the Western Macedonian zone, the Pelagonian massif, the Vardar zone, and the Serbo-Macedonian massif.

The Serbo-Macedonian massif (SMM) consists of Riphean/Cambrian mafic plutonic and volcanic rocks and early Paleozoic schist and phyllite all intruded by large bodies of Paleozoic granite. With the exception of the north-plunging nose of the Pelagonian anticlinorium, the structures in the pre-Cenozoic basement rocks are dominated by NW-trending foliation, folds and faults that form an important crustal anisotropy that controlled many of the basin bounding faults in Cenozoic time.

CENOZOIC STRUCTURES AND MORPHOSTRUCTURES

The detailed scientific studies and morphostructural analysis have enabled us to understand the processes which preceded the formation of the zone of Cenozoic activation. Contribution to the more complete understanding of the Cenozoic activization and definition of real longitudinal structures and large morphostructural segments at the Balkan Peninsula was in given in workings of Janković and Petković (1974); Petković (1978); Kocneva et al. (1978), Janković et al. (1979); Serafimovski (1993); Janković and Serafimovski (1997); Serafimovski et al. (1997); Serafimovski and Jelenković (1998); Tomson et al. (1998); Tomson et al. (2004); Burchfiel et al. (2008.).

The zone of Cenozoic autonomous activation of the Balkan Peninsula is characterized by a specific structural plan, multiphase volcanic-intrusive magmatism and interesting mineral deposits.

Striking transcurrent faults can be recognized from air and satellite pictures, striking in the same direction as the zone of activation, as well as systems of smaller parallel faults, systems of diagonal jagged faults and systems of straight, tension faults. A special characteristic of the zone of autonomous activation is its many ringlike structure. These megastructures correspond to broad, gentle arches, are elliptical or circular in shape and have a diameter of 60 to 100 km (Petković et al. 1982). Their internal structure features a wealth of forms. They are built of concentric ringlike segments, and sometimes have the appearance of a coil. Central parts are usually raised, while the other rings are alternately lowered and raised. The

radially arranged faults separate internal parts of the megastructure into sector blocks. These structures are contoured along the periphery by depressions which are either bow-shaped or oval-shaped. Within the megastructure there are numerous smaller ringlike forms ranging from several hundred meters to a few kilometers in diameter (Fig. 2).

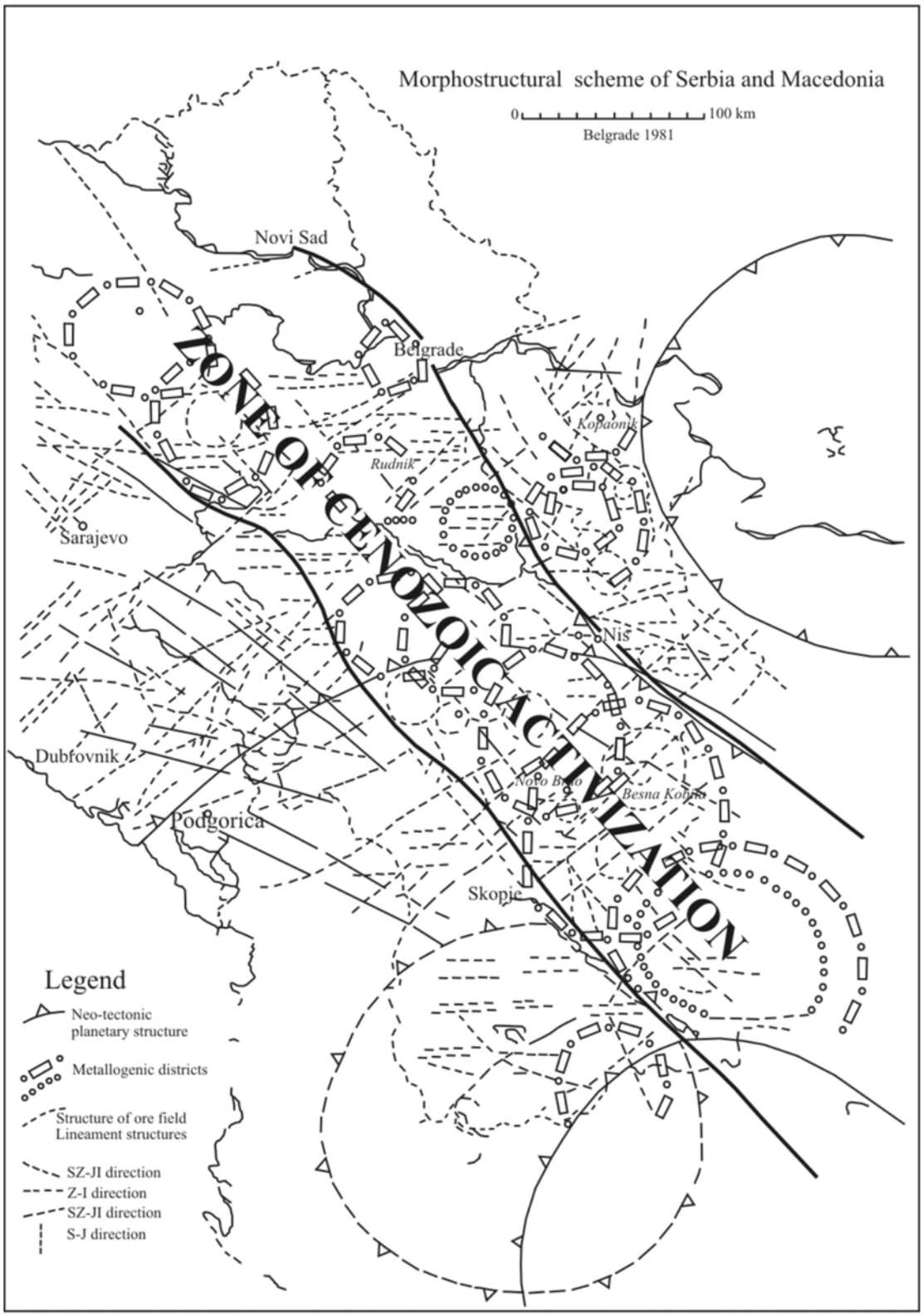

Fig. 2. Morphostructural sketch of Serbia and Macedonia (Petković et al. 1982)

The first signs of magmatic activity in the zone of Tertiary autonomous activation had already occurred at the end of the Eocene, but it is still not clear what connection they have with this zone. The magmatism culminated in the Miocene, while it gradually calmed down in the Pliocene, occasionally extending into the Quaternary. The magmatic rocks correspond to the volcanic-intrusive granodiorite complexes chemically they belong to the Ca-alkali rocks and in later phases are rich in potassium. Besides dacite-andesites, we also find trachyandesites, quartz-latites, latites, trachybasalts, trachytes and subordinate leucite roks (lamprophyric facies). The rocks are accompanied by pyroclastics, agglomerates and breccia. Tuffs are extremely rare. Intrusives of quartzdiorite, granodiorite and quartzmonconites are, in principle, synchronous with analogous volcanic rocks. Magmatic rocks are consolidated at the subvolcanic-volcanic level, in the process of which plutons are formed as "high plutons". According to more recent ideas, granites in the zone of autonomous activation were formed by metasomatic transformation of granodioritic plutons.

There are numerous and varied mineral deposits in the zone of Cenozoic autonomous activation. Interesting occurrences of tin and niobic tantalum are the only ones genetically linked with the granites (Cer, Bukulja). All the other endogenous deposits are paragenetically linked with the volcanic-intrusive complexes of granodioritic magma. The magnetite deposits (Suva ruda type) magnetite and hematite (Damjan type) – belong to typical metasomatic scarns. The copper deposits are either porphyric (Bucim) or vein-impregnation (Zlatica, Plavica). The molybdenum deposits are stockwork impregnated (Mackatica). The lead and zinc deposits are of scarn type (Rudnik), hydrothermal-metasomatic (Sasa, Toranica) or vein type (Zletovo). The antimony deposits are usually monomineral (Krstov Dol), but there are also transitions to lead-antimony, arsenic-antimony deposits.

Logical metallogenic analysis was made possible for the first time by the distinguishing of the megastructures in the Tertiary autonomous activation zone. Thus the megastructures correspond to the ore districts and coincide with the centres ofmagmatic activity, while the distribution of mineral deposits in them is found to be distinctly laterally zoned. The lesser ringlike structures correspond to the structure of the ore fileds or mineral deposits, as we are showing that later on the Bukovik-Kadiica polymetallic ore system.

SOME MORPHOSTRUCTURES RELATED TO THE CENTRAL PART OF THE SERBO-MACEDONIA MASSIF

From the general point of view the Macedonian territory have passed through the detailed geological evolution. One part of the territory of the Macedonia belongs to the SMM and Pelagonian massif as old crystaline complexes. These two complexes are divided by the riftogene Vardar zone, which has been represented by ophiolite melange and Jurassic and Cretaceous molasse sediments. Within the SMM dominate Precambrian, Riphean-Cambrian and Paleozoic rocks.

The Cenozoic tectono-magmatic activizitation happened in the eastern parts of Macedonia and has been manifested by deposited structural elements in the existing relief and occurrence of volcanogene-intrusive magmatic complexes in conditions of disseminated spreading. In frame of the newly formed structures dominate fissure zones of lineament type, riftogene zones with emphasized concentric structures of different sizes etc (Fig. 3).

Serbo-Macedonian massif as a remarkable geotectonic unit has been built of two structural-lithological complexes or more precisely two metamorphic complexes (upper and lower). Lower metamorphic complex is represented by highly metamorphic rocks such as gneiss, amphibolites followed by quartzites, marbles and migmatites. Upper metamorphic complex is lying trangresivelly over the lower complex. It is repreented by greenschist facies, where dominate chlorite, chlorite-sericite, chlorite-amphibolite and graphite schists and quartzites. These complexes were intruded by different types of granitoide intrusions during the Baikal, Caledonian, Herzinian and Alpine cycle. Metamorphic rocks represented as complex forma and cumulates have direction NW-SE and sometimes are forming submeridian flexures.

Cenozoic activization at the territory of the Republic of Macedonia enclosed the most complex geotectonic units such as Vardar zone and SMM. Its occurrence is mainly along fissures of general NW-SE direction and activated meridian cracking zones and faulting systems of general NE-SW direction. In a such conditions came to complete re-

distribution of the lineament structures network when on the main direction of Mesozoic structures NW-SE (340°) occurred fault system of the same direction but slightly different angle (320°). Later ones determined the structural plan of the area of the Cenozoic activization. The results from the satellite images and morphostructural analysis of modern relief allowed determination of three zones of similar direction, mainly NW-SE (Fig. 4).

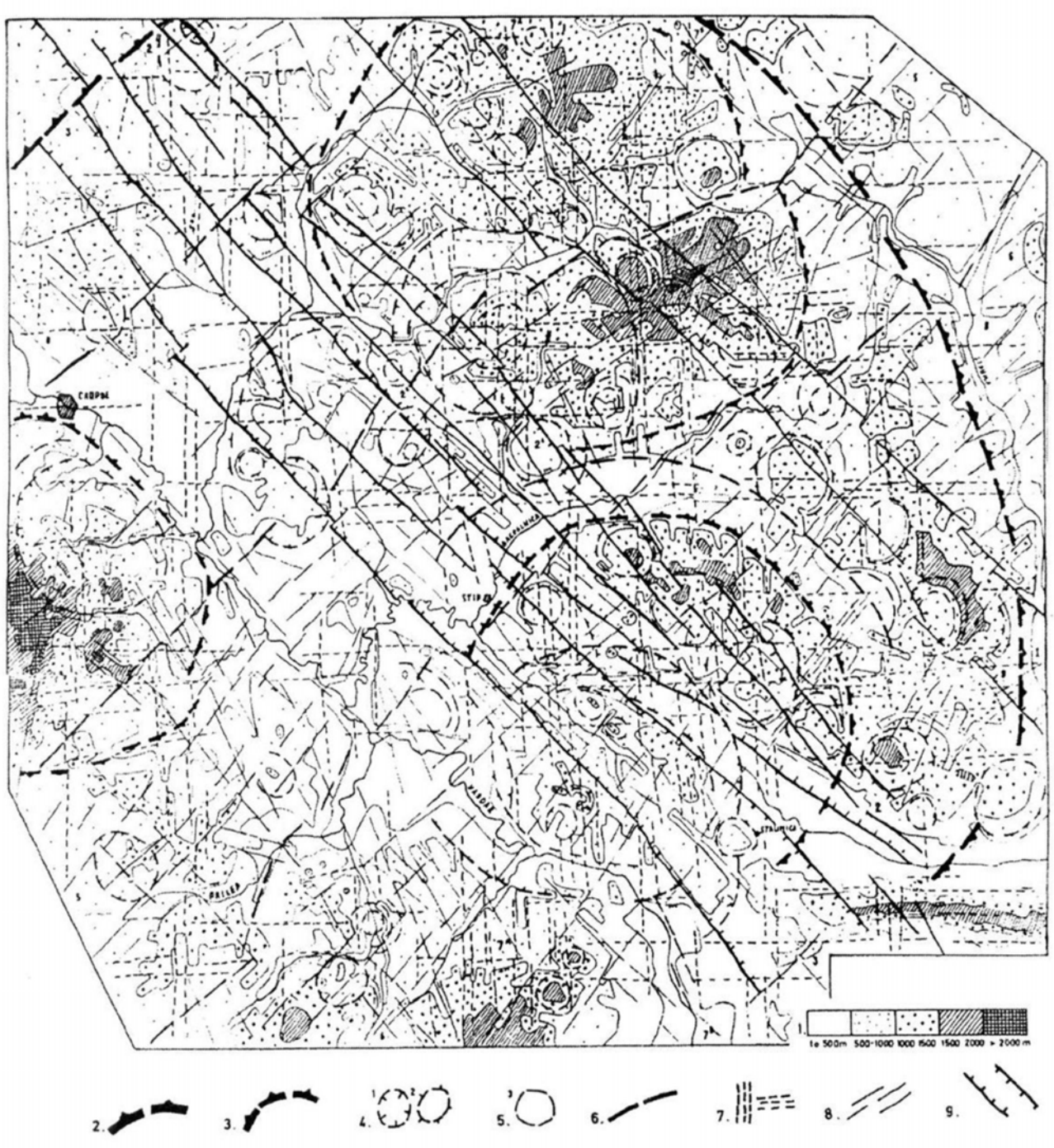

Fig. 3. Morphostructural scheme of the Eastern Macedonia
1) Height peak, 2) Boundary of Macedonian dome, 3) Boundary of local dome, 4) Boundary of concentric structures, 5) Occurences of structures by satellite images, 6) Faults, 7) Faults zone systems of ortogonal strike, 8) Zones of oblique cuts of N-W strike.

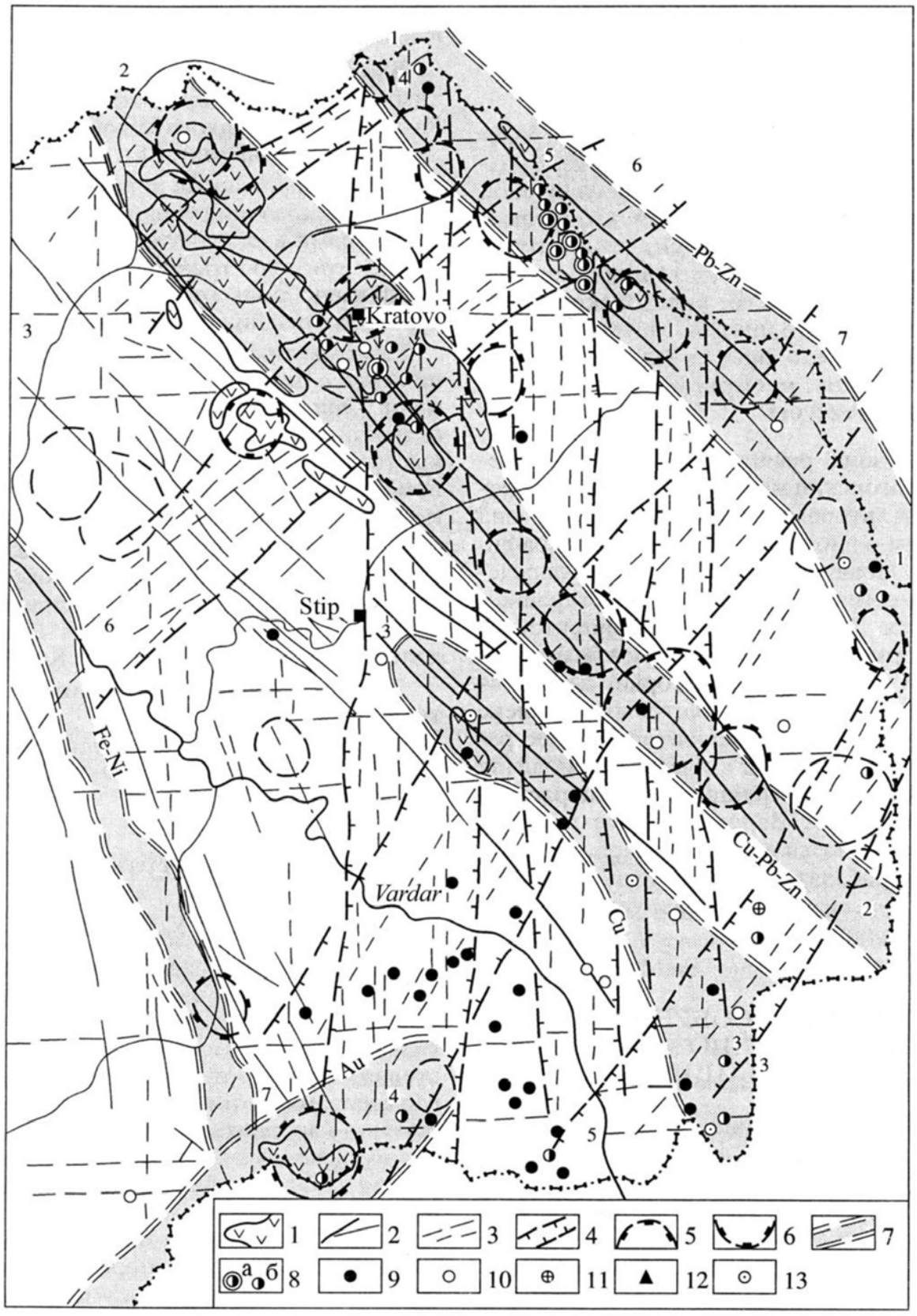

Fig. 4. Scheme of the Cenozoic metallogeny in the Eastern Macedonia
1) Cenozoic magmatic rocks, 2) Followed fissure, 3) Faults defined by satellite images and morphostructural analysis, 4) Fissure zones and cracking systems, 5) Semi-curved structures and calderas, 6) Pericline structures, 7) Metallogenetic zones, 8) Polymetallic deposits (a) and ore occurrences (b), 9) Copper deposits and occurrences, 10) Uranium deposits, 11) Tungsten deposits, 12) Antimony deposits, 13) Iron deposits

These systems practically determined the angle of graben structures, which have been filled with Cenozoic sediments. Numerous drill holes drilled in the Kocani geothermal area confirmed the composition of those graben structures. It should be pointed out that along the fissure structures, of general direction NW-SE, was localized Tertiary magmatism, also. It controled the Cenozoic metallogenetic zones (Fig. 4).

Activated cracking zones of meridian direction quite common comply with flexures directions of flexures in already formed sediments in grabens. Mainly were distinguished three crack zones, which have played an important role as ore bearing structures and localization of the ore fields and ore knots (Fig. 4).

Especial feature within these structural elements are the faulting structures with general direction NE-SW which relicts are saved up to date. They have controled seismic zones and have shown influence to the loalization of mamatic bodies and ore mineralization on places where structures of NW-SE cross cut. These types of structures are common in so called wide zones of relaxation. After the activization of Cenozoic faults followed stage of formation of pericline structures and systems of concentric structures of volcanic type. In that context were distinguished numerous volcanic calderas in frame of the Kratovo-Zletovo volcanic area. With satellite images and morphostructural analyses has been determined that within older concentric structures occurred radial fissures which have been manifested by common presence of faults with NW-SE direction (Fig. 4).

MORPHOSTRUCTURAL FEATURES OF THE BUKOVIK-KADIICA MINERALIZED SYSTEM

The Bukovik-Kadiica ore district has been located in the most eastern parts of the Besna Kobila-Osogovo-Tassos metallogenic zone (Aleksandrov, 1992) and it has been characterized by complex polymetallic mineralization. Within this ore district were determined ore body systems and intersected dykes of quartz-latites with an absolute age of 24–12 Ma. In this zone were located some ore districts while by the detailed analyses were found structures of the Osogovo polymetallic ore district, where it was confirmed that the deposits are situated on the dome's margins and their intersection and crossing with the fissures of SW meridian system and fissures of NW direction (Serafimovski et al. 1997; Janković and Serafimovski, 1997; Thompson et al. 1998). All structural elements were determined with detailed morphostructural analysis and interpretation of satellite imagery. Since earlier it was proven that the Macedonian territory had long and uninterrupted development that allows use of the tectonic elements in the field in determination of the ore controling structures.

By analogy to Osogovo, structural-geomorphological analysis helped in the study of the Bukovik-Kadiica ore district. Determination of tectonic elements in the recent relief was done by use of different set of metodologies: generalization of horizontals, study of river network, interpretation of satellite imagery etc. Relief analysis was based on the topographic map at 1 : 100 000 scale and remote prospecting materials at different scales. For eaxmple, we were using Earth Sat satellite images at scale range 15 to 50 m (step 5m) and covered area in range of 7.5 × 7.5 km to 25 × 25 km (step 2.5 km). Also, it was performed detailed desk study of some previous materials related to the area of interest.

Studied area has been located in the upper parts of the Bregalnica River, Pehcevska River and Celevica. In these water streams were formed two systems: *centrifugal* in the upper parts of Bregalnica and *centripetal* within the boundaries of the Kadiica Mountain. the northern part of the area is of mild mountain character and raises up to 1700-1900 m above the sea level, while the southern part is slightly lower with altitude of 1000–1300 m, divided by wide valley with loose direction and numerous water streams inflowing into the main water-way (Tasev et al. 2008).

From north to the east, the lower part of the area, has been surrounded by the raised arc with altitudes of 1600–1700 m. Radial and radial-centrifugal form of raised water-ways and lowered parts allowed determination of two crossed oval structures: southern one (11 × 8 km) and northern one (7.5 × 6 km). Higher points, erosion study and alluvial accummulation are pointing our to a slope-like development with characteristic valleys and slopes on the southern oval structure and raise of the northern oval structure (Fig. 5).

Intersection of the oval forms has been complicated by the ring structure 3.5 km in diameter. The central part of that structure overlaps with the

independently raised bukovik (1700 m). Around the raised area there is a depression belt, which has been articulated with the highest parts of Celevica, Pehcevska-Rakocevica river valleys. To the east, outer side of the structure has been limited by an arc raised up to 1700–1900 m.

Located group of ring structures has been located on the intersection between the two metallogenic zones: the polymetallic Besna Kobila-Osogovo-Tassos and Kožuf-Aridea (encloses Alšar deposit) with associated Pliocene mineralization.

The area of intersection is higher than earlier mentioned zones and have complex composition. According to that the Bukovik ring structure has been located within the intersection of orthogonal system of fissures determined on the linear tectonic elements of the recent relief (Serafimovski et al. 2010). Dispositions of meridian direction represented as more fractured zones were determined from the satellite imagery, while on the topographic they were shown as fine linear elements in the relief.

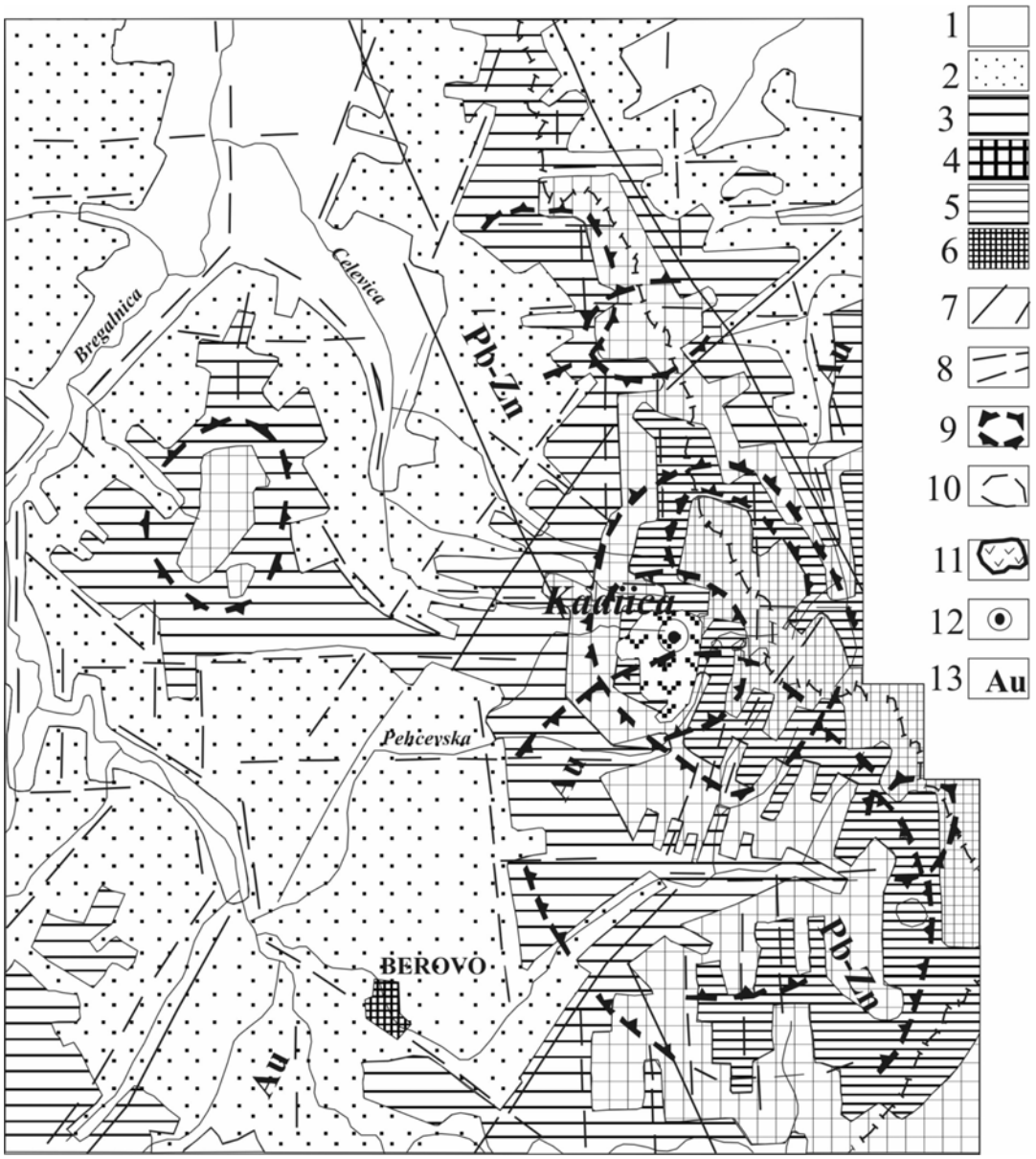

Fig. 5. Morphostructural map of the Bukovik-Kadiica area, Macedonia (Tasev et al. 2008)
1–6 – hypsometric levels (in m): 1) lower than 800 m; 2) 800–1000 m; 3) 1000–1200 m; 4) 1200–1500 m; 5) 1500–1700 m; 6) more than 1700 m; 7) metallogenetic zones, structures, ocurrences on the topographic and satellite imagery; 8.) linear dislocations; 9) concentric structures boundaries; 10) concentric dislocations; 11) pliocene volcanics manifestations; 12) Bukovik-Kadiica ore deposit; 13) specialized metallogenetic zones

These linear lineaments are directly exposed to the upright systems (articulated tectonic flatening, large water-ways curves recent graben incavations). As it has been said already, orthogonal systems run by direction and quite often are connected by the fissure zones. Within the Bukovik-Kadiica area has been detected linear zone that can be followed from Gradiska until the Kadan Bunar, in the corner of the upright Kožuf-Aridea metallogenetic zone. It is a deeply eroded zone defined by welded rectilinear valleys, which can indicate deep zones with the highest permability at the surface.

According to the field and desk study of reality in the field, satellite imagery, metallogenetic features, professional literature etc., we have concluded that morphostructural parameters of the Bukovik-Kadiica area are characterized by structures of two general directions, NW-SE and NE-SW ones. Also this study that mineralization was closely associated to the intersection knots of major structures have shown.

CONCLUSION

Macedonia experienced two periods of extension separated by two abbreviated periods of shortening in Cenozoic time.

The Cenozoic activization of NW-SE strike diagonaly crossed through the large tectonic units Dinarides, Vardar Zone, central parts of the Serbo-Macedonian Massif and Rhodope massif. This activization significantly contributed to the localization of the Cenozoic mineralizations within the Eastern Macedonia

The disruption structures of of NW-SE direction control three major Cenozoic metallogenetic zone. Two of them are characterized by the Oligocene-Miocene magmatism and mineralization in the major ore region Kratovo-Zletovo and Bucim-Damjan-Borov Dol and the third one has been characterized by Miocene volcanics and related mineralization in the Osogovo ore region (Bukovik-Kadiica).

REFERENCES

Aleksandrov M., 1992: *Metallogenetic features of the polymetallic ore field Sasa-Eastern Macedonia*. Ph. D. Thesis, Faculty of Mining and Geology in Štip, Macedonia, 264 p. (in Macedonian).

Arsovski M., Ivanov T., 1977: *Neotectonics magmatism and metallogeny on the territory of Yugoslavia. – Metallogeny and platetectonics in the NE Mediterranean*, Belgrade, pp. 471–482

Burchfiel B. C., Nakov R., Dumurdžanov N., Papanikolaou D., Tzankov T., Serafimovski T., King R. W., Kotzev V., Todosov A. and Nurce, B., 2008: Evolution and dynamics of the Cenozoic tectonics of the South Balkan extensional system, *Geosphere*; December 2008; **4**, 6, 919–938; DOI: 10.1130/GES00169.1

Dumurdžanov N., Serafimovski T. and Burchfiel B. C., 2005: Cenozoic tectonics of Macedonia and its relation to the South Balkan extensional regime. *Geosphere*, **1**, 1, 1–22,

Janković S., Petković M., Tomson I. N., Kravcov V., (1980): *Porphyry copper deposits in the Serbo-Macedonian province, Southeastern Europe*. SGA Special Publication No. 1, Janković, S. and Sillitoe, R. H. (eds.), Belgrade, p.96–102

Janković S. and Petković M., 1974: *Metallogeny and Concepts of the Geotectonic Development of Yugoslavia. Metallogeny and Concepts of the Geotectonic Development of Yugoslavia*, 443–477, Rud. geol. fak., Beograd.

Janković S., Serafimovski, T., 1997: Alpine Metallogeny of SE Europe: regional geotectonic setting and major ore deposits. *Annual General Meeting of IGCP 356 Carpatho-Balkan Metallogeny*, Glasgov University, January 8–11.

Janković S., Serafimovski, T., 1997: Specific Features of Mineralization Related to Different Tectonic Environments in the Serbo-Macedonian Metallogenic Province. *Symposium – Annual Meeting*, Proceeding-Abstract, 285–286, Dojran.

Kocneva N. T,, Romić K., Petković M., 1978: Rekonstrukcija struktura neogene aktivizacije u Srbiji i Makedoniji. *IX Kongres geologa Jugoslavije*, Sarajevo.

Petković M., 1978: *Neogene activation and its importance for the Yugoslavian metallogeny*. II Counceling for the Pb-Zn mineralizations in Yugoslava, Štip (in Serbian).

Petković M., Grubić, A. and Romić, K., 1982: The structural and metallogenic analysis of the zone of Cenozoic autonomous activation. *Symposium International Commission VII International Society for Photogrammetry and Remote Sensing*, Toulouse, Actes 2, pp. 203–208.

Serafimovski, T., 1990: *Metallogeny of the Lece-Chalkidiki zone*. Ph. D. Thesis (in Macedonian), Faculty of Mining and Geology, Štip, 380 p.

Serafimovski T., Janković S., Čifliganec V., 1995. Alpine Metallogeny and Plate Tectonics in the SW Flank of the Carpatho-Balkanides. *Geologica Macedonica*, **9**, 1, 3–14, Štip.

Serafimovski T., 1993: *Structural metallogenetic characteristics of the Lece-Chakidiki zone: Types of Mineral Depos-*

its and Distribution). Special edition of RGF Štip, No 1, 328 pgs. With extended summary in English, Štip,

Serafimovski T., Tomson, I. N., Kochneva, N. T., 1997: Alpine orogenic structures and metallogeny in the Serbo-Macedonian massif and the Vardar zone of the territory of Macedonia. *Symposium-Annual Meeting*, Proceeding 113–117, Dojran.

Serafimovski T., Jelenković, R., 1998: Principle metallogenic units in the SW part of the Carpatho-Balkanides: Geotectonic setting and metallogenic features. *XVI Congress of the Carpathian-Balkan geological Association*, Vien, Austria.

Serafimovski, T., Blažev, K., Tasev, G. and Volkov, A., 2010: Relationship between Cenozoic structures and polymetallic mineralizations in the central part of the Serbo-Macedonian massif. *XIX Congress of the Carpathian-Balkan Geological Association*, Abstracts Volume (eds. Chatzipetros, A., Melfos, V., Marchev, P. and Lakova, I. – *Special Issue of Geologica Balcanica*), Thessaloniki, Greece, pp. 356–357.

Tasev G., Serafimovski, T., Volkov, A. and T. Kochneva, N., 2008: Morphostructural features of the ore zone Bukovik-Kadiica, R. Macedonia. *First Congress of geologists of the Republic of Macedonia*, Proceeding book, pp.201–206 (in Macedonian).

Tomson I. N., Serafimovski T. and Kochneva N., 1998a: Cenozoic metallogeny in Eastern Macedonia. *Geology of ore deposits*, **40**, 3, 195–204 (in Russian).

Tomson N. I., Serafimovski, T., Kochneva, T. N. and Stojanov, R., 2004: New structural background and relation between the Cenozoic structural and metallogenic zones in the Republic of Macedonia. *Geologica Macedonica*, **18**, pp. 1–6, Štip.

Р е з и м е

ГЛАВНИТЕ АЛПИСКИ СТРУКТУРИ И Cu-ПОРФИРСКА МИНЕРАЛИЗАЦИЈА ВО СРПСКО-МАКЕДОНСКИОТ МАСИВ

Тодор Серафимовски[1], Горан Тасев[1], Крсто. Блажев[1], Александр Волков[2]

[1]Институт за геологија, Факултет за природни и технички науки, Универзитет "Гоце Делчев" Гоце Делчев 89, МК-2000 Штип, Република Македонија
[2]ИГЕМ-Руска Академија на Науките, Москва, Русија
todor.serafimovski@ugd.edu.mk

Клучни зборови: Српско-Македонски масив; морфоструктури; Кенозојска активизација; полиметалични минерализации; рудни системи

Геодинамичката еволуција на Српско-Македонскиот масив може да се разгледува во неколку геолошки и геотектонски епохи, но многу специфична е Кенозојската еволуција геодинамички, геотектонски, структурен, магматски и металогенетски аспект. Кенозојските лонгитудинални структури се длабоки и претставуваат граница кон Вардарската зона од една страна и Струма зоната од друга страна.

Морфоструктурните формии од различен ранг и интензитет се од големо значење за просторната дистрибуција на рудната минерализација (Pb-Zn-Cu рудна област Кратово-Злетово, Cu-Au-Fe рудна област Бучим-Дамјан, рудоносен систем Cu-Au-Ag-Fe Буковик-Кадиица и др.). Доминантни структури во рамките на Српско-Македонскиот масив се оние со правец СЗ-ЈИ, кои служеле како рудоносни системи, исто така (рудна зона Бесна Кобила-Осогово-Тасос и металогенетска зона Леце-Халкидики).

Geologica Macedonica, Vol. **24** (1), pp. 49–52 (2010)
ISSN 0352 – 1206
UDC: 553.7 : 546.6(497.7)

GEOME 2
Manuscript received: April 15, 2010
Accepted: October 15, 2010

Original scientific paper

FLUORIDE CONTENT AND DEPENDENCE ON OTHER ELEMENTS IN SOME GEOTERMAL WATERS IN REPUBLIC OF MACEDONIA

Tena Šijakova-Ivanova[1], Vesna Ambarkova[2], Vassiliki Topitsogloy[3], Vesna Paneva-Zajkova[1]

[1]Faculty of Natural and Technical Sciences, "Goce Delčev" University, Goce Delčev 89, MK–2000, Štip, Republic of Macedonia
[2]Faculty of Dentistry, Department of preventive dentisivy, Ss. Cyril and Methodius" University in Skopje, Republic of Macedonia
[3]Faculty of Dentisty, Aristotle University of Thessaloniki, Greece
tena.ivanova@ugd.edu.mk

A b s t r a c t: The paper presents the results obtained for the fluoride content in some geothermal waters in Republic of Macedonia. The results made it possible to determine the dependence between fluoride and other chemical elements in the geothermal water. Fluoride content was determined with jon-analyser (EA 920 ORION) and Ion selective electrode for detection of trace fluoride. For chemical analysis was used 10% TISAB Alumina. Samples were collected in plastic bottles and kept in dark place not longer than two months. Examination on other chemical elements was carried out with AES-ICP. First, the samples were filtered and preserved with HNO_3.

Key words: fluoride; jon analyzer; AES-ICP

INTRODUCTION

Fluoride is an ion of the element fluorine, and is a natural component in most water resources.

Fluoride is an essential element notably for health (Frencken, J. E. 1992; USNRC 1993; USPHS 1991). Fluoride is present in surface, more in ground water and much more in geothermal and mineral water (Allmann, R. and Koritnig,1974; Deshmukh A. N. and Maple D. B. 1996; Gaciri S. J. and Davies 1993; Handa B. K. 1975). Fluorine content varies widely.

Fluoride content in water depends on several factories such as:

– geology of the terrain,
– porosity and alkali of soil,
– type of rocks,
– pH values and temperature,
– chemical and physical properties of water–bearing layer,
– content of calcium ion which limits dissolution of fluorine to 3.1 mg/l concentration,
– depth of source,

Specific geological conditions which result in higher concentration of fluoride in water are related to volcanic activity. Acidic rocks which are poor in calcium and rich in fluoride under high temperature activity release fluoride from the rocks or fluids after eruptive processes and hydration in water bodies.

Volcanic rocks and geothermal fluids can be regarded as key factor for the high concentration on fluoride in water (Lottermoser, B. G., and Cleverley, J. S. 2007; Hem, J. D.,1989; Sharma S. K.2003).

Fluoride is dissolved salt whose major sources in ground waters are apatite, mica and fluorapatite. They are associated with water with high pH values and low calcium concentration (Karthikeyan,.G, A. Shunmugasundarraj, 2008; Alagumuthu G and Rajan M 2008).

RESULTS AND DISCUSSION

Table 1 shows the chemical composition of investigated waters. Dependence between F^-–Cl^-, F^-–Na, F^-–Ca, F^-–Mg, F^-–As, F^-–Al, F^-–Fe, F^-–Cr is shown on Figs. 1–8. Correlation coefficient can be seen from the results given in Table 2

Table 1

Chemical composition of investigated geothermal waters

	Kežovica	Kumanovo	Katlanovo	Konjari	Bansko	Istibanja
As	0.177	0.076	0.004	0.060	0.016	0.187
Al	0.025	0.000	0.008	0.004	0.008	0.025
Sr	0.379	1.08	0.334	0.354	1.10	1.26
Ca	14.6	127.6	54.7	124.6	54.4	9.3
Ba	0.024	0.316	0.541	0.050	0.145	0.086
Mn	0.029	0.004	0.005	0.070	0.004	0.002
Fe	0.037	0.015	0.013	0.013	0.012	0.033
Cr	0.017	0.007	0.007	0.006	0.006	0.005
Mg	0.734	46.2	16.98	24.8	15.6	9.2
Na	524	311	27	70	189	543
F^-	14	0.58	1.5	0.33	1.8	5.4
P	0.024	0.022	0.022	0.761	0.005	0.003
Zn	0.019	0.008	0.596	0.178	0.007	0.005
Pb	0.011	0.003	0.014	0.001	0.001	0.006
Co	0.007	0.007	0.005	0.007	0.006	0.006
K	12.7	16.8	3.6	13.7	10.7	26.5
Cl^-	1368	312	354	1259	232	267
NO_3^-	0.059	0.068	0.029	0.066	0.029	0.016
NH_4^+	0.029	0.044	0.098	0.050	0.058	0.057
Hardness concentracion $CaCO_3$ (mg/l)	39.5	508.3	206.4	413.4	200.0	60.8
Classification	soft water	very hard	hard	very hard	hard	soft water

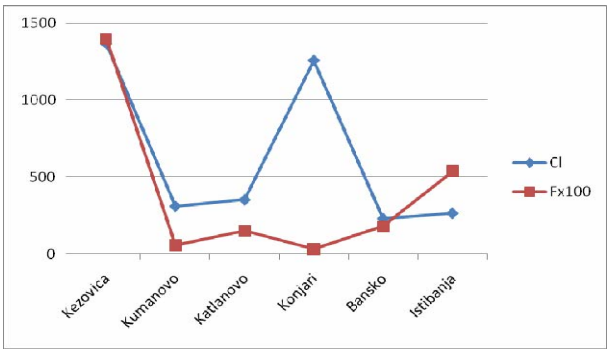

Fig. 1. Dependence between F^- and Cl

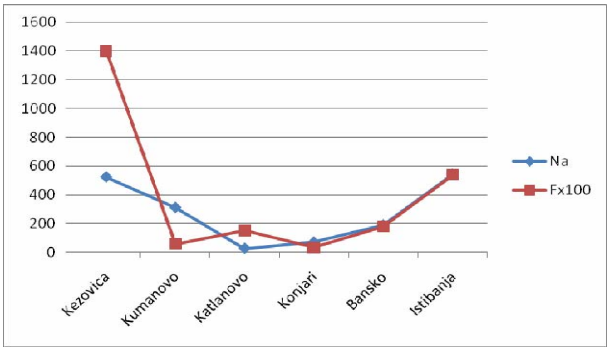

Fig. 2. Dependence between F^- and Na

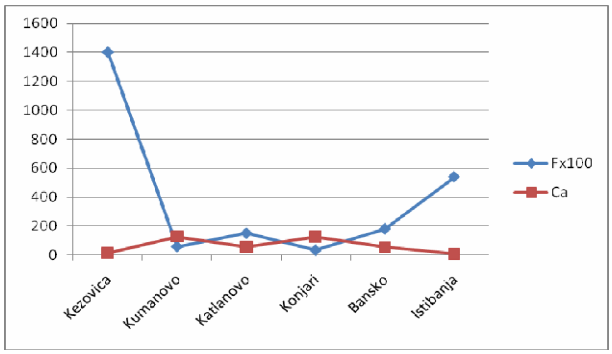

Fig. 3. Dependence between F^- and Ca

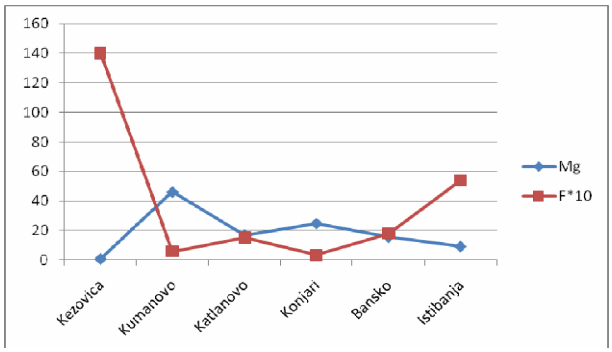

Fig. 4. Dependence between F^- and Mg

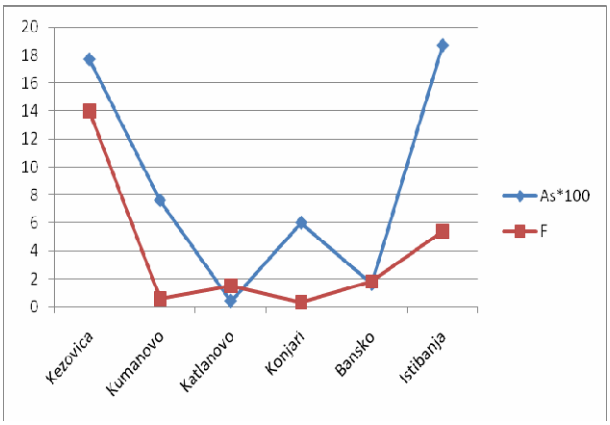

Fig. 5. Dependence between F^- and As

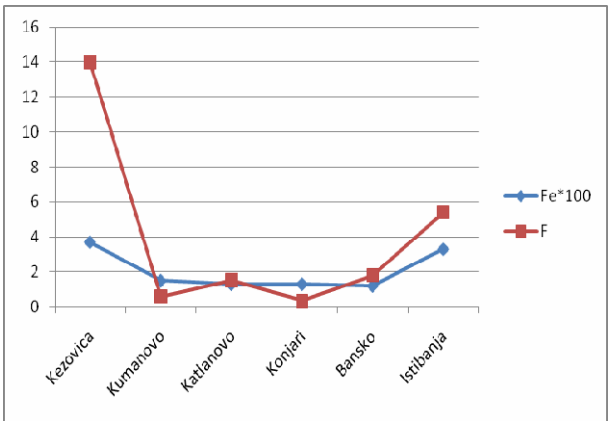

Fig. 7. Dependence between F^- and Fe

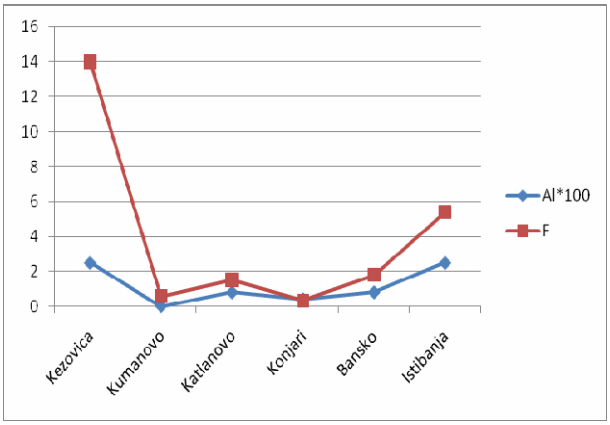

Fig. 6. Dependence between F^- and Al

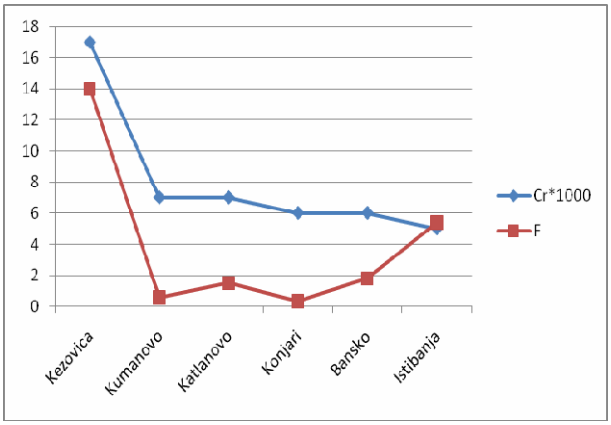

Fig. 8. Dependence between F^- and Cr

Table 2.

Correlation coefficient between F^- and Cl^-, Na, Ca, Mg, Al, As. Fe and Cr

	Cl^-	Na	Ca	Mg	Al	As	Fe	Cr
Correlation coefficient (r)	0.5174	0.7383	–0.7121	–0.7268	0.8400	0.7456	0.8930	0.8801

CONCLUSION

Investigations carried out led to the conclusion as follows.

Fluoride content is higher in Kežovica water and lowest in Konjare water. Dependence between F^-–Cl^-, Na, Al, As, Fe and Cr is proportional. Correlation coefficient for F^- and Cl^- has lower value, 0.5174 and correlation coefficient for F– and Fe has higher value, 0.8930 Non-proportional dependence was established between F^-–Ca and F^- Mg with correlation coefficient, –0.7121 and –0.7268. Kežovica and Istibanja are soft water. Kumanovo and Konjari are very hard water. Kežovica water, except higher concentration on F^- has higher value on Cl^-, Na, Al, Fe and Cr.

	Higher value	Lower value
F^-	Kežovica	Konjare
Cl^-	Kežovica	Bansko
Na	Istibanja, Kežovica	Katlanovo
Ca	Kumanovo	Istibanja
Mg	Kumanovo	Kežovica
Al	Kežovica, Istibanja	Kumanovo
As	Istibanja	Katlanovo
Fe	Kežovica	Bansko
Cr	Kežovica	Istibanja

REFERENCE

Allmann R. and Koritnig S., 1974: Fluorine. In: Wedepohl, K.H. (editor), *Handbook of Geochemistry*, vol**. II**/1. Berlin, Heidelberg; Springer Verlag,

Alagumuthu G. and Rajan M., 2008: Monitoring of fluoride concentration in ground water of Kadayamblock of Tirunel Velidistrict, India, Correlation with physic–chemical parameters *Rasayan J. Chem.*, **1 (**4),757–765, (2008).

Deshmukh A. N. and Maple D. B., 1996: *Fluorine in environment, Special publication*, Gondwana geological Society, Bagpur, pp 1–13.

Frencken J. E. (editor), 1992: *Endemic Fluorosis in developing countries, causes, effects and possible solutions*. Publication number 91.082, NIPG–TNO, Leiden, The Netherlands,

Gaciri S. J., and T. C. Davies, 1993: The occurrence and geochemistry of fluoride in some natural waters of Kenya. *J. Hydrol. (Amst)*, 143, 395–412.

Handa B. K., 1975: *Ground Water*, Volume **13**, Issue 3, pages 275–281,

Karthikeyan G, A. Shunmugasundarraj, 2008: *Fluoride***, 33,** 121–127

Lottermoser B. G., and Cleverley J. S., 2007: Controls on the genesis of a high–fluoride thermal spring: Innot Hot Springs, North Queensland. *Australian Journal of Earth Sciences*, **54** (4). pp. 597–607. ISSN 1440–0952

Hem, J. D., 1989: Study and interpretation of the chemical characteristics of natural water [3d ed]: U.S. *Geological Survey Water –Supply Paper*, 2254–263 p

Sharma S. K. 2003: *High fluoride in ground water crippleslife in parts of India*, Diffuse Pollutation Conference Dublin 2003.

USNRC 1993 *Health effects of Ingested fluoride*, United States national research Council national Academy Press Washington.

USPHS, 1991: *Review fluoride benefits and risks. report of ad hoc subcommittee on fluoride*. Committeeto coordinate Environmental health and related Program.

Р е з и м е

ЗАВИСНОСТ ПОМЕГУ КОНЦЕНТРАЦИЈАТА НА ФЛУОР И ОСТАНАТИТЕ ЕЛЕМЕНТИ ВО НЕКОИ ГЕОТЕРМАЛНИ ВОДИ ВО РЕПУБЛИКА МАКЕДОНИЈА

Тена Шијакова-Иванова[1], Весна Амбаркова[2], Vassiliki Topitsogloy[3], Весна Панева-Зајкова[1]

[1]Факултет за природни и технички науки, Универзитет Гоце Делчев, ул. Гоце Делчев, 89, МК-2000 Штип, Република Македонија
[2]Стоматолошки факултет, Катедра за превентивна стоматологија, Универзитет Св. Кирил и Методи во Скопје,Република Македонија
[3]Стоматолошки факултет , Аристотел Универзитет , Солун, Грција
[1]Faculty of Natural and Technical Sciences, "Goce Delčev" University, Goce Delčev 89, MK–2000, Štip, Republic of Macedonia
tena.ivanova@ugd.edu.mk

Клучни зборови: флуор; јон анализатор; AES-ICP

Содржината на флуоридните јони е највисока во водата од Кежовица, а најниска во водата од Коњаре. Корелацијата помеѓу содржината на флуоридни јони со содржината на Cl^-, Na, Al, As, Fe и Cr пропорционална. Коефициентот на корелација за F^-–Cl^- има најниска вредност, 0,5174, а за F^-–Fe највисока, 0,8930. Корелацијата помеѓу концентрацијата на F^-–Ca и F^-–Mg е обратно пропорционална со коефициенти на корелација –0,7121 и –0,7268. Водите од Кежовица и Истибања се меки води, а водите од Куманово и Катланово се многу тврди. Во водата од Кежовица се одредени највисоки концетрации не само за флуоридните анјони, туку и за Cl^-, Al, Fe и Cr.

Geologica Macedonica, Vol. **24, No.** 1, pp. 53–62 (2010)
ISSN 0352 – 1206
UDC: 631.416.4(497.714)

GEOME 2
Manuscript received: March 5, 2010
Accepted: September 7, 2010

Original scientific paper

DETERMINATION OF ACTIVITY CONCENTRATION OF ^{40}K AND GROSS BETA ACTIVITY IN SOIL FROM KAVADARCI AND ITS ENVIRONS

Snežana Dimovska[1], Trajče Stafilov[2], Robert Šajn[3]

[1]*Institute of Public Health, 50 Divizija 6, MK-1000 Skopje, Macedonia*
[2]*Institute of Chemistry, Faculty of Science, St. Cyril and Methodius University in Skopje, POB 162, MK-1001 Skopje, Macedonia,*
[3]*Geological Survey of Slovenia, Dimičeva ul. 14, 1000 Ljubljana, Slovenia*
trajcest@pmf.ukim.mk

A b s t r a c t: A survey was carried out to determine the activity concentration and distribution of ^{40}K and gross beta activity in the soil from the city of Kavadarci, Republic of Macedonia, and its environs. A total of 45 surface soil samples were collected from evenly distributed sampling sites over an area of 360 km^2. The activity concentrations of ^{40}K were measured using a high purity germanium (HPGe) gamma-ray detector, while the gross beta activity measurements were made using a low background gas-flow proportional counter. The obtained values for the activity concentrations of ^{40}K were found to be in the range of 286±6 and 801±12 Bq/kg with an average value of 545±118 Bq/kg. The gross beta activities varied between 438±21 and 1052±36 Bq/kg, with an average value of 681±146 Bq/kg. These values allowed the determination of the elemental concentrations of potassium as well as the air absorbed gamma dose rate, which were found to range from 0.92±0.02 to 2.56±0.04% and from 11.9±0.1 to 33.4±0.5 nGy/h, respectively. The mean values of these parameters were 1.74±0.37% and 22.8±4.9 nGy/h. All obtained values fall within the worldwide range as reported in the literature. A strong correlation between the content of potassium in the soils and their geological origin was observed.

Key words: potassium; soil; gamma spectrometry; gross beta activity, activity concentration; absorbed dose rate, lithological units

INTRODUCTION

External exposures outdoors arise from terrestrial radionuclides present at trace levels in all soils and the specific levels are related to the types of rock from which the soils originate. There have been many surveys to determine the background levels of radionuclides in soils, which can in turn be related to the absorbed dose rates in air. The spectrometric measurements indicate that the three components of the external radiation field, namely from the gamma-emitting radionuclides in the ^{238}U and ^{232}Th series and ^{40}K, make approximately equal contribution to the external gamma radiation dose to individuals (UNSCEAR, 2000).

Potassium is an essential element of human metabolism and can be found in all living cells, mainly in the muscular tissue. Natural potassium is composed of three isotopes: ^{39}K, ^{40}K and ^{41}K. Of these naturally occurring potassium isotopes only ^{40}K is unstable, having a half-life of 1.28×10^9 years. It occurs to an extent of 0.012 % in natural potassium, thereby imparting a specific activity of approximately 30 Bq/g potassium. ^{40}K is a beta and gamma emitter (89 % and 11 % of its radiation, respectively) with respective energies of 1.3 and 1.46 MeV (Bowen, 1979).

Because of its relative abundance and its energetic beta emission, ^{40}K is easily the predominant radioactive component in normal foods and human tissues. It is important to recognize that the potassium content of the body is under strict homeostatic control and is not influenced by variations in environmental levels (Eisenbud, 1987).

Radioactivity levels of the environment depend on geological aspects, mainly on rocks and soil, where the radionuclides are found in varying concentrations (Tzortzis and Tsertos, 2004). Representative values of the potassium content of rocks, as summarized by Kohman and Saito (1954)

indicate a wide range of values, from 0.1 % for limestones trough 1 % for sandstones and 3.5 % for granite. The potassium content of soils of arable lands is controlled by the use of fertilizers. It is estimated that about 1.11×10^{14} Bq is added annually to the soils of the United States in the form of fertilizer (Guimond, 1978).

The mean natural radionuclide contributions to gross beta activity in soil are ^{40}K and ^{226}Ra beta emitting decay products (Kücükömeroglu et al., 2008).

The aim of the present study is to measure the beta activity levels in the surface soil over the Kavadarci region, to assess the radiation hazard to the population due to ^{40}K and to investigate the connection between the potassium content in the soils and the geology of the terrain. The importance of this work arises from the fact that there is no reference regarding this area concerning the ^{40}K activity concentrations in the soil.

MATERIAL AND METHODS

Study area

The city of Kavadarci is situated in Tikveš valley, about 100 km south of Skopje, the capital of The Republic of Macedonia (Fig. 1). The study area is limited with coordinates (Gauss Krueger zone 7) 7574000 (W) -7592000 (E) and 4582000 (S) – 4602000 (N).

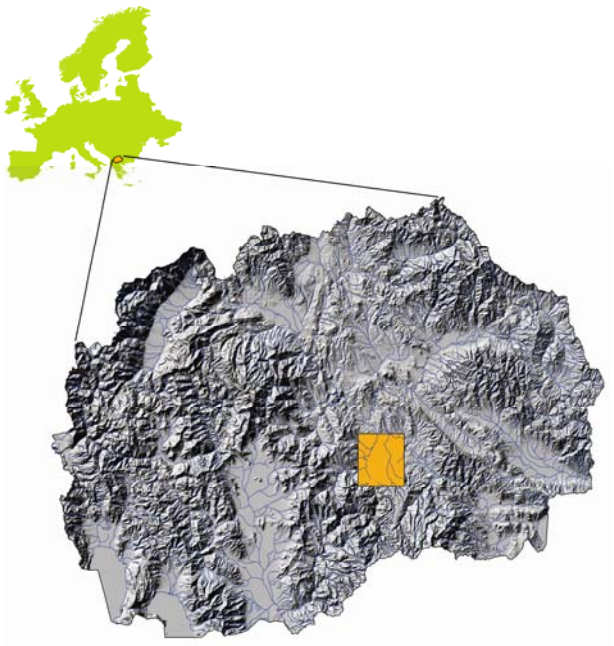

Fig. 1. Location of the study area

The urban area is surrounded by hills from east and south. Of the total 360 km^2 of the study area, rivers and lakes cover 6 km^2, cultivable land 221 km^2, non-cultivable area 120 km^2 and urbanized area 13 km^2 (Fig. 2). The Kavadarci region is the main center of vine production in Macedonia and south-eastern Europe and it is known for its ferro-nickel industrial activity (Stafilov et al., 2008; 2010).

The geological description of the study area (Fig. 3) was made according to Rakićević et al. (1965) and Hristov et al. (1965).

The region of Paleozoic and Mezozoic rocks (Pz-Mz) cover approximately 39 km^2 in the SW and W part of the investigated area and 7 soil samples were taken from this area. The Upper Eocene flisch sediments and yellow sandstones (E-Flis) are developed along Vardar, Crna Reka and Luda Mara valleys, they cover approximately 34 km^2, mainly in the north part of the investigated area, where 4 sampling sites are located. The Pliocene sediments (Pl-sand) fill the Tikveš basin, they cover the biggest part of the study area (about 182 km^2) and from this region 23 soil samples were collected. The Quaternary pyroclastic vulcanites (Q) are found on the south-east from Kavadarci, they are spread over an area of around 25 km^2 and 5 soil samples were taken. Quaternary ages is represented with deluvial (12 km^2), terrace (23 km^2) and aluvial sediments (40 km^2). On this lithyological units 6 sampling sites are located.

Sampling

The soil samples from the city of Kavadarci and its environs were collected for preparing a geochemical atlas of this region and according to the European guidelines for soil pollution studies (Teocharopulos et al., 2001; Šajn, 2004). The investigated region was covered by a sampling grid of 4×4 km^2 (Fig. 4) and a total of 45 soil samples were taken. The samples were collected from the upper 5 cm layer. Each sample represents a composite material collected at the central sample point and four points within the radius of 10 m around it towards N, E, S and W. The mass of such sample was about 1 kg.

Fig. 2. Land use map of the study area

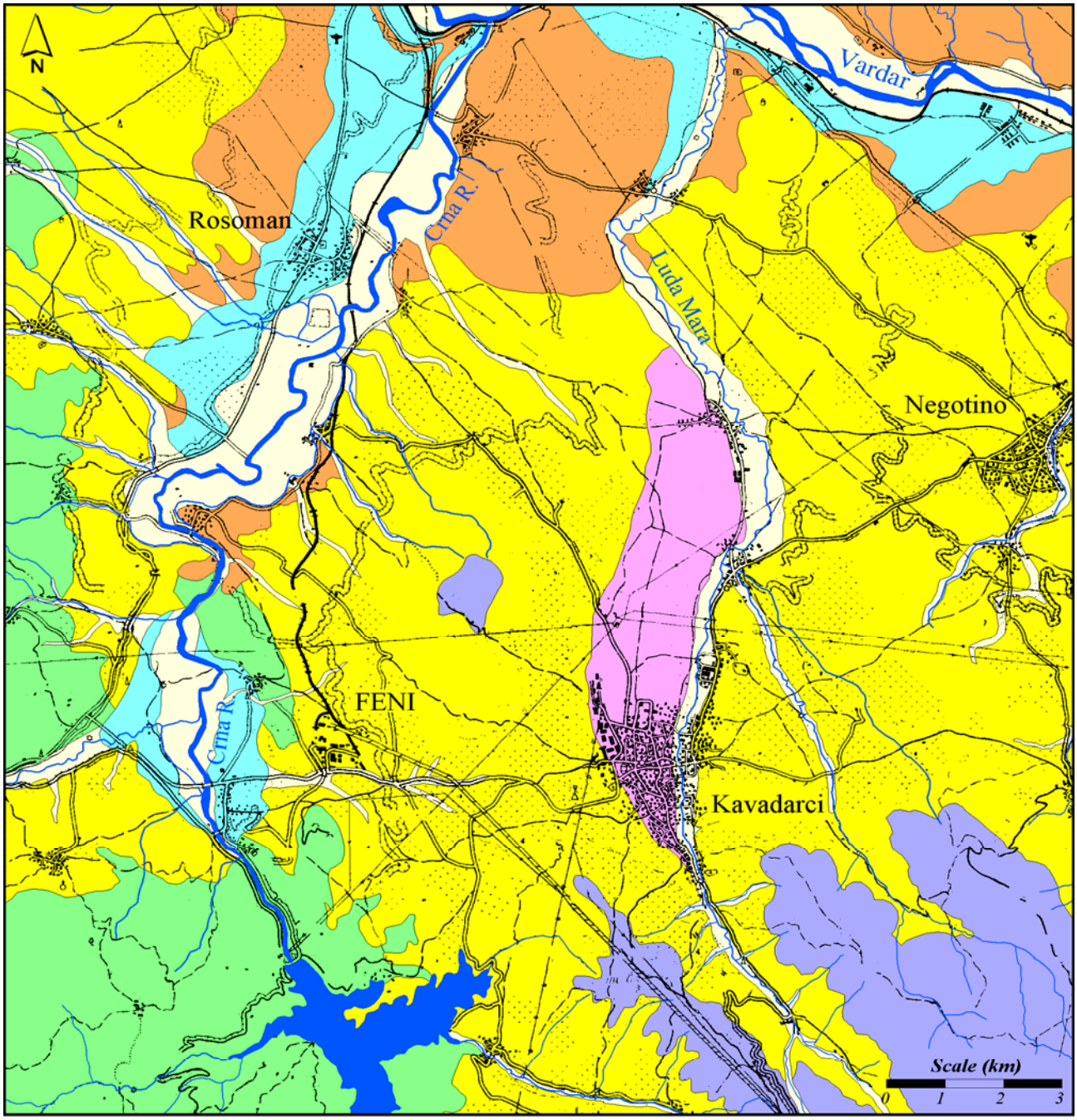

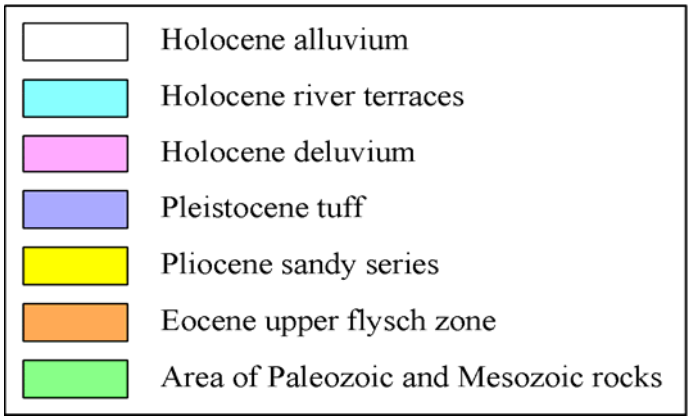

Fig. 3. Lithological map of the study area

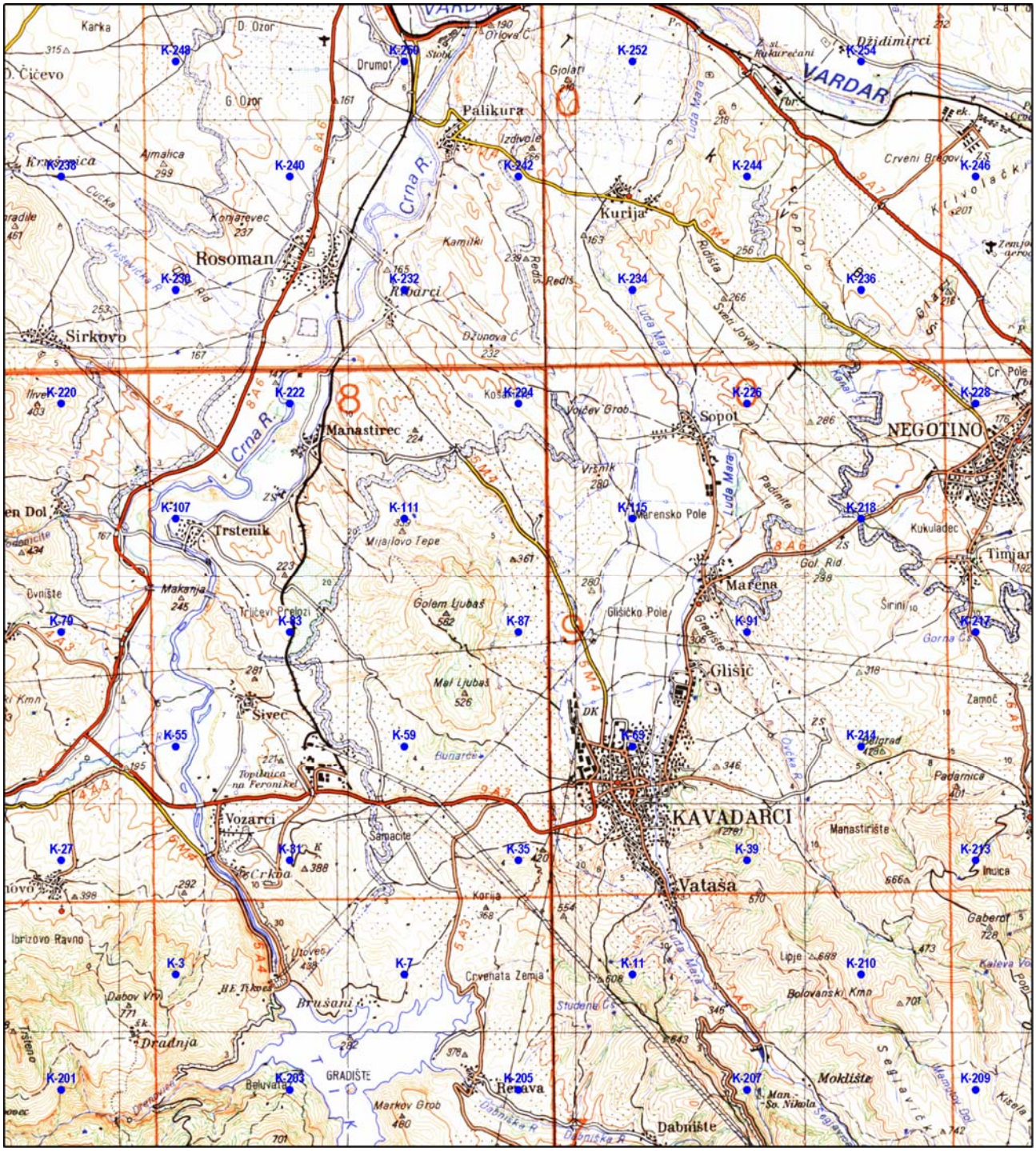

Fig. 4. Soil samples locations in the Kavadarci area

Sample preparation

The samples were mixed thoroughly, collected in plastic bags and labeled properly. In the laboratory, after removing the roots and stones, the samples were air dried for about two weeks, grounded, sieved and homogenized. The fraction below 2 mm was used for the analyses. The data have been expressed on dry weight basis.

About 200 mg of each soil sample were taken for measurement of the gross beta activity, transferred into a 2-in. diameter stainless steel planchete, evenly spread, fixed with acetone and dried under infrared lamp.

For gamma spectrometric analyses of ^{40}K prepared soil samples of about 150 g each were stored in standardized cylindrical plastic containers.

Radiological analyses

The measurement of gross beta activity in all soil samples was performed using MINI 20 Very low background multiple detector counting system for low alpha/beta activities, Eurysis Measures. The detectors used were gas flow proportional counters. The system was calibrated with prepared standard samples which contain known concentration of ^{40}K. The counting time was 60 minutes, by four independent detectors in the system, simultaneously. Each sample was counted for three times in a row and the results were given as an arithmetic mean with the statistical error.

For the measurement of activity concentrations of ^{40}K in the soil samples a high resolution gamma-ray spectrometer consisting of a coaxial P-type HPGe detector with a relative efficiency of 27.1 % was used. The detector was coupled to a Canberra multi-channel analyzer (MCA). The resolution was 2 keV at 1.33 MeV of ^{60}Co. The detector was shielded in an 8 cm lead chamber with an inner lining of 2 cm thick copper plate to reduce the background. The results were analyzed by Genie-2000 software (Canberra). A reference sample (Soil-375) provided by the International Atomic Energy Agency was used for the efficiency calibration of the system. Each sample was counted for 60 000 s.

The activity concentration of ^{40}K was determined using its single 1460.8 keV gamma-ray line and converted to total elemental concentration of potassium, reported in %, using the following equation (Tzortzis and Tsertos, 2004):

$$F_E = \frac{M_E \cdot C \cdot A_E}{\lambda_E \cdot N_A \cdot f_{A,E}}$$

where F_E is the fraction of element E in the sample, M_E, λ_E, $f_{A,E}$ and A_E are the atomic mass (kg/mol), the radioacivity decay constant (s^{-1}), the fraction atomic abundance in nature and measured activity concentration (Bq/kg) of the corresponding radionuclide, respectively, N_A is Avogadro's (6.023×10^{23} atoms/mol) and C is a constant with a value of 100 for potassium.

The absorbed gamma dose rate in air 1 m above the ground (D_K), proceeding from the gamma emissions of ^{40}K, in nGy/h, was calculated on the basis of guidelines provided by UNSCEAR, 2000:

$$D_K = 0.0417 \cdot A_K$$

where A_K is the activity concentration of ^{40}K (Bq/kg).

RESULTS AND DISCUSSION

The obtained results for the minimum, maximum and average values of gross beta activity and the activity contrations of ^{40}K in Bq/kg of dry soil, the calculated content of potassium (in %) and the absorbed gamma dose rate (in nGy/h) are presented in Table 1.

Table 1

The minimum, maximum and average values of gross beta activity, activity concentration of ^{40}K, elemental concentration of potassium and the absorbed gamma dose rate

	Minimum	Maximum	Average
Gross beta activity (Bq/kg)	438±21	1052±36	681±146
^{40}K (Bq/kg)	286±6	801±12	545±118
K (%)	0.92±0.02	2.56±0.04	1.74±0.37
D_K (nGy/h)	11.9±0.1	33.4±0.5	22.8±4.9

The gross beta activity of the soils varied between 438±21 and 1052±36 Bq/kg, with an average of 681±146 Bq/kg. The map of the distribution of the gross beta activity in the studied area is shown in Fig. 5.

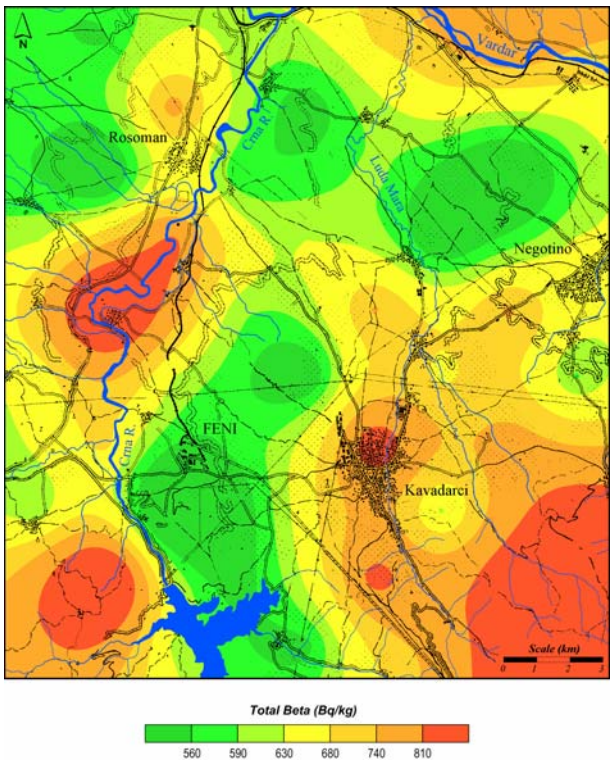

Fig. 5. Map of the distribution of gross beta activity

The activity concentration of potassium in the soil samples was found to be in the range from 286±6 to 801±12 Bq/kg, with an average of 545±118 Bq/kg. The elemental concentration of potassium ranged from 0.92±0.02 to 2.56±0.04%, with an average of 1.73±0.37%. The distribution of potassium in the studied area is shown in Fig. 6.

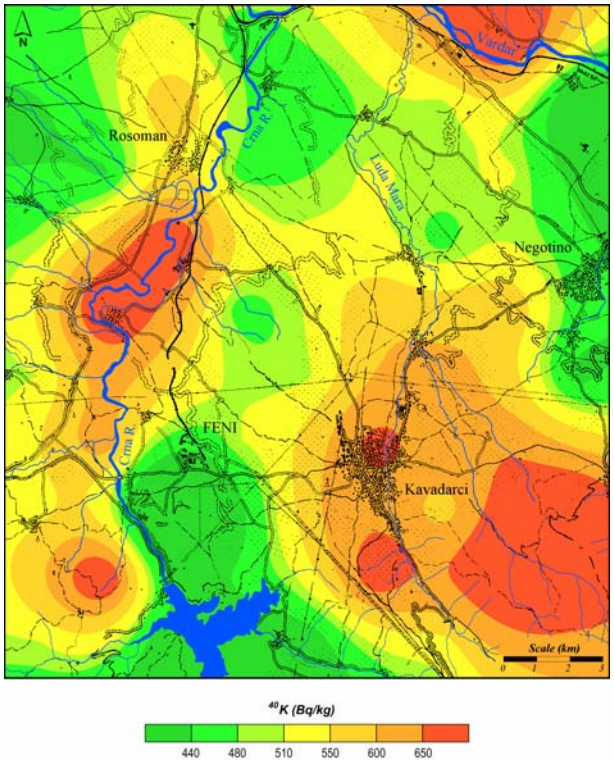

Fig. 6. Map of the distribution of ^{40}K

The measured activity concentration of ^{40}K were compared with the values reported worldwide as shown in Table 2.

Table 2

Activity concentrations of ^{40}K (Bq/kg) measured worldwide

Region	References	^{40}K
Pernambuco, Brazil	Santos Jr., et al. 2005	1827
Thanjavur, India	Senthilkumar et al., 2010	149.5±3.1
Riyadh, Saudi Arabia	Alaamer, 2008	225±63
Ontario, Canada	Vanden Bygaart et al., 1999	461.5±168.4
Marmara Region, Turkey	Kilic et al., 2007	442.5±189.9
West Bank, Palestina	Dabayneh et al., 2008	630
Ptolemais, Greece	Psichoudaki and Papaefthymiou, 2008	496±56
Punjab, Pakistan	Tahir et al., 2005	307±101
Vojvodina, Serbia	Bikit et al., 2005	554±92
Nigeria	Ajayi, 2009	286.5±308.5
Turkey	Kücükömeroglu et al., 2008	51-1605
Veles region, Macedonia	Dimovska et al., 2010	585.7 ± 86.4
Worldwide average	UNSCEAR, 2000	400 (140-850)
This work		545±118

The calculated air absorbed gamma dose rate values varied from 11.9±0.1 to 33.4±0.5 nGy/h, with a mean of 22.8±4.9 nGy/h.

The statistical data for gross beta activity and the activity concentration of ^{40}K, according to the basic lithological units, are given in Table 3.

Table 3

The minimum, maximum and average values of gross beta activity and activity concentration of ^{40}K according to the basic lithological units

	Lithological unit	Minimum	Maximum	Average
Gross beta activity (Bq/kg)	Pz-Mz	438±21	1052±36	681±146
	E-Flis	494±25	688±28	591±91
	Pl-sand	490±27	868±33	625±91
	Q-Tuf	744±29	1030±34	880±102
	Q-Al	612±26	1012±33	790±136
^{40}K (Bq/kg)	Pz-Mz	286±6	756±11	481±144
	E-Flis	374±6	541±7	450±69
	Pl-sand	400±6	754±11	523±77
	Q-Tuf	588±8	780±11	677±73
	Q-Al	469±7	801±12	662±121

The highest average values for the activity concentration of ^{40}K and gross beta activity (677±73 Bq/kg and 880±102 Bq/kg, respectively) are found in the regions of Pleistocene tuff (Q-Tuf), whereas the lowest average values (450±69 Bq/kg and 591±91 Bq/kg, respectively) occur in the areas of the Eocene upper flysch zone (E-Flis) (Figs. 7 and 8).

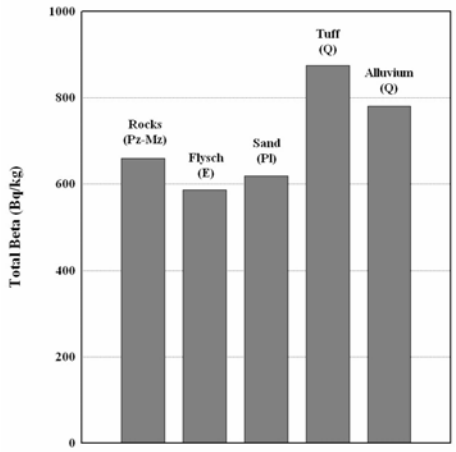

Fig. 7. Average gross beta activity according to the basic lithological units

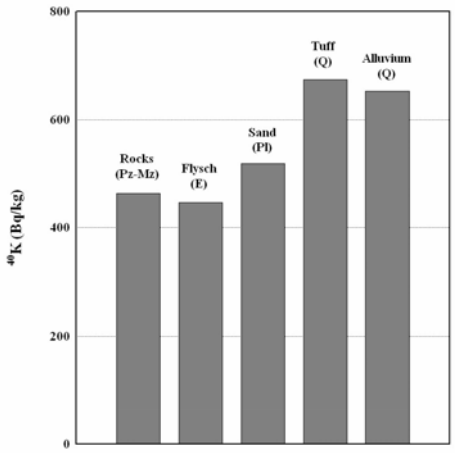

Fig. 8. Average activity concentration of ^{40}K according to the basic lithological units

CONCLUSION

The calculated average value for the gross beta activity in the analyzed soil samples is 681±146 Bq/kg. The common values range from several hundreds to 1000 Bq/kg (ISO 18589-3, 2007). The gross beta activity in environmental samples derives mainly from the presence of ^{40}K and also the other natural beta emitting radionuclides. The high obtained value for the linear coefficient of correlation *r* (0.82) between the gross beta activity and the activity of ^{40}K is in an agreement with the literature data.

The average activity concentration of ^{40}K measured in the soil samples from the region of Kavadarci and its environs (545±118 Bq/kg) is comparable with the values for the activity concentration of ^{40}K in the soils from other region in Macedonia and the neighboring countries (Serbia, Greece). It is slightly higher than the worldwide average, but still in the range of UNSCEAR 2000 report, which is 140-850 Bq/kg.

The highest average values for the investtigated parameters are found in the regions of Pleistocene tuff and Holocene alluvium of the rivers Vardar, Crna Reka and Luda Mara, whereas the lowest average values occur in the areas of the Eocene upper flysch zone, which proves the relation between the content of potassium in soils and their geological origin.

REFERENCES

Ajayi O. S., 2009: Measurement of activity concentrations of ^{40}K, ^{226}Ra and ^{232}Th for assessment of radiation hazards from soils of the southwestern region of Nigeria, *Radiation and Environmental Biophysics*, **48**, 323-332.

Alaamer A. S., 2008: Assessment of human exposures to natural sources of radiation in soil of Riyadh, Saudi Arabia, *Turkish Journal of Engineering and Environmental Sciences,* **32**, 229-234.

Bikit I., Slivka J., Čonkić Lj., Krmar M., Vesković M., Žikić – Todorović N., Varga E., Ćurčić S., Mrdja D., 2005: Radioactivity of the soil in Vojvodina (northern province of Serbia and Montenegro), *Journal of Environmental Radioactivity*, **78**, 11-19.

Bowen H. J. M., 1979: *Environmental Chemistry of the Elements*, Academic Press, New York.

Dabayneh K. M., Mashal L. A., Hasan F. I., 2008: Radioactivity concentration in soil samples in the southern part of the West Bank, Palestina, *Radiation Protection Dosimetry*, **131**, 265-271.

Dimovska, S., Stafilov, T., Šajn, R., Frontasyeva, M. V., 2010: Distribution of some natural and man-made radionuclides in soil from the city of Veles (Republic of Macedonia) and its environs, *Radiation Protection Dosimetry*, **138,** 144–157.

Eisenbud M., 1987: *Environmental Radioactivity*, Academic Press, New York.

Guimond R. J., 1987: The radiological aspects of fertilizer utilization in radioactivity in consumers products. USNRC Rep. NUREG/CP0003, p. 381-393. NTIS, Springfield, Virginia.

Hristov C., Karajovanović M., Stračkov M., *Basic Geological Map of SFRJ, Sheet Kavadarci, M 1:100,000 (map & interpreter)*, Federal Geological Survey, Beograd, 1965, 62 pp.

ISO International Organization for Standardization, 18589-3, 2007: Measurement of radioactivity in the environment - Soil, Part 3: Measurement of gamma-emmitting radionuclides.

O. Kilic O., Belivermis M., Topcuoglu S., Cotuk Y., Coskun M., Cayir A., Kucer R., 2007: Radioactivity concentrations and dose assessment in surface soil samples from east and south of Marmara region, Turkey, *Radiation Protection Dosimetry*, **128**, 324-330.

Kohman T., Saito N., 1954: Radioactivity in geology and cosmology, *Annual Review of Nuclear Science,* **4**, 401-462.

Kücükömeroglu B., Kurnaz A., Keser R. , Korkmaz F., Okumusoglu N. T., Karahan G., Sen C., Cevik U., 2008: Radioactivity in sediments and gross alpha-beta activities in surface water of Firtina River, Turkey, *Environmental Geology*, **55**, 1483-1491.

Psichoudaki M., Papaefthymiou, H., 2008: Natural radioactivity measurements in the city of Ptolemais (Northern Greece), Journal of Environmental Radioactivity, 99, 1011-1017.

Rakićević T., Stojanov S., Arsovski M., *Basic Geological Map of SFRJ, Sheet Prilep, M 1:100,000 (map & interpreter)*, Federal Geological Survey, Beograd, 1965, 62 pp.

Šajn R., 2004: Distribution of mercury in surface dust and topsoil in Slovenian rural and urban areas, *RZM-Materials and Geoenvironment*, **51**, 1800-1803.

Santos Jr. J. A., Cardoso J. J. R. F., Silva C. M., Silveira S. V., Amaral R. dos S., 2005: Analysis of the ^{40}K Levels in Soil using Gamma Spectrometry, *Brazilian Archives of Biology and Technology*, **48**, 221-228.

Senthilkumar B., Dhavamani V., Ramkumar S., Philominathan P., 2010: Measurement of gamma radiation levels in soil samples from Thanjavur using γ-ray spectrometry and estimation of population exposure, *Journal of Medical Physics*, **35**, 48-53.

Stafilov T., Šajn R., Boev B., Cvetković J., Mukaetov D., Andreevski M., 2008: *Geochemical Atlas of Kavadarci and the Environs*, Faculty of Natural Sciences and Mathematics, Skopje.

Stafilov T., Šajn R., Boev B., Cvetković J., Mukaetov D., Andreevski M., Lepitkova, S., 2010: Distribution of some elements in surface soil over the Kavadarci Region, Republic of Macedonia, *Environmental Earth Sciences*, **61**, 1515–1530..

Tahir S. N. A., Jamil K., Zaidi J. H., Arif M., Ahmed N., Ahmad S. A., 2005: Measurement of activity concentrations of naturally occuring radionuclides in soil samples from Punjab province of Pakistan and assessment of radiological hazard, *Radiation Protection Dosimetry*, **113**, 421-427.

Theocharopulos S. P., Wagner G., Sprengart, Mohr M-E., Desaules A., Muntau H., Christou M., Quevauviller P., 2001: European soil sampling guidelines for soil pollution studies, *The Science of the Total Environment*, **264**, 51-62.

Tzortzis M., Tsertos H., 2004: Determination of thorium, uranium and potassium elemental concentrations in surface soils in Cyprus, *Journal of Environmental Radioactivity*, **77,** 325-338.

UNSCEAR United Nation Scientific Committee on the Effects of Atomic Radiation, 2000: *Sources, effects and risks of ionizing radiation*. Report to general assembly, with scientific annexes, United Nations, New York.

Vanden Bygaart A. J., Protz R., McCabe D. C., 1999: Distribution of natural radionuclides and ^{137}Cs in soils of southwestern Ontario, *Canadian Journal of Soil Science*, **79,** 161-171.

Р е з и м е

ОПРЕДЕЛУВАЊЕ НА АКТИВНОСТА НА ^{40}K И ВКУПНАТА БЕТА АКТИВНОСТ ВО ПОЧВАТА ОД КАВАДАРЦИ И НЕГОВАТА ОКОЛИНА

Снежана Димовска[1], Трајче Стафилов[2], Роберт Шајн[3]

[1]Институт за јавно здравје, 50 Дивизија 6, МК-1000 Скопје, Македонија
[2]Институт за хемија, Природно-математички факултет, Универзитет „Св. Кирил и Методиј“ во Скопје, п. фах 162, МК-1001, Скопје, Република Македонија
[3]Геолошки завод на Словенија, Димичева 14, 1000 Љубљана, Словенија
trajcest@ pmf.ukim.mk

Клучни зборови: калиум; почва; гама спектрометрија; вкупна бета активност, специфична активност, брзина на гама доза, литолошки единици.

Испитување беше извршено со цел да се определи активноста и дистрибуцијата на ^{40}K и вкупната бета активност во почвата од Кавадарци, Република Македонија, и неговата околина. Земени се вкупно 45 примероци од површински почви од рамномерно распоредени локации, на површина од 360 km^2. Специфичните активности на ^{40}K беа мерени со помош на П-тип коаксијален гама детектор од германиум со висока чистота, додека мерењата на

вкупната бета активност беа извршени со користење на нискофонов гасно-проточен пропорционален бројач. Добиените вредности за специфичната активност на ^{40}K се движат од 286±6 до 801±12 Bq/kg, со средна вредност од 545±118 Bq/kg. Вкупната бета активност варира помеѓу 438±21 и 1030±36 Bq/kg, со средна вредност од 681±146 Bq/kg. Овие податоци овозможија да се пресмета концентрацијата на калиум, како и брзината на гама дозата на зрачење, кои изнесуваа од 0,92±0,02 до 2,56±0,04 % и од 11,9±0,1 до 33,4±0,5 nGy/h, соодветно. Средните вредности на овие параметри беа 1,74±0,37 % и 22,8±4,9 nGy/h. Сите добиени вредности се споредливи со просечните во светски рамки, објавени во литературата. Резултатите од анализата укажуваат на силна поврзаност помеѓу застапеноста на калиумот во почвите и нивното геолошко потекло.

GEOME 2
Manuscript received: April 21, 2010
Accepted: October 10, 2010

Geologica Macedonica, Vol**. 24**, No. 1, pp. 63–71 (2010)
ISSN 0352 – 1206
UDC: 550.84 : 553.3(497.715)

Original scientific paper

FLUID INCLUSIONS AND K/Ar DATING OF THE ALLŠAR Au-Sb-As-Tl MINERAL DEPOSIT, MACEDONIA

Sabina Strmić Palinkaš[1], Sibila Borojević Šoštarić[2], Ladislav Palinkaš[1], Zoltan Pecskay[3], Blažo Boev[4], Vladimir Bermanec[1]

[1]Faculty of Science, University of Zagreb, Horvatovac 95, HR-10000 Zagreb, Croatia
[2]Faculty of Mining, Geology and Petroleum Engineering, University of Zagreb, Pierottijeva 6. HR-10000 Zagreb, Croatia
[3]Institute of Nuclear Research, Hungarian Academy of Sciences, Bem tér. 18c, HU-4001 Debrecen, Hungary
[4]Faculty of Natural and Technical Sciences, "Goce Delčev" University, Goce Delčev 89, MK-2000, Štip, Republic of Macedonia
blazo.boev@ugd.edu.mk

A b s t r a c t: The Allšar Au-Sb-As-Tl mineral deposit, Macedonia, occurs in the southern part of the Vardar zone. The deposit carries Carlin-type of mineralization hosted by calcareous sedimentary complex. Mineral assemblages and alterations display characteristic zonal distribution. According to the fluid inclusion data, mineral deposition occurred as a result of cooling, dilution and neutralization of the ore-bearing fluids. Neogene magmatism (4.6 to 5.8 Ma) served as the heat source responsible for driving convective hydrothermal circulation at the Allšar deposit.

Key words: carlin; gold; thallium; arsenic; antimony; fluid inclusions; K/Ar dating

INTRODUCTION

The Allšar Au-Sb-As-Tl mineral deposit is located at the north-western margins of Kožuf Mts. in the southern part of the Vardar zone, 110 km SE from Skopje, Macedonia (Fig. 1). The deposit is unique in the world because of the presence of the mineral lorandite ($TlAsS_2$), which is of particular interest for nuclear physicists and geochemists. Lorandite offers the possibility of geochemical detection of proton–proton-solar neutrinos which have very low detection limits and threshold energies (Pavićević et al., 2006).

Several studies have been carried out at the Allšar deposit, including ore-stage mineral paragenesis (Janković, 1988; Janković & Jelenović, 1994; Percival & Radtke, 1994), characterization of the petrological and geochemical features of the volcano-intrusive complex of the Kožuf Mts. (Boev, 1988; Karamata et al., 1994), age of volcanic and hydrothermal activity in the area (Jakupi et al., 1982; Lippolt & Fuhrmann, 1986; Kolios et al., 1988; Boev, 1988; Troesch & Franz, 1992), and others. However, the questions about the nature of mineralizing fluids (Beran et al., 1994), sources of metals and the role of magmatism (Frantz et al., 1994) are still open. Similar problems remain a contentious issue for the worldwide Carlin-type deposits as well (e.g., Hofstra & Cline, 2000; Su et al., 2010).

The deposit displays distinctive features of the Carlin-type of mineralization as (1) strong structural control of mineralization by faults and folds; (2) calcareous sedimentary host rocks of diverse facies ± igneous rocks; (3) decarbonation, silicification, argillization and sulfidation alterations; (4) submicron gold in association with pyrite, arsenian pyrite and arsenopyrite and (5) geochemical signature of Au, As, Hg, Sb and Tl (Radtke, 1985; Hofstra & Cline, 2000).

The mineralization occurs within the three, not sharply defined, zones (Fig. 1): (1) Southern, high temperature, zone characterized by dominance of Au mineralization accompanied with variable amount of Sb and As minerals; (2) Central

part of the deposit beside Au, Sb and As mineralization contains significant amounts of Tl minerals, minor amount of Ba, Hg and traces of Pb and (3) Northern, low temperature, zone is represented by As and Tl mineralization, accompanied by minor Sb and traces of Hg and Au (Ivanov, 1986; Janković et al., 1997).

The aim of the present study is to elucidate the characteristics of fluid evolution by constraining the physico-chemical condition of Sb-As-Tl mineralization based on the analysis of fluid inclusions. Beside microthermometry, analyses of evaporate mound by scanning electron microscope with an attached X-ray energy dispersive system (SEM/EDX) is performed. Whereas the Au-Sb-As-Tl mineralization shows close spatial relationship to the volcanics, K/Ar dating of quartz latite is used for the refinement of the mineral deposition age.

GEOLOGICAL SETTING

The Allšar deposit is situated along a regional fault belt between the Vardar zone on the east and Pelagonian massif on the west. The deposit is related with a Neogene calc-alkaline volcano-intrusive complex intruded into Paleozoic-Mezozoic basement of the Vardar zone. The basement is composed of Precambrian gneisses, metamorphosed Triassic complex (marble, dolostones, minor schist) and Jurassic ophiolites followed by Cretaceous and Tertiary flysch, carbonate rocks and Neogene molasse deposits (Percival & Radtke, 1994; Janković & Jelenović, 1994). Volcanic activity in the area lasted between 7.0 and 1.8 Ma (Boev, 1988). Its products are extrusive rocks, ranging in composition from andesite, quartz-latite to dacite, occasionally trachyte and latite, generally enriched in K and Rb (Karamata et al., 1994), and pyroclastic equivalents.

The mineralization, represented by disseminated submicrometer-sized gold particles and Sb-As-Tl sulphides and sulfosalts and distributed over an area extending 2500 m WE and 200 m SN, shows a zonal pattern (Fig. 1). Zone I occupies the southernmost part of the deposit. It is characterized by extensive widespread replacement-induced silicification containing variable concentrations of gold, antimony and arsenic. The silicification varies in intensity from partial to total replacement (jasperoid). Central part of the deposit (Zone II) beside gold, antimony and arsenic contains significant amounts of thallium and minor amounts of barium, mercury and lead. The mineralization is hosted by argillized tuffs, Tertiary dolostones and rarely Triassic carbonate rocks. Thallium mineralization prevails within northern part of the deposit (Zone III). The principal host rocks are altered carbonate and tuffaceous rocks (Ivanov, 1986; Percival & Radtke, 1994, Janković et al., 1997).

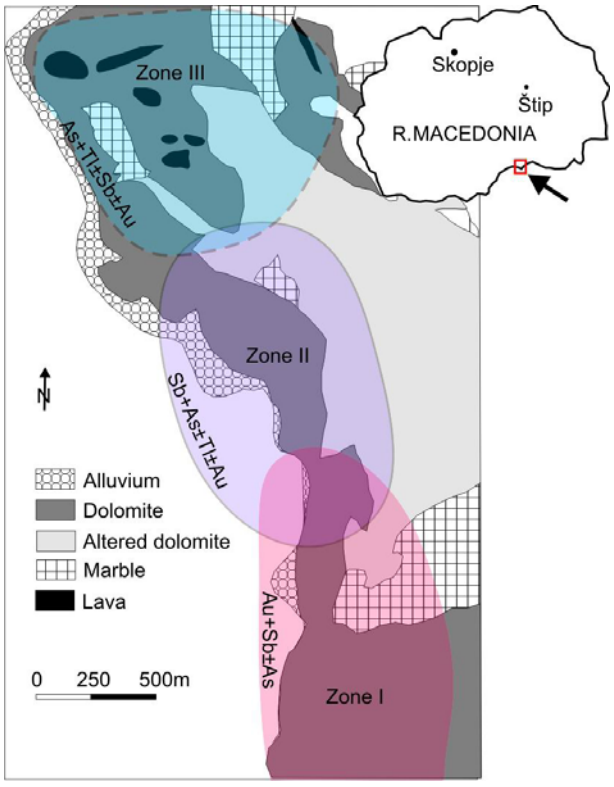

Fig. 1. Geographical and geological setting of the Allšar mineral deposit, Macedonia (after Janković et al., 1997)

SAMPLES AND METHODS

Fluid inclusion studies were carried out to estimate the P-T-X conditions during the mineralization. Microthermometric measurements were performed on primary fluid inclusions within doubly polished, ~0.3 mm thick, wafers of: (1) Quartz associated with high temperature sulfide mineralization (Zone I, Fig. 1); (2) Quartz and calcite from central part of deposit (Zone II, Fig. 1), (3) Real-

gar, orpiment, lorandite and dolomite associated with sulfide mineralization barren of Sb and enriched in As and Tl (Zone III, Fig. 1) and (4) Agate associated with an low temperature mineralization northernmost of Zone III (Fig. 1). Measurements were conducted at Linkam THMS 600 stage mounted on Olympus BX 51 microscope using 10x and 50x Olympus long-working distance objective lenses for visible light. Two synthetic fluid inclusion standards (SYN FLINC; pure H_2O, mixed H_2O-CO_2) were used to calibrate equipment. The precision of the system was ±2.0°C for homogenization temperature, and ±0.2°C in the temperature range between –60 and +10°C.

Ultraviolet (UV) fluorescence microscopy of hydrocarbons bearing inclusions was performed at Olympus BH 2 photomicroscope under magnification of 300×. The technique involves stimulation of a thin section by UV (ultraviolet light at 450–490 nm wavelength), which causes the specimen to fluoresce in the visible light spectrum. This visible light is captured in a specially adapted optical microscope. Organic materials, mostly hydrocarbons in the form of mobile oil, bitumen and "dead" oil, kerogen and other detrital organic components, are activate UV fluorescence. Therefore, mineral hosts with organic inclusions can be identified. Maturation degree of hydrocarbons is a function of colors displayed under UV and can be approximated using method described after Hagemann & Hollenbach (1986) and McLimans (1987).

Analyses of evaporate mounds were carried out to constrain the chemical composition of mineralizing fluid. Analyses were focused on realgar and orpiment used for microthermometry. Evaporate mounds were prepared according to the procedure described by Kontak (2004). The doubly polished wafers of realgar and orpiment were rapidly heated at heating-freezing stage described above. Massive decrepitation of fluid inclusions within realgar occurs in the range between 180 and 220°C. Although leaking of fluid inclusions within orpiment starts at temperature below 100°C, samples were heated at 160°C to produce enough evaporate mounds. Decrepitated wafers were removed on Cu tape attached to metal plate and transferred to the SEM, ready for chemical analysis. Evaporate mounds were located using backscattered (BSE) and secondary electron (SE) imagining. The analyses were done using the following operating conditions: 3–40 μm beam, accelerating voltage 15 kV, current 10 nA and counting time 40 seconds.

Measurements of K/Ar ages were performed at the Institute of Nuclear Reasearch of the Hungarian Academy of Science (ATOMKI), Debrecen. The samples were crashed to 0.063–0.315 mm size. Mineral separation was done by magnetic field and heavy liquids. One aliquot of samples (100 mg) was pulverized for potassium determination. Powders were digested in HF with the addition of some sulphuric and perhloric acids. The digested samples were dissolved in 100 ml 0.25 mol/1 HCl and diluted fivefold. Na and Li (100 ppm) were added as buffer and internal standard. Potassium concentration was measured with a digitalized flame photometer. Another aliquot of samples (500 mg) was used for Ar analyses. The samples were degassed by high-frequency induction heating, and the conventional getter materials were used for cleaning Ar. The ^{38}Ar spike was introduced to the system from a gas pipette before degassing. The cleaned Ar was directly introduced into the mass spectrometer, operated in the static mode. Recording and evolution of Ar spectra was controlled by a microcomputer. Details of the instruments, the applied methods and results of calibration have been described by Balogh (1985).

X-ray diffraction spectra were obtained on random oriented powders with a Phillips PW 3040/60 X'Pert PRO X-ray diffractometer with Cu Kα radiation at 45 kV and 40 mA (a counting time of 0.5 s per 0.5° step was used for 2θ in the 4–63° range). Samples powder was pressed on holder before measurements in order to minimize possible orientations effects.

RESULTS

Microthermometry of fluid inclusions

Microthermometric measurements were performed on primary, L+V, inclusions within quartz samples from the Zone I (Fig. 2.a). First melting (eutectic temperature, Te) obtained in interval between –44.0 and –58.0°C (Fig. 3.a) indicates the presence of bivalent cations, probably Ca^{2+} or Mg^{2+}, within the system (Crawford, 1981). Final melting of hydrate ($T_m$hyd1) was recorded in temperature range between –24.2 and –42.0°C (Fig. 3.b). Ice melting temperatures ($T_m$ice) in interval from –2.4 to –18.1°C (Fig. 3.c) point to salinity between 4 to 21.3 wt.% NaCl equ. Homogeniza-

tion (T_h) by vapor disappearance occurred in temperature range from 131 to 200°C (Fig. 3.d). Only one fluid inclusion nucleate recognizable chlatrate phase melted at temperature of –0.5°C ($T_m$chl), suggesting presence of CO_2 and salinity of 16 wt.% NaCl equ. Homogenization temperature was recorded at 201°C.

Microthermometric measurements within quartz (Fig. 2.b) and calcite (Fig. 2.c) from Zone II were conducted on two-phase (L+V) inclusions of the primary origin. The initial melting temperature (T_e) in range between –50.0 and –56.0°C indicates presence of bivalent cations (Fig. 3.a). Final melting of hydrate ($T_m$hyd1) was noticed between –27.2 and –39.0°C (Fig. 3.b). Ice melting temperatures ($T_m$ice) in interval from –10.5 to –13.1°C (Fig. 3.c) is in concordance with salinity between 14.5 and 17.1 wt.% NaCl equ. Homogenization into liquid phase occurred in range from 120 to 165°C (Fig. 3.d).

Microthermometric measurements were carried out on the primary, L+V, inclusions hosted by realgar (Fig. 2.d), orpiment (Fig. 2.e), dolomite (Fig. 2.f) and lorandite (Fig. 2.g) from Zone III. The eutectic temperature (T_e) in an interval between –50.3 and –54.2°C indicates presence of bivalent cations (Fig. 3.a). Melting runs in the temperature range between –35 and 0°C determined existence of two hydrates. Melting of the first hydrate ($T_m$hyd1) was recorded in temperature interval between –22.0 and –24.5°C (Fig. 3.b). Temperature interval of the final melting of the second hydrate ($T_m$hyd2) is observed between –11.0 and –15.4°C (Fig. 3.b). The ice melting temperature ($T_m$ice) the interval between –1.5 and –4.1°C (Fig. 3.c) corresponds to salinity of 2.6 to 6.9 wt.% NaCl equ. Homogenization within quartz and dolomite into liquid phase (T_h) was recorded between 120 and 152°C (Fig. 3.d). Temperature of total homogenization within orpiment and lorandite was not recorded due to massive decrepitation of fluid inclusions at lower temperatures.

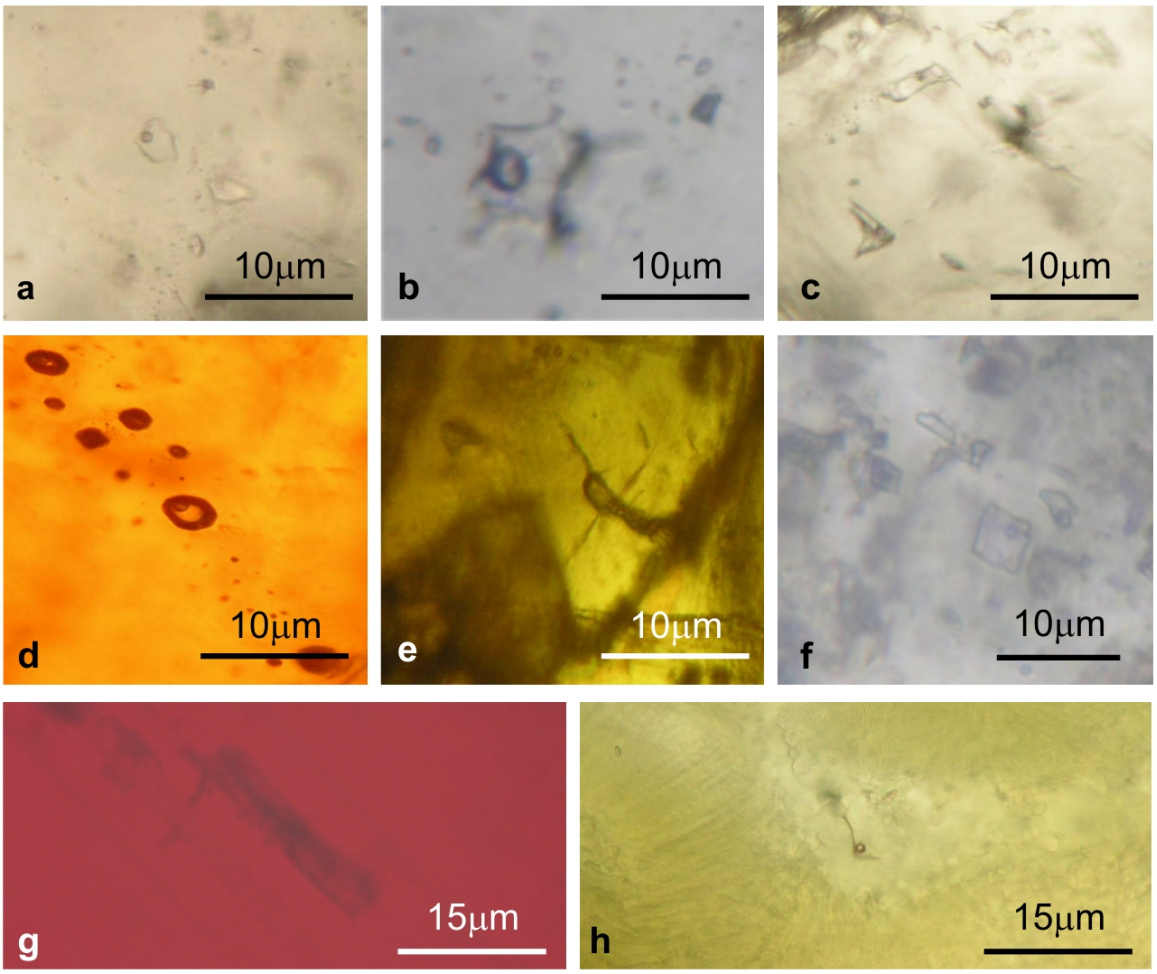

Fig. 2. Fluid inclusions within a) quartz (Zone I); b) quartz (Zone II); c) calcite (Zone II); d) realgar (Zone III); e) orpiment (Zone III), f) dolomite (Zone III); g) lorandite (Zone III); h) agate (north of Zone III).

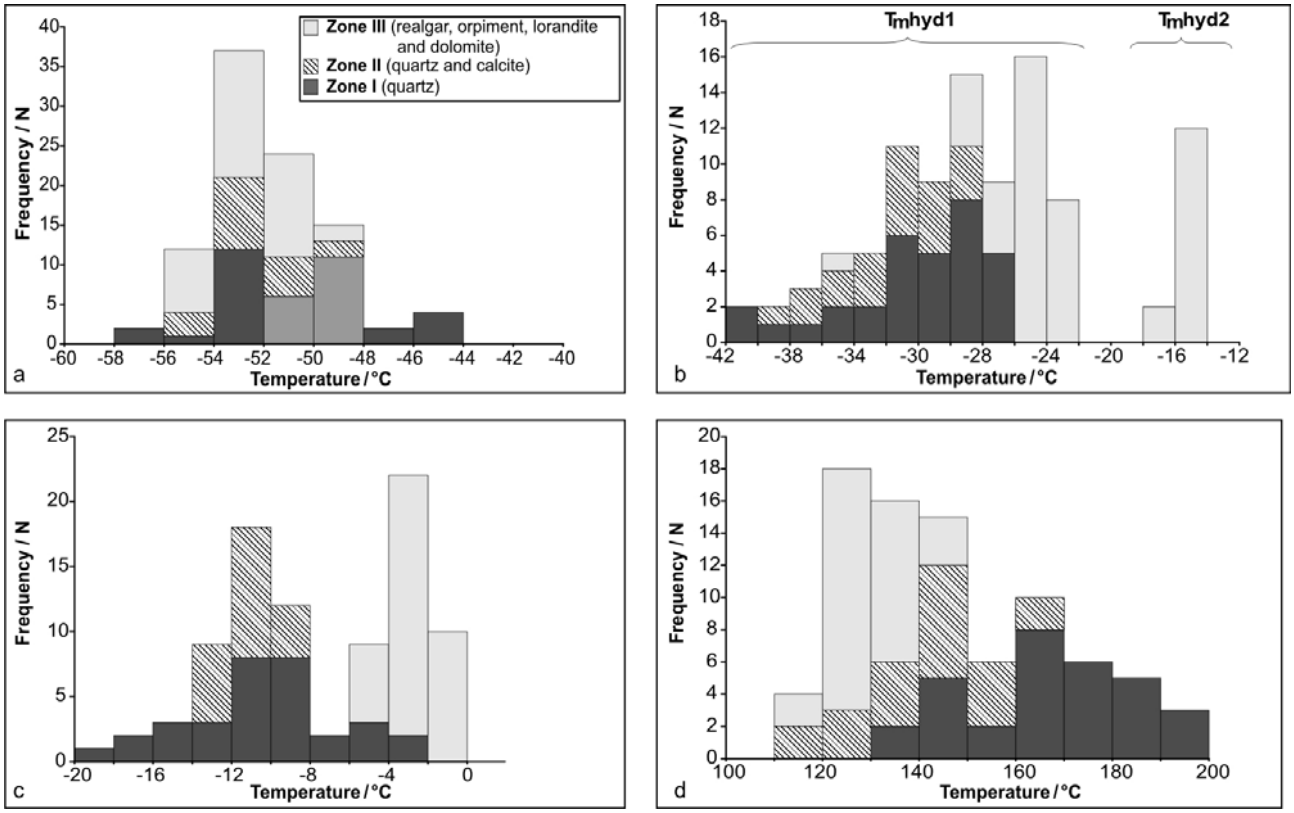

Fig. 3. Frequency distribution of a) the eutectic temperature; b) melting temperatures of hydrates; c) the last melting temperature of ice; d) homogenization temperature within vapor phase.

Microthermometric measurements were performed on aqueous inclusions containing CO_2 and hydrocarbons and multiphase hydrocarbon inclusions within agate (Fig. 2.h). During heating of aqueous inclusions containing CO_2 and hydrocarbons first homogenization in temperature range from +31.0 to +33.0°C occur within vapor bubble (liquid to vapor transition). Total homogenization to liquid state was recorded between 102 and 125°C (Fig. 3). Melting of chlatrates at temperature range from 2.4 to 7.0°C corresponds salinity from 6.0 to 13.5 wt.% NaCl equ.

Complex hydrocarbons bearing inclusions are remaining unfrozen at minimum stage temperature of –180°C. During subsequent heating, only observed changes within these inclusions were reduction in size or shape of some of the components, omitting the complete phase transitions. None of these inclusions were homogenized before decripitation, which occurred at temperatures range from 170 to 180°C.

Ultraviolet fluorescence microscopy

Ultraviolet (UV) fluorescence microscopy was performed on hydrocarbons bearing inclusions trapped within agate. This type of inclusion shows yellow and green fluorescence suggesting immature organic matter (e.g., Hagemann & Hollerbach 1986; McLimans 1987; Bodnar 1990). The intensity of fluorescence is increasing with the size of inclusions. Also, UV microphotographs show presence of various pieces of organic matter trapped within agate, with similar fluorescence colours to the described inclusions.

Composition of evaporate mounds

Analyses of realgar samples indicate Na and K chlorides composition of evaporate mounds. The presence of Al is also observed. A comparison of composition of evaporates mounds and microthermometric measurements points to composition of hydrates present within frozen inclusions. Hydrate with final melting temperature in the range between –22.0 and –24.5°C ($T_m$hyd1) is hydrohalite ($NaCl \times 2H_2O$). Hydrate with temperature interval of the final melting between –11.0 and –15.4°C ($T_m$hyd2) is $KCl \times 2H_2O$.

Analyses of orpiment samples point that evaporate mounds consist only of Na and K chlorides (Fig. 4).

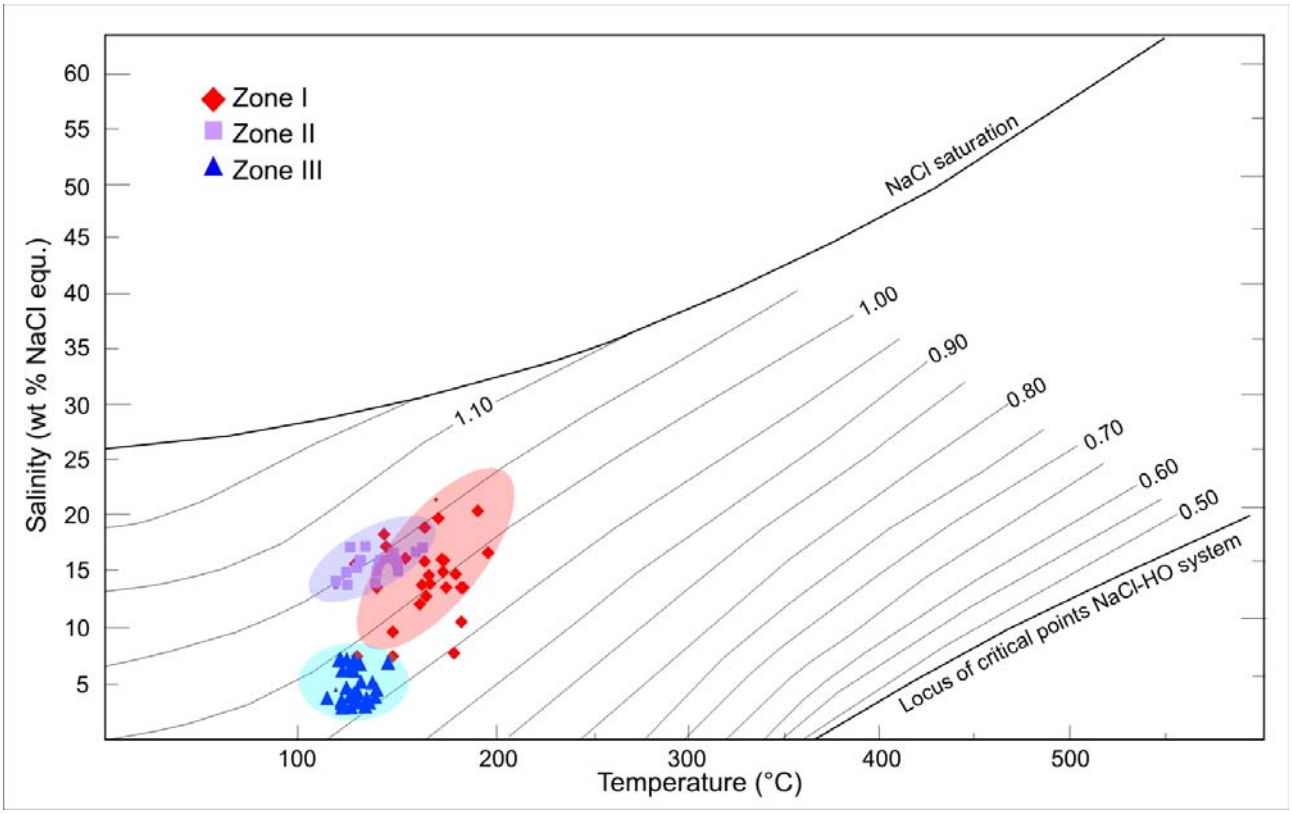

Fig. 4. Bivariate plot of homogenization temperature versus salinity

K/Ar dating

The K/Ar age dating was performed on quartz-latite sample collected on the Kožuf Mts., approximately 0.5 km N from the deposit. The whole rock and separated concentrate of hornblende, feldspar and biotite obtained K/Ar ages range from 4.6 to 5.8 Ma. The analytical data and ages of whole rock sample and separated minerals are shown in Table 1.

Table 1

The K/Ar data obtain on quartz-latite from the Kožuf Mts., Macedonia.

Sample	Dated fraction	K %	^{40}Ar* cm^3/g	^{40}Ar* %	K/Ar age (Ma)
MK-1.	Whole rock	3.05	5.486×10^{-7}	40.6	4.62 ± 0.19
MK-1.	hornblende	1.90	4.399×10^{-7}	33.1	5.79 ± 0.21
MK-1.	Biotite	4.45	9.719×10^{-7}	36.2	5.61 ± 0.20
MK-1.	feldspar	2.14	4.291×10^{-7}	38.9	5.15 ± 0.21

DISCUSSION

The Allšar deposit shares several common features with the Carlin-type deposits worldwide: (1) structural controls of mineralization; (2) calcareous sedimentary host rocks mostly accompanied with igneous rocks; (3) alterations including decarbonization, silicification, argillization and sulfidation; (4) submicron-sized gold in association with Fe-sulfides and (5) enrichment in Au, As, Hg, Sb and Tl.

The deposit is characterized by a zonal distribution of mineral assemblages and alterations. The fluid inclusions study reveals a change in temperature and composition of the mineralizing fluid across the different zones of the deposit (Fig. 4). Homogenization temperatures and salinities decrease from the southern toward the northern part of the deposit interpreted as a result of cooling and dilution. The main dissolved salts in the southern zone are Ca-Na-chlorides with a Na/Ca molar ratio between 0.2 and 19.3. In the central part of the deposit, the Na/Ca molar ratio varies in a narrow range between 0.3 and 1.3. In the northern part of the deposit, fluids are enriched in potassium. The presence of CO_2 is related to Sb-bearing jasperoids (Zone I) and to the opal precipitated north of the Zone III.

The ore fluids transported gold, arsenic, antimony, thallium, mercury and iron. The dominance of marcasite over pyrite in Zone I suggests a pH below 5. The mineralization consisting mainly of sulfides suggests that the ore forming fluids were enriched in reducing sulfur. Under such condition thallium is a very mobile element (Vink, 1993). Chemical analyses of country rocks within the Allšar deposit suggest volcanic and tuffaceous rocks as a possible source of thallium (Percival & Radtke, 1994; Frantz et al., 1994). Reaction of the ore fluids with the host carbonates resulted in an increase of pH in the northern part of the deposit. Whereas thallium sulfides show a small stability field under alkaline and reducing conditions (Vink, 1993) an increase in pH would optimize the thallium precipitation.

Although the Carlin-type deposits worldwide are spatially affiliated to organic rich carbonate rocks the role of organic matter in this type of mineralization is still unknown. Early observations on the Carlin deposit, Nevada, USA (e.g. Joralemon, 1951) suggested that metals were precipitated by reactions between mineralizing fluids and organic matter from the wall rocks which had served as a reductant or that metals were transported by organometallic complexes. Furthermore, the metal sources of the world's largest mercury deposits, Almadén (Spain: Saupé & Arnold, 1992) and Idrija (Slovenia: Palinkaš et al., 2004), are inferred to be in organic rich volcano-sedimentary complex. Contrary, some of recent works have suggested that the organic matter did not play an important role during the formation of Carlin-type mineralization (e.g. Kuehn & Rose, 1995; Gize et al., 2000).

However, it is important to notice that Beran et al. (1990) reported hydrocarbon bearing fluid inclusions within realgar from the Allšar deposit (Zone III) and that fluid inclusions hosted by opal show involvement of organic matter as well.

According to the fluid inclusion data Neogene magmatism (4.6 to 5.8 Ma) was the heat source responsible for driving convective hydrothermal circulation at the Allšar deposit, similar to that proposed for other Carlin-type deposits worldwide (e.g., Sillitoe & Bonham, 1990; Henry & Ressel, 2006; Johnston et al., 2008).

CONCLUSION

The Allšar mineral deposit occurs within sedimentary complex of the southern Vardar zone. Structurally controlled mineralization comprises mostly disseminated submicrometer-sized gold particles and Sb-As-Tl sulphides and sulfosalts. The mineralization and alterations display zonal pattern which coincides with fluid inclusion data. The southern zone (Zone I) hosts Au mineralization together with variable amount of Sb and As minerals. Alteration consists primarily of moderate to strong silicification (jasperoids). Fluid inclusion data accompanied with mineralogical features (predominance of marcasite, strong silicification) suggest participation of high temperature (T_h = 131 – 200°C), saline (up to 21.3 wt.% NaCl equ.) and low pH fluids. The central zone (Zone II), beside Au, Sb and As, carries significant amounts of Tl minerals, minor amount of Ba, Hg and traces of Pb. The mineralization is hosted by argillized tuffs, Tertiary dolostones and Triassic carbonate rocks. Decrease in both, homogenization temperature (T_h = 120 – 165°C) and salinity (14.5 and 17.1 wt.% NaCl equ.) points to the cooling and the dilution of ore-forming fluids. The northern zone (Zone III) represents the most important source of Tl mineralization. The deposition of thallium sulfides required reducing conditions. Fluid inclusion data suggest precipitation from relatively cooled (T_h = 120 – 152°C) and diluted (2.6 to 6.9 wt.% NaCl equ.) solutions. An involvement of organic matter within ore-bearing fluids was recorded by its contribution in ore-forming processes is still obscure. The authors suggest that Neogene magmatism (4.6 to 5.8 Ma) represented the heat source responsible for driving convective hydrothermal circulation at the Allšar deposit.

REFERENCES

Balogh K., 1985: K/Ar dating of Neogene volcanic activity in Hungary: experimental technique, experiences and methods of chronological studies, *ATOMKI report, Debrecen*, **D/1**, 277–288.

Beran A., Götzinger M.A., Rieck B., 1994: A fluid inclusion study of realgar from the Allšar deposit, FYR Macedonia, *N. Jahrb. Mineral. Abh.*, **167**, 345–348.

Bodnar R. J., 1990: Petroleum migration in Miocene Monterey Formation. California. USA: constraints from fluid-inclusion studies. *Mineral. Mag.*, **54**, 295–304.

Boev, B., 1988: Petrologic, Geochemical and Volcanologic Characteristics of the Volcanic Rocks of Mt. Kožuf. Ph.D. Thesis, Rudarsko-Geol. Fak., Štip, 195 pp. (in Macedonian).

Crawford M. L., 1981: Phase equilibria in aqueous fluid inclusions. Fluid inclusions: applications to petrology. In: Hollister L.S., Crawford M.L. (Eds.): *Fluid Inclusions: Applications to Petrology, Mineralogical Association of Canada Short Course Handbook*, **6**, 75–100.

Frantz E., Palme H., Todt W., El Goresy A., Pavičević M. K., 1994: Geochemistry of Tl–As minerals and host rocks at Allšar (FYR Macedonia). Solar neutrino detection with TI-205 the "LOREX" Project; geology, mineralogy and geochemistry of the Allšar deposit locality Crven Dol, *N. Jb. Miner. Abh.*, **167**, 359–399.

Gize A. P., Kuehn C. A., Furlong K. P., Gaunt J. M., 2000: Organic maturation modeling applied to ore genesis and exploration. In: Giordano T. H., Kettler R. M., Wood S. A. (Eds.) *Ore genesis and exploration: the roles of organic matter, Reviews in Economic Geology*, **9**, 87–104.

Hagemann H. W., Hollerbach A., 1986: The fluorescence behavior of crude oils with respect to their thermal maturation and degradation, *Org. Geochem.*, **10**, 473–480.

Hofstra, A. H., Cline, J. S., 2000: Characteristics and models for Carlin-type gold deposits. In: Hagemann S. G., Brown P. E. (Eds.): *Gold 2000, SEG Reviews in Economic Geology*, **13**, 163–220.

Ivanov T., 1986: Allšar the richest ore deposit of Tl in the world. *GSI-report 86–9*, Darmstadt, 6 pp.

Jakupi B., Kostić A., Anatanasijević R., Jovanović L., Torović Z., Pereygin V. P., Stetsenko S. G., 1982: On the geological age determination of orpiments from Alshar (Macedonia) by fission fragment track method, *S. G. Bull. du Mus. d'Histoir. Natur. Ser. A.*, 37.

Janković S., 1988: The Allšar Tl–As–Sb Deposit, Yugoslavia and its specific metallogenic features, *Nucl. Instrum. Methods Phys. Res., Sect. A*, **271**, 286.

Janković S., Boev B., Serafimovski T., 1997: Magmatism and Tertiary mineralization of the Kožuf metalogenetic district, the Republic of Macedonia, with particular reference to the Alšar deposit. Univerzitet "Sv. Kiril i Metodij" – Skopje, Rudarsko-geološki fakultet, Štip, Special issue, **5**, 262 pp.

Janković S., Jelenković R., 1994: Thallium mineralization in the Allšar Sb-As-Tl-Au deposit, *N. Jb. Miner. Abh.*, **167**, 283–297.

Johnston M. K., Thompson T. B., Emmons D. L., Jones K., 2008: Geology of the Cove Mine, Lander County, Nevada, and a genetic model for the McCoy-Cove hydrothermal system, *Econ. Geol.*, **103**, 759–782.

Joralemon P., 1951: The occurrence of gold at the Getchell Mine, Nevada, *Econ. Geol.,* **46**, 267–310.

Karamata S., Pavičević M. K., Korikovkij S. K., Boronikhin V. A., Amthauer G., 1994: Petrology and mineralogy of Neogene volcanic rocks from the Allšar area, the FY Republic of Macedonia, *N Jahrb Mineral Abh*, **167**, 317–328.

Kolios N., Innocenti F., Maneti P., Peccerillo A., Giuliani O., 1988: The Pliocene volcanism of the Voras Mts. (Central Macedonia, Greece), *Bull. Volcanol.*, **1**, 3–43.

Kontak D. J., 2004: Analysis of evaporate mounds as a complement to fluid-inclusion thermometric data: case studies from granitic environments in Nova Scotia and Peru. *Can. Mineral.*, **42**, 1315–1329.

Kuehn C. A., Rose, A. W., 1995: Carlin Gold Deposits, Nevada: Origin in a Deep Zone of Mixing between Normally Pressured and Overpressured Fluids, *Econ. Geol.*, **90**, 17–36.

Lippolt H. J., Fuhrmann U., 1986: K–Ar Age deteminations on volcanics of Alshar Mine, Yugoslavia. *GSI-report 86–9*, Darmstadt, 2 pp.

McLimans R. K., 1987: The application of fluid inclusions to migration of oil and diagenesis in petroleum reservoirs, *Appl. Geochem.*, **2**, 585–603.

Palinkaš L., Strmić S., Spangenberg S., Prochaska W., Herlec U., 2004: Ore-forming fluids in the Grübler orebody, Idrija mercury deposit, Slovenia, *Schweiz. Miner. Petrog.*, **84**, 173–188.

Pavičević M. K., Cvetković V., Amthauer G., Bieniok A., Boev B., Brandstatter F., Gotzinger M., Jelenković R., Prelević D., Prohaska T., 2006: Quartz from Allšar as monitor for cosmogenic ^{26}Al: Geochemical and petrogenetic constraints, *Mineral. Petrol.*, **88**, 527–550.

Percival T. J., Radtke A. S., 1994: Sedimentary-rock-hosted disseminated gold mineralization in the Alšar district, Macedonia, *Can. Mineral.*, **32**, 649–665.

Radtke A. S., 1985: Geology of the Carlin gold deposit, Nevada. *U.S. Geological. Survey Professional Paper*, **1267**, 124 p.

Ressel M. W., Henry C. D., 2006: Igneous geology of the Carlin trend, Nevada: Development of the Eocene plutonic complex and significance for Carlin-type gold deposits, *Econ. Geol.*, **101**, 347–383.

Saupé A. F., Arnold M., 1992: Sulphur isotope geochemistry of the ores and country rocks at the Almadén mercury deposit, Ciudad Real, Spain, *Geochim. Cosmochim. Acta*, **56**, 3765–3780.

Sillitoe R. H., Bonham H. F., 1990: Sediment-hosted gold deposits: Distal products of magmatic-hydrothermal systems, *Geology*, **18**, 157–161.

Su W., Heinrich C. A., Pettke T., Zhang X., Hu R., Xia B., 2010: Sediment-Hosted Gold Deposits in Guizhou, China: Products of Wall-Rock Sulfidation by Deep Crustal Fluids, *Econ. Geol.*, **104**, 73–93.

Troesch M., Frantz E., 1992: ^{40}Ar/^{39}Ar Alter der Tl-As Mine von Crven Dol, Allšar (Macedonia), *Eur. J. Mineral.*, **4**, 276.

Vink B. W., 1993: The behavior of thallium in the (sub) surface environment in terms of Eh and pH, *Chem. Geol.*, **109**, 119–123.

Р е з и м е

ГАСНО-ТЕ×НИ ИНКЛУЗИИ И ОДРЕДУВАЊЕ НА СТАРОСТА СПОРЕД МЕТОДОТ K/Ar НА Au-Sb-As-Tl НАОЃАЛИШТЕТО АЛШАР, МАКЕДОНИЈА

Сабина Стрмиќ Палинкаш [1], Сибила Боројевиќ Шоштариќ [2], Ладислав Палинкаш[1], Золтан Печкај[3], Блажо Боев[4], Владимир Берманец[1]

[1]Природно-математички факултет, Универзитет во Загреб, Хорватовац 95, 10000 Загреб, Хрватска
[2]Факултет за рударство, геологија и нафтно инженерство, Универзитет во Загреб, Пиеротиева 6, 10000 Загреб, Хрватска
[3]Институт за нуклеарни истражувања, Унгарска Академија на науките, БемТер 18ц, 4001 Дебрецен, Унгарија
[4]Факултет за природни и технички науки, Универзитет "Гоце Делчев", Гоце Делчев 89, 2000 Штип, Република Македонија
blazo.boev@ugd.edu.mk

Клучни зборови: карлин; злато; талиум; арсен; антимон; гасно-течни инклузии; одредување на старост според методот K/Ar

Au-Sb-As-Tl наоѓалиштето Алшар, Македонија, се јавува во јужниот дел на Вардарската зона. Наоѓалиштето е носител на Карлински тип на минерализација сместено во карбонатен седиментен комплекс. Минералните асоцијации и алтерации пројавуваат карактеристична зонална дистрибуција. Во согласност со податоците од гасно-течните инклузии, формирањето на минерализацијата е резултат на ладењето, разблажувањето и неутрализацијата на рудоносните флуиди. Неогениот магматизам (4.6 до 5.8 Ma) служел како извор на топлина одговорен за одржување на конвектината хидротермална циркулација во наоѓалиштето Алшар.

INSTRUCTIONS TO AUTHORS

The *Geologica Macedonica* is an official publication of the "Goce Delčev" University, Faculty of Natural and Technical Sciences, Štip, Republic of Macedonia. It is published a yearly. The journal publishes **original scientific papers, short communications, reviews, professional** and **educational papers** from all fields of Mining, Geology, Petrology, Mineralogy and Geochemistry....

The journal also publishes, continuously or occasionally, the bibliographies of the members of the Faculty, book reviews, reports on meetings, information on future meetings, important events and dates, and various heading which contribute to the development of the corresponding scientific field.

Original scientific papers report unpublished results of completed original scientific research. Experimental data should be presented in a way that enables reproduction and verification of analyses and deductions on which the conclusions are based. Manuscripts should normally not exceed 6000 words.

Short communications should also contain completed but briefly presented results of original scientific research. Manuscripts should normally not exceed 2000 words.

Reviews are submitted at the invitation of the Editorial Board. They should be critical surveys of an area in which preferably the author himself is active. The reviews can be longer than typical research articles but should generally be limited to 10 000 words including references, tables and figures.

Professional papers report on useful practical results that are not original but help the results of the original scientific research to be adopted into scientific and production use. Manuscripts should normally not exceed 4 000 words.

SUBMISSION OF MANUSCRIPTS

The authors bear the sole responsibility for the content of the contributions. It is assumed that by submitting their paper the authors have not violated any internal rules or regulations of their institutions related to the content of the contributions. Submission of a paper implies that it has not been published previously, that it is not under consideration for publication elsewhere, and that, if accepted, it will not be published elsewhere in the same form, in English or in any other language, without the written consent of the Publisher.

For the first submission, please send two hard copies of the manuscript and an identical electronic copy of the manuscript on a disc (in MS Word) to the Editor-in-Chief of Geologica Macedonica, the "Goce Delčev" University, Faculty of Natural and Technical Sciences, Goce Delčev 89, MK 2000 Štip, Republic of Macedonia. Electronic version of the manuscript can be also sent by email at todor.serafimovski@ugd.edu.mk

A cover letter must accompany every new submission. It should contain full names of all authors and their affiliation, the manuscript title and the name and contact information for the corresponding author. Please provide a mailing address, e-mail address, and phone and fax numbers. Authors are requested to submit, with the manuscript, the names and full contact details (including e-mail addresses) of 3 potential referees.

PREPARATION OF MANUSCRIPTS

Prepare the entire manuscript in double-space typing, on numbered pages of A4 format with margins of 2.5 cm on each side. Do not use footnotes.

The papers should be written in the shortest possible way and without unnecessary repetition. The original scientific papers, short communications and reviews should be written in English. Abstract and key words in Macedonian, must accompany each manuscript.

Manuscript should contain: title, authors names and addresses, abstract, key words, introduction, experimental or theoretical background, results and discussion, acknowledgement (if desired) and references.

Title. It should be brief and informative but should define the subject of the manuscript. It should include most of the key words.

Authorship. List the first and last name of each author. Omit professional and official titles. Give the complete mailing address of each author. For the corresponding author include an e-mail address and a phone and fax numbers. The name of the corresponding author should carry an asterisk.

Abstract. Each manuscript should be provided with an abstract of about 100–150 words. It should give the aim of the research, methods or procedures, significant results and conclusions. Define any abbreviations used in the abstract.

Key words. Up to 5 key words or phrases should be given to facilitate indexing and online searching.

Introduction. The most important previous results related to the problem in hand should be reviewed avoiding a detailed literature survey, and the aim and importance of the research should be clearly stated.

Experimental section. This section should contain a description of the materials used and methods employed in form which makes the results reproducible, but without detailed description of already known methods.

Manuscripts that are related to theoretical studies, instead of experimental section should contain a subheading **theoretical background** where the necessary details for verifying the results obtained should be stated.

Results and discussion. The authors should discuss their findings, postulate explanations for the data, elucidate models and compare their results with those of other works. Irrelevant comparisons and speculations unsupported by the new information presented in the manuscript should be avoided. The conclusions should be not given separately but included in this section.

Tables. They should be given with a suitable caption and should be numbered consecutively with Arabic numerals. Footnotes to tables should be typed below the table and should be referred to by superscript lowercase letter. Each table should be typed on a separate sheet. The correct position of the tables should be marked on the manuscript.

Figures. Figures (photographs, diagrams and schemes) should be numbered consecutively with Arabic numerals in order to which they referred. They should accompany the manuscript but should not be imbedded in the text. Each figure should be clearly marked with the figure number and the first author's name. All figures should have captions that

should be supplied on a separate sheet. Correct position of the figures should be marked on the manuscript. The size of the symbols for the physical quantities and units as well as the size of the numbers and letters used in the reduced figures should be comparable with the size of the letters in the main text of the paper. Each figure or group of figures should be planned to fit, after appropriate reduction, into the area of either one or two columns of text. The maximum finished size of a one column illustration is 8.0 cm and that of a two column illustration is 17.0 cm width. Make sure you use uniform lettering and sizing of your original artwork. All figures should be printed on a high quality graphics plotter. Figures should be also sent in electronic form as TIFF or JPG files with minimum 300 dpi or higher resolution.

Color illustrations in print can be included only at the author's expense.

Units. The SI (Systeme Internationale d'Unites) for quantities and units should be used throughout the whole text. If nomenclature is specialized, nomenclature section should be included at the end of the manuscript, giving definitions and dimensions for all terms.

The **names of chemical substances** should be in accordance with the IUPAC recommendations and rules or *Chemical Abstract* practice.

Acknowledgement. Financial support, advice or other kinds of assistance can be included in this section.

REFERENCES

Literature references should be numbered and listed in order of citation in the text. They should be selective rather than extensive with the exemption to review articles. Avoid references to works that have not been peered-reviewed. Citation of a reference as "in press" implies that it has been accepted for publication.

The surname of one or two authors may be given in the text, whereas in case of more than two authors they should be quoted as, for example, Julg *et al.* [1]. References should be cited as follows:

Journals:

(Boev et al., 1992): Boev Blažo, Čifliganec Vančo, Stojanov Risto, Lepitkova Sonja, 1992: Oligocene-Neocene magmatism in the region Bučim block. *Geologica Macedonica,* **6,** 23–32.

(Makreski et al., 2004): Makreski Petre, Jovanovski Gligor, Stafilov Trajče, Boev Blažo, 2004: Minerals from Macedonia, XII. The dependence of quartz and opal color on trace element composition – AAS, FT IR and micro-Raman spectrocsopy study. *Bull. Chem. Technol. Macedonia,* **23,** 2, 65–212.

Scientific meetings:

(Stojanov, 1990): Stojanov Risto, Serafimovski Todor, 1990: The volcanism in the Zletovo–Kratovo volcanic area. In: "XII Congress of Geologists in Yugoslavia", Ohrid, 405–124.

Books:

(Boev, 1996): Boev Blažo, Janković S., 1996: *Nickel and nickel-ferrous iron deposits of the Vardar zone (SE Europe) with particular reference to the Ržanovo–Studena Voda ore bearing series*. Faculty of Mining and Geology, Spec. Iss. No. **3,** pp. 273.

(Manahan, 2000): Manahan S. E., *Environmental Chemistry,* Seventh editions. CRC Press LLC, Boca Raton.

For the web references, as a minimum the full URL should be given. Any further information, if available (author names, dates, reference to a source publication, etc.) should also be given.

EDITORIAL PROCESS

Receipt of manuscripts. Receipt of each manuscript is acknowledged by e-mail to the corresponding author within three working days. The manuscript is read and examined for conformity to these Instructions to Authors. Failure to meet the criteria outlined may result in return of the manuscript for correction before evaluation.

Peer review/evaluation. Papers received by the Editorial Board are sent to two referees (one in the case of professional and educational papers). Although authors are invited to suggest reviewers who are competent to examine their manuscript, the Editorial Board is not limited to such suggestions. Identities of the reviewers will not be released to the authors. The review process is expected to be complete within 3 months, but conflicting recommendations and other unpredictable events may cause some delay.

The comments and recommendations of the referees and the Editorial Board are sent to the authors for further action. The authors are allowed 30 days to undertake revisions and return the corrected text to the Editorial Board. The final decision on acceptance or rejection is made by the Editorial Board. This decision, together with any relevant reasons, will be send to the corresponding author.

Publication process. The accepted manuscript is checked for conformation to the Instructions to Authors and to ensure that all necessary paperwork is present. Any areas that are identified as problematic will be addressed by the Editorial Board in consultation with the corresponding author. The papers will be prepared for publication by a professional copy editor responsible for ensuring that the final printed work is consistent in form and style.

Galley proofs. A galley proof is sent to the corresponding author. It should be checked very carefully and must be returned within 2 days of receipt. The proof stage is not the time to make extensive corrections, additions, or deletions.

Reprints. The corresponding author will receive, free of charge, 20 reprints of the paper published in the *Geologica Macedonica.* Additionally he will receive a complementary copy of the journal.